The Effect of Calcium Binding on Adhesion and Pilus Biogenesis in the PilC Family of Proteins

Michael D. L. Johnson

A dissertation submitted to the faculty of the University of North Carolina at Chapel Hill in partial fulfillment of the requirements for the degree of Doctor of Philosophy in the Department of Biochemistry and Biophysics.

Chapel Hill
2011

Approved by:

Professor Matthew Redinbo, Ph.D.

Professor Edward Collins, Ph.D.

Professor Matthew Wolfgang, Ph.D.

Professor Jack Griffith, Ph.D.

Professor Joseph St. Geme III, M.D.

ABSTRACT

MICHAEL D. L. JOHNSON: The Effect of Calcium Binding on Adhesion and Pilus Biogenesis in the PilC Family of Proteins
(Under the direction of Matthew Redinbo)

Pseudomonas aeruginosa is an opportunistic pathogen prevalent in people on immunosuppressants, recent open wounds, or cystic fibrosis patients. P. aeruginosa attaches to the host cell via polar type IV pili (tfp). These tfp are composed of many proteins including the major pilus subunit PilA, retraction protein PilT, and one focus of this dissertation, 1163 residue protein PilY1. PilY1 shares homology to other bacterial adhesion and pilus biogenesis proteins such as the PilC family of proteins in *Neisseria gonorrhoeae*, *Neisseria meningitidis*, and *Kingella kingae* thus, it is often characterized as a pilus biogenesis protein and the *P. aeruginosa* adhesin. However, no known mechanism for either situation had been elucidated. In this study, we have identified two calcium binding sites which affect both functional pilus biogenesis and adhesion to host cells. In addition, we have also located an RGD (integrin binding motif) that mediates PilY1 binding to integrin.

The C-terminal most PilY1 calcium binding site (CBS) was found from residues 851-859 in PAK and is conserved in other strains of *P. aeruginosa*. This CBS is also conserved in the PilC proteins over 100 different bacteria. We found, through mutating the bidentate aspartic acid *in vitro* and *in vivo*, that this CBS controlled functional pilus biogenesis with the calcium bound and unbound states corresponding to pilus extension and retraction respectfully. We also characterized the homologous CBSs in *N. gonorrhoeae* and *K. kingae* finding similar results.

Upon further examination, we also located separate CBS from residues 600-608. This site was in close proximity to an RGD. This CBS was conserved in other strains of *P. aeruginosa*, but not in other bacteria. We found that purified PilY1 bound integrin in an RGD dependent manner. Furthermore, we found that this interaction was mediated by the calcium bound states of both CBSs.

Here, we demonstrate that *P. aeruginosa* PilY1 uses calcium to mediate both functional pilus biogenesis factor and adhesion to host cells. Future studies will hopefully include exploiting both calcium binding domains to prevent pilus formation and binding to host cells and characterizing the in vivo effects of these three sites.

Dedication

To all the wonderful women in my life, my wife Elisha, my daughters Michaela and the one still cooking, and my mother Barbara

ACKNOWLEDGEMENTS

First and foremost, I must thank God. On December 14th, 2003, in my then girlfriend, now wife's church, I was told to pursue science. Since that moment, God has put a great number of people who have been positively essential to in my life as a researcher, a father, and a husband.

Thank you to Dr. Gary Johnson for your wonderful advice, which guided me to giving my CV Paula Harrington, which in turn, led me to first lab mentor, Dr. Jeffery Frelinger. You "grew hair" on my scientific chest; thanks for giving me my first shot in the Show. I'd also like to think Cindy Hensley who was my first lab mom. These relationships led me to Dr. Barbara Vilen who encouraged me to apply to the IBMS program in which I met the program director, Dr. Sharon Milgram. Thanks for the letters of recommendation and scoring me that sweet talk at the NIH. Thanks to my first IBMS family, specifically Kate, Bret, Deb, Rose, Deepak, Erica, Alaina and Pam, you all were my class before I had a class.

I'd like to give a big thanks to my current research mentor, Dr Matthew Redinbo. I still remember our first interview in which we talked about Duke basketball and you told me to a rotation in your lab. I don't know if I could describe a better interview. Since joining your lab, you have given me a lot of scientific rope and I have been made a better researcher because of it. I hope you can get a grant out of it. While in the Redinbo lab, my apartment burned down. Thank you to all the past and present members of the lab as well as my IBMS family that helped me move and helped with donations.

There are a number of people who are not in the Redinbo lab that have been very helpful. Here I would like to thank Kevin and Michelle for your friendship and Leah for your realism. I have also had the opportunity to mentor people on this journey, Justin, Stephani, Angela, and Brian, you all have taught me so much about myself and who I want to be.

Thank you to my collaborators; Dr. Matthew Wolfgang, Kimberly, Dr, Joe St. Geme, Eric, Dr. Christopher Thomas, Jeff, and Christine. I would like to thank a number of people in the Redinbo lab. Joe, you were always like a big brother/mentor to me and I will always appreciate that, Rebekah, for showing how to think on the other side of the road, and Monica, the other half of the original happy corner, my lab wife, and just a good overall friend, thanks for not making lab seem like work all the time; and yes, the plans are still set. I'd also like to thank Keith, the walking UNC encyclopedia, Yuan, and all the past and present members of the Redinbo Lab for great scientific and mindless conversations.

So much of what I accomplished in graduate school would not have been possible without Pat Phelps. Your Midas touch on my graduate school life has been much appreciated. Thanks for the outreach opportunities, giving me the tools to succeed, and for being extremely helpful in me getting a postdoc at St. Jude. Meeting you made me a better person.

Most of all, I couldn't have completed this work without the support of my loving family. Thank you Mom, for all you have done for me throughout my life. Words cannot describe how much I appreciate what you have done for me. Most of all, thank you to my wife for talking me up, down, and whatever other direction I needed thought out my grad school life. Thank you for being my other half.

Table of Contents

List of Tables

List of Figures

List of Abbreviations and Symbols

Å – angstrom

α – alpha

Ala, A – alanine

Amp – ampicillin

ANOVA – analysis of variance

Asn, N – asparagine

Asp, D – aspartic acid

ATP – adenosine triphosphate

β – beta

BSA – bovine serum albumin

C – Celsius

Ca – calcium

CaM – calmodulin

CBD – calcium binding domain

CBS – calcium binding site

CD – circular dichroism

CD – cluster of differentiation

CFU – colony forming unit

Cl – chloride

CTD- C-terminal domain

C-terminus, C-term, C-terminal – carboxy terminus

Δ – deletion

DNA – deoxyribonucleic acid

DTT – D,L-dithiothreitol

DxDxDG – aspartic acid-x-aspartic acid-x-aspartic acid-glycine calcium binding motif

EC_{50} – half maximal effective concentration

EDTA – ethylenediaminetetraacetic acid

EGTA – ethylene glycol tetraacetic acid

EF – helix-loop-helix

F – fluorine

FL – full length

g – gravity

Glu, E – glutamic acid

GM – sialotetrahexosylganglioside

GRADSP – glycine- arginine-alanine-aspartic acid-serine-proline control peptide

H – hydrogen

h – hour

HEPES - 4-(2-hydroxyethyl)-1-piperazineethanesulfonic acid

His, H – histidine

HRP – horseradish peroxidase

I - isoleucine

IC_{50} - half maximal inhibitory concentration

IPTG – isopropyl β-D-1-thiogalactopyranoside

ITC – isothermal titration calorimetry

K, Lys – lysine

K – potassium

K_d – dissociation constant

kD – kilodalton

λ – wavelength

L – liter

L – leucine

LB – lurea broth

LDV – leucine-aspartic acid-valine integrin binding motif

LIC – ligation independent cloning

MBP – maltose binding protein

μ – micro

μg – microgram

μL – microliter

μm – micron

μM - micromolar

MBP- maltose binding protein

mdeg – millidegrees

mg – milligram

min – minutes

mL – milliliters

mm – millimeter

Mn – manganese

mol – mole

M - methionine

MW – molecular weight

Na – sodium

NHS PEO4 Biotin – 12-biotinylamino-4,7,10-trioxadodecanoic acid N-hydroxysuccinimidyl ester

Ni – nickel

nM – nanomolar

nm – nanometer

nN – nano Newton

N-terminus, N-term N-terminal – amino terminus

O – oxygen

OD – optical density

P – phosphate

p – p-value

PAGE - polyacrylamide gel electrophoresis

PAK – *Pseudomonas aeruginosa* strain K

PBS – phosphate buffered saline

PBST – phosphate buffered saline .1% Tween

PDB – Protein Data Bank

PEG – polyethyleneglycol

pH – negative log (base 10) of the molar concentration of hydronium ions

Phe, F – phenylalanine

PMSF - phenylmethanesulfonylfluoride

pN – pico Newton

RGD – arginine-glycine-aspartic acid integrin binding motif

RGDS – arginine-glycine-aspartic acid integrin binding inhibitor peptide

RIPL – BL21-CodonPlus (DE3)-RIPL cells

rpm – revolutions per minute

s – seconds

SAD – single wavelength anomalous dispersion

SDS – sodium dodecyl sulfate

SEM – standard error of the mean

TB – terrific broth

Tb – terbium

Tet – tetracyclin

TEV – tobacco etch virus

T4P – Type IV Pili

TFP – Type IV Pili

T_m – melting temperature

TPR – tetratricopeptide

TRIS – 2-Amino-2-hydroxymethyl-propane-1,3-diol

Tyr, Y – tyrosine

UNC-CH – University of North Carolina at Chapel Hill

U.S. – United States

WT – wild type

w/v – weight by volume

% – percent

° – degree

$^{+}$ - positive

$^{-}$ - negative

Chapter 1

Introduction to *Pseudomonas aeruginosa* Type IV Pili

1.1 Pseudomonas aeruginosa Overview

Pseudomonas aeruginosa is a rod-shaped Gram-negative opportunistic pathogen that is highly prevalent in people with cystic fibrosis, on immunosuppressants, or with recent open wounds or burns. Needing only minimal nutrients to live, *P. aeruginosa* has been found living on or in a variety of environments, including steel, soil, deionized distilled water, and gasoline [1,2]. Having the ability to undergo both aerobic and anaerobic respiration, this nosocomial pathogen has the ability to infect any part of the body; however infections typically occur in the respiratory system, broken skin, blood, or urinary tract [3]. Hospital acquired infections, which killed an estimated 100,000 people in 2002, infected an estimated 1.7 million people in the U.S.; *P. aeruginosa* accounting for about 11% of those infections [4,5]. In addition to humans, this pathogen can infect other organisms, such as plants, insects, and other members of the animal kingdom, making it a bacterium of interest with significant relevance for studying the general mechanisms regulating pathogenesis [6,7].

P. aeruginosa is resistant to many antibiotics, such as β-lactams, macrolides, tetracyclines, co-trimoxazole, and most fluoroquinolones; it further has the ability to develop resistance to many more antibiotics including penicillins, monobactams, and the remaining fluoroquinolones [8]. This bacterium evades antibiotics by using a variety of mechanisms. *P. aeruginosa* has a thick cell wall that makes it difficult for antibiotics to get through the membrane, it ejects antibiotics using efflux pumps, and it attenuates antibiotic effects by forming a protective biofilm [9,10,11]. *P. aeruginosa* can also evade antibiotic treatments

targeting vital bacterial pathways through an SOS response, a process where the organism purposely mutates its genes in an attempt to adapt to and thus overcome stress [12].

1.2 P. aeruginosa Infection

P. aeruginosa causes infection via multiple stepwise actions: first, using flagella, it swims to approach its target; second, it adheres to the surface of the target using arm-like protrusions called type IV pili (tfp) that are also responsible for "walking" on the surface, a process known as twitching motility; third, it undergoes quorum sensing (ability to detect other bacteria) and forms a protective alginate biofilm; and fourth, somewhat concurrently with the third step, it begins secreting virulence factors such as LasA and LasB elastase, exotoxin A, and alkaline protease [13,14,15,16,17]. Finally, individual bacterium can separate from the parent colony to cause infections in other host sites. A critical step in causing virulence is the tfp's ability to attach to cells, tissues, or other surfaces, thereby allowing biofilm formation [2,13,18]. Without tfp, and hence the ability to anchor to a surface, *P. aeruginosa* cannot congregate to form a functional biofilm for its own protection and thus facilitate host infection [14].

1.3 Type IV Pili

P. aeruginosa tfp typically extend from one end of the rod-shaped bacterial cell. Pili give the bacteria the ability to travel in two different ways. One method, which is more directional is where the pili pull or drag the bacteria on the long edge, while the other method, which leads to more random movement, is walking upright, or on the tip of the rod-shaped bacteria [19]. Through twitching motility mediated pilus extension and retraction, tfp allow *P. aeruginosa* to move at speeds of 1 μm s^{-1} in a process that assembles and disassembles approximately 1,500 pilus subunits s^{-1} [20]. This process is ATP-dependent

and occurs during directed movement toward a nutritional gradient [21]. As can be expected, lack of tfp eliminates *P. aeruginosa*'s pathogenesis to host organisms due to lack of motility [15,18,22].

1.4 Proteins in the Type IV Pilus

There are more than forty proteins involved in the tfp. These proteins include PilA as the major pilin subunit; PilQ as the membrane pore protein through which the pilus extends and retracts; PilT, a key component in pilus retraction; PilB, which is responsible for pilus extension, and PilD, which is responsible for cleaving the membrane leader sequence on the pilus proteins [15,20,23,24]. There are also a number of pseudopilins (pilin-like proteins) that are incorporated into the main pilus fiber [25]. These proteins include FimU, PilV, PilW, PilX, and PilE, which are all located in the PilY1 operon controlled by AlgR [26,27]. Other members of this operon are PilY1 and PilY2 [26].

P. aeruginosa tfp are long fibers containing polymerized PilA. Although the sequences can be quite divergent between strains, the consensus monomer structure (based on solved crystal structures) contains a long α-helix with a head group of four β-strands, similar to the homologous protein PilE in *Neisseria gonorrhoeae* [28,29,30,31]. PilA is often thought to function as an adhesin in *P. aeruginosa* [28,32]. C-terminal disulfide-connected loops may control binding at the tip of the pilus to gangliosides GM1 and GM2; however, this evidence has been disputed because it is not consistent throughout the bacterial strains [28,32,33,34,35].

The current opinion on how these subunits polymerize is that, post PilD-mediated cleavage, PilA monomers are held in place in the membrane with the long α-helix tail

embedded in the membrane and the β-sheet head group sticking out, extracted using approximately three ATP molecules, and attached via electrostatic interactions using a conserved negatively charged glutamic acid of one PilA subunit attaching to the positively charged N-terminal region of another monomer [36,37,38,39]. The resultant polymer can be 6-9 nm wide and up to 1-4 μm long [36]. It has been estimated that six ATP molecules are used to assemble a pilus subunit and it is possible that the other three are needed for the polymerization step [40]. Accordingly, pilus polymerization is regulated by the tfp elongation ATPase, PilB [41,42]. Mutations to the His box, Walker-A, or –B motifs eliminate surface piliation, twitching motility, and the pilus dependent process of phage susceptibility [43].

Functional tfp extension and retraction occurs through a pore made by a dodecameric protein, PilQ, as observed in *Nesseria meningitidis* [44,45]. PilQ is also thought to play a role in pilus assembly because of its conformational change upon tfp engagement and its association with only one end of the pilus fiber [46]. The necessary process of *P. aeruginosa* PilQ multimerization and insertion into the bacterial membrane is regulated by PilF [47]. PilF has been found to attach to the outer membrane of *P. aeruginosa* and control PilQ pore assembly through six tetratricopeptide repeat (TPR) protein-protein interaction motifs [47]. TPRs are helical structures usually involved in large protein complex formation [48].

Pilus retraction occurs though ATPases PilT and PilU [41,42,49,50,51]. Consistent with what is seen in PilB and *N. gonorrhoeae,* mutations to the ATP binding domains in both of these proteins in *P. aeruginosa* eliminate functional pilus biogenesis, twitching motility, and results in phage resistance [43,50,52]. The retraction power of PilT can generate forces of more than 100pN per fiber [53]. The apo and ATP bound crystal structures of *P. aeruginosa* PilT have been solved and reveals a homohexamer [51]. It is also thought that

PilT works in concert with *P. aeruginosa* PilC, N, O, and P to coordinate individual pilus subunit depolymerization via a “paddle-wheel” type mechanism [51].

1.5 The f*imUpilVWXY1Y2E* Operon

The *fimUpilVWXY1Y2E* operon constitutes gene products for factors that fit into three families: pseudopilins/ minor pilin/ pilin-like protein family (FimU, PilV, W, X, and E), an uncharacterized group (PilY2), or the PilC family of proteins from the *Neisseria* family (PilY1) [26]. FimU, PilV, W, X, and E have been found to be necessary for functional pilus biogenesis and are integrated into the pilus [25]. All of these proteins share high homology to PilA with some minor differences. For example, PilW has a large predicted loop region within the head group of the protein. Integrated tfp minor pilins make a cuff in 1:1 stoichiometric ratios at various parts of the pilus fiber [25]. It is possible that these cuffs provide the grip for PilT-mediated retraction. PilY2 shows no known homology to other proteins, and PilY2 deletion mutants exhibit reduced twitching motility and pilus biogenesis [26].

1.6 PilY1

Another protein involved in the tfp is an 1163 amino acid (PAK strain) protein called PilY1. PilY1, which contains a 30 amino acid leader sec-dependent periplasmic signal sequence that is cleaved by PilD, is found in the pilus and outer membrane of *P. aeruginosa* [15,26,54,55]. Targeting PilY1 to the periplasm also helps facilitate disulfide formation in the reducing environment. PilY1 is a *P. aeruginosa* pilus protein necessary for functional pilus biogenesis [26]. PilY1 has also been characterized as the *P. aeruginosa* adhesin; however,

there have been no previous reports of the attachment mechanism directly involving PilY1 [15].

PilY1 is a member of the PilC class of proteins found in organisms such as *N. gonorrhoeae*, *N. meningitides*, and *Kingella kingae.* PilC proteins have been characterized as both tfp biogenesis proteins and as the adhesins of their respective organisms; however, the evidence for these respective host cell receptors is not concrete [56,57,58]. Typically, the N-terminal regions of PilC are characterized as the adhesion domains, while the C-terminal regions are known to be tfp biogenesis domains. PilY1 shares sequence homology with the C-terminal region of the PilC proteins but no N-terminal homology to any of proteins in this family. The lack of PilY1 N-terminal homology is consistent in that all of these organisms have different mechanisms for infection, and therefore, most likely have differing host target proteins. Investigating the role of these similar proteins may lead to broad-spectrum treatments. It is the goal of this dissertation to further characterize the PilC family of proteins to obtain new information about their role in pilus biogenesis and adhesion.

1.7 References

1. Foght JM, Westlake DW, Johnson WM, Ridgway HF (1996) Environmental gasoline-utilizing isolates and clinical isolates of Pseudomonas aeruginosa are taxonomically indistinguishable by chemotaxonomic and molecular techniques. Microbiology 142 (Pt 9): 2333-2340.

2. Stanley PM (1983) Factors affecting the irreversible attachment of Pseudomonas aeruginosa to stainless steel. Can J Microbiol 29: 1493-1499.

3. Richards MJ, Edwards JR, Culver DH, Gaynes RP (1999) Nosocomial infections in pediatric intensive care units in the United States. National Nosocomial Infections Surveillance System. Pediatrics 103: e39.

4. Klevens RM, Edwards JR, Richards CL, Jr., Horan TC, Gaynes RP, et al. (2007) Estimating health care-associated infections and deaths in U.S. hospitals, 2002. Public Health Rep 122: 160-166.

5. Schaberg DR, Culver DH, Gaynes RP (1991) Major trends in the microbial etiology of nosocomial infection. Am J Med 91: 72S-75S.

6. Apidianakis Y, Rahme LG (2009) Drosophila melanogaster as a model host for studying Pseudomonas aeruginosa infection. Nat Protoc 4: 1285-1294.

7. Starkey M, Rahme LG (2009) Modeling Pseudomonas aeruginosa pathogenesis in plant hosts. Nat Protoc 4: 117-124.

8. Driscoll JA, Brody SL, Kollef MH (2007) The epidemiology, pathogenesis and treatment of Pseudomonas aeruginosa infections. Drugs 67: 351-368.

9. Hoiby N, Ciofu O, Bjarnsholt T (2010) Pseudomonas aeruginosa biofilms in cystic fibrosis. Future Microbiol 5: 1663-1674.

10. Mah TF, O'Toole GA (2001) Mechanisms of biofilm resistance to antimicrobial agents. Trends Microbiol 9: 34-39.

11. Poole K (2004) Efflux-mediated multiresistance in Gram-negative bacteria. Clin Microbiol Infect 10: 12-26.

12. Cirz RT, O'Neill BM, Hammond JA, Head SR, Romesberg FE (2006) Defining the Pseudomonas aeruginosa SOS response and its role in the global response to the antibiotic ciprofloxacin. J Bacteriol 188: 7101-7110.

13. Giltner CL, van Schaik EJ, Audette GF, Kao D, Hodges RS, et al. (2006) The Pseudomonas aeruginosa type IV pilin receptor binding domain functions as an adhesin for both biotic and abiotic surfaces. Mol Microbiol 59: 1083-1096.

14. Hahn HP (1997) The type-4 pilus is the major virulence-associated adhesin of Pseudomonas aeruginosa--a review. Gene 192: 99-108.

15. Mattick JS (2002) Type IV pili and twitching motility. Annu Rev Microbiol 56: 289-314.

16. Miller MB, Bassler BL (2001) Quorum sensing in bacteria. Annu Rev Microbiol 55: 165-199.

17. Van Delden C, Iglewski BH (1998) Cell-to-cell signaling and Pseudomonas aeruginosa infections. Emerg Infect Dis 4: 551-560.

18. O'Toole GA, Kolter R (1998) Flagellar and twitching motility are necessary for Pseudomonas aeruginosa biofilm development. Mol Microbiol 30: 295-304.

19. Gibiansky ML, Conrad JC, Jin F, Gordon VD, Motto DA, et al. (2010) Bacteria use type IV pili to walk upright and detach from surfaces. Science 330: 197.

20. Burrows LL (2005) Weapons of mass retraction. Mol Microbiol 57: 878-888.

21. Kearns DB, Robinson J, Shimkets LJ (2001) Pseudomonas aeruginosa exhibits directed twitching motility up phosphatidylethanolamine gradients. J Bacteriol 183: 763-767.

22. D'Argenio DA, Gallagher LA, Berg CA, Manoil C (2001) Drosophila as a model host for Pseudomonas aeruginosa infection. J Bacteriol 183: 1466-1471.

23. Strom MS, Nunn DN, Lory S (1993) A single bifunctional enzyme, PilD, catalyzes cleavage and N-methylation of proteins belonging to the type IV pilin family. Proc Natl Acad Sci U S A 90: 2404-2408.

24. Turner LR, Lara JC, Nunn DN, Lory S (1993) Mutations in the consensus ATP-binding sites of XcpR and PilB eliminate extracellular protein secretion and pilus biogenesis in Pseudomonas aeruginosa. J Bacteriol 175: 4962-4969.

25. Giltner CL, Habash M, Burrows LL (2010) Pseudomonas aeruginosa minor pilins are incorporated into type IV pili. J Mol Biol 398: 444-461.

26. Alm RA, Hallinan JP, Watson AA, Mattick JS (1996) Fimbrial biogenesis genes of Pseudomonas aeruginosa: pilW and pilX increase the similarity of type 4 fimbriae to the GSP protein-secretion systems and pilY1 encodes a gonococcal PilC homologue. Mol Microbiol 22: 161-173.

27. Belete B, Lu H, Wozniak DJ (2008) Pseudomonas aeruginosa AlgR regulates type IV pilus biosynthesis by activating transcription of the fimU-pilVWXY1Y2E operon. Journal of bacteriology 190: 2023-2030.

28. Hazes B, Sastry PA, Hayakawa K, Read RJ, Irvin RT (2000) Crystal structure of Pseudomonas aeruginosa PAK pilin suggests a main-chain-dominated mode of receptor binding. J Mol Biol 299: 1005-1017.

29. Parge HE, Forest KT, Hickey MJ, Christensen DA, Getzoff ED, et al. (1995) Structure of the fibre-forming protein pilin at 2.6 A resolution. Nature 378: 32-38.

30. Craig L, Taylor RK, Pique ME, Adair BD, Arvai AS, et al. (2003) Type IV pilin structure and assembly: X-ray and EM analyses of Vibrio cholerae toxin-coregulated pilus and Pseudomonas aeruginosa PAK pilin. Mol Cell 11: 1139-1150.

31. Craig L, Volkmann N, Arvai AS, Pique ME, Yeager M, et al. (2006) Type IV pilus structure by cryo-electron microscopy and crystallography: implications for pilus assembly and functions. Mol Cell 23: 651-662.

32. Audette GF, Irvin RT, Hazes B (2004) Crystallographic analysis of the Pseudomonas aeruginosa strain K122-4 monomeric pilin reveals a conserved receptor-binding architecture. Biochemistry 43: 11427-11435.

33. Craig L, Pique ME, Tainer JA (2004) Type IV pilus structure and bacterial pathogenicity. Nat Rev Microbiol 2: 363-378.

34. Emam A, Yu AR, Park HJ, Mahfoud R, Kus J, et al. (2006) Laboratory and clinical Pseudomonas aeruginosa strains do not bind glycosphingolipids in vitro or during type IV pili-mediated initial host cell attachment. Microbiology 152: 2789-2799.

35. Schroeder TH, Zaidi T, Pier GB (2001) Lack of adherence of clinical isolates of Pseudomonas aeruginosa to asialo-GM(1) on epithelial cells. Infect Immun 69: 719-729.

36. Craig L, Li J (2008) Type IV pili: paradoxes in form and function. Curr Opin Struct Biol 18: 267-277.

37. Lemkul JA, Bevan DR (2011) Characterization of interactions between PilA from Pseudomonas aeruginosa strain K and a model membrane. J Phys Chem B 115: 8004-8008.

38. Macdonald DL, Pasloske BL, Paranchych W (1993) Mutations in the fifth-position glutamate in Pseudomonas aeruginosa pilin affect the transmethylation of the N-terminal phenylalanine. Can J Microbiol 39: 500-505.

39. Nunn DN, Lory S (1991) Product of the Pseudomonas aeruginosa gene pilD is a prepilin leader peptidase. Proc Natl Acad Sci U S A 88: 3281-3285.

40. Maier B, Koomey M, Sheetz MP (2004) A force-dependent switch reverses type IV pilus retraction. Proc Natl Acad Sci U S A 101: 10961-10966.

41. Nunn D, Bergman S, Lory S (1990) Products of three accessory genes, pilB, pilC, and pilD, are required for biogenesis of Pseudomonas aeruginosa pili. Journal of bacteriology 172: 2911-2919.

42. Turner LR, Lara JC, Nunn DN, Lory S (1993) Mutations in the consensus ATP-binding sites of XcpR and PilB eliminate extracellular protein secretion and pilus biogenesis in Pseudomonas aeruginosa. Journal of bacteriology 175: 4962-4969.

43. Chiang P, Sampaleanu LM, Ayers M, Pahuta M, Howell PL, et al. (2008) Functional role of conserved residues in the characteristic secretion NTPase motifs of the Pseudomonas aeruginosa type IV pilus motor proteins PilB, PilT and PilU. Microbiology 154: 114-126.

44. Collins RF, Davidsen L, Derrick JP, Ford RC, Tonjum T (2001) Analysis of the PilQ secretin from Neisseria meningitidis by transmission electron microscopy reveals a dodecameric quaternary structure. Journal of bacteriology 183: 3825-3832.

45. Martin PR, Hobbs M, Free PD, Jeske Y, Mattick JS (1993) Characterization of pilQ, a new gene required for the biogenesis of type 4 fimbriae in Pseudomonas aeruginosa. Mol Microbiol 9: 857-868.

46. Collins RF, Frye SA, Balasingham S, Ford RC, Tonjum T, et al. (2005) Interaction with type IV pili induces structural changes in the bacterial outer membrane secretin PilQ. J Biol Chem 280: 18923-18930.

47. Koo J, Tammam S, Ku SY, Sampaleanu LM, Burrows LL, et al. (2008) PilF is an outer membrane lipoprotein required for multimerization and localization of the Pseudomonas aeruginosa Type IV pilus secretin. Journal of bacteriology 190: 6961-6969.

48. Blatch GL, Lassle M (1999) The tetratricopeptide repeat: a structural motif mediating protein-protein interactions. Bioessays 21: 932-939.

49. Chiang P, Habash M, Burrows LL (2005) Disparate subcellular localization patterns of Pseudomonas aeruginosa Type IV pilus ATPases involved in twitching motility. J Bacteriol 187: 829-839.

50. Wolfgang M, Lauer P, Park HS, Brossay L, Hebert J, et al. (1998) PilT mutations lead to simultaneous defects in competence for natural transformation and twitching motility in piliated Neisseria gonorrhoeae. Mol Microbiol 29: 321-330.

51. Misic AM, Satyshur KA, Forest KT (2010) P. aeruginosa PilT structures with and without nucleotide reveal a dynamic type IV pilus retraction motor. J Mol Biol 400: 1011-1021.

52. Wolfgang M, Park HS, Hayes SF, van Putten JP, Koomey M (1998) Suppression of an absolute defect in type IV pilus biogenesis by loss-of-function mutations in pilT, a twitching motility gene in Neisseria gonorrhoeae. Proc Natl Acad Sci U S A 95: 14973-14978.

53. Maier B, Potter L, So M, Long CD, Seifert HS, et al. (2002) Single pilus motor forces exceed 100 pN. Proc Natl Acad Sci U S A 99: 16012-16017.

54. Bendtsen JD, Nielsen H, von Heijne G, Brunak S (2004) Improved prediction of signal peptides: SignalP 3.0. J Mol Biol 340: 783-795.

55. Bohn YS, Brandes G, Rakhimova E, Horatzek S, Salunkhe P, et al. (2009) Multiple roles of Pseudomonas aeruginosa TBCF10839 PilY1 in motility, transport and infection. Mol Microbiol 71: 730-747.

56. Nassif X, Beretti JL, Lowy J, Stenberg P, O'Gaora P, et al. (1994) Roles of pilin and PilC in adhesion of Neisseria meningitidis to human epithelial and endothelial cells. Proc Natl Acad Sci U S A 91: 3769-3773.

57. Kallstrom H, Liszewski MK, Atkinson JP, Jonsson AB (1997) Membrane cofactor protein (MCP or CD46) is a cellular pilus receptor for pathogenic Neisseria. Mol Microbiol 25: 639-647.

58. Kirchner M, Heuer D, Meyer TF (2005) CD46-independent binding of neisserial type IV pili and the major pilus adhesin, PilC, to human epithelial cells. Infect Immun 73: 3072-3082.

CHAPTER 2

Crystal Structure Analysis Reveals *Pseudomonas* PilY1 as an Essential Calcium-Dependent Regulator of Bacterial Surface Motility

Jillian Orans[a], Michael D. L. Johnson[b]*, Kimberly A. Coggan[c]*, Justin R. Sperlazza[a], Ryan W. Heiniger[c], Matthew C. Wolfgang[c,d], and Matthew R. Redinbo[a,b]

[a]Department of Chemistry, University of North Carolina at Chapel Hill, CB 3290, Chapel Hill, NC 27599, USA. [b]Department of Biochemistry and Biophysics, University of North Carolina at Chapel Hill, CB 7260, Chapel Hill, NC 27599, USA. [c]Department of Microbiology and Immunology, University of North Carolina at Chapel Hill, CB 7290, Chapel Hill, NC 27599, USA. [d]Cystic Fibrosis/Pulmonary Research and Treatment Center University of North Carolina at Chapel Hill, University of North Carolina at Chapel Hill, CB 7248, Chapel Hill NC, 27599, USA.

*Contributed equally to this work

Orans, J., Johnson, M.D.L., Coggan, K.A., Sperlazza, J.R., Heiniger, R.W. Wolfgang, M.C., Redinbo, M.R. . Proc Natl Acad Sci U S A. 2010 Mar 16;107(11):5260.

Data Deposition: coordinates and structure factors have been deposited to the PDB and assigned accession code 3HX6.

Michael D. L. Johnson contributed Fig. 2.2 C and D, Figure 2.4B, Fig. S2.2, Fig. S2.5, Fig. S2.6, and Fig. S2.7. He also contributed additional figures, now found in the text, Fig A2.1A-C and Fig A2.2A-C, that were not part of this manuscript, but supportive of the overall conclusion.

2.1 SUMMARY

Several bacterial pathogens require the “twitching” motility produced by filamentous type IV pili (T4P) to establish and maintain human infections. Two cytoplasmic ATPases function as an oscillatory motor that powers twitching motility via cycles of pilus extension and retraction. The regulation of this motor, however, has remained a mystery. We present the 2.1 Å resolution crystal structure of the *Pseudomonas aeruginosa* pilus-biogenesis factor PilY1, and identify a single site on this protein required for bacterial translocation. The structure reveals a modified β-propeller fold and a distinct EF-hand calcium-binding site conserved in pathogens with retractile T4P. We show that preventing calcium binding by PilY1 using either an exogenous calcium chelator or mutation of a single residue disrupts *Pseudomonas* twitching motility by eliminating surface pili. In contrast, placing a lysine in this site to mimic the charge of a bound calcium interferes with motility in the opposite manner – by producing an abundance of non-functional surface pili. Our data indicate that calcium binding and release by the unique PilY1 EF-hand loop identified in the crystal structure controls the opposing forces of pilus extension and retraction. Thus, PilY1 is an essential, calcium-dependent regulator of bacterial twitching motility.

2.2 INTRODUCTION

The pathogenesis of bacterial infections typically depends on microbial adherence to host tissue, aggregation of the pathogen at the site of infection, and subsequent dissemination to other anatomical sites within the host. Type IV pili (T4P) are thin surface filaments involved in biofilm formation, bacterial aggregation and microbial adherence to biotic and abiotic surfaces. T4P biogenesis requires more than a dozen proteins conserved across a range of bacterial species [1]. A subset of bacteria, including the opportunistic human pathogen *Pseudomonas aeruginosa,* cyclically extend and retract their T4P, facilitating a form of surface movement termed twitching motility [2,3,4]. Retractile T4P are required for *P. aeruginosa* adherence to host tissue, virulence and dissemination of infection [5,6,7].

The pilin subunits that form T4P are incapable of self-assembly. Instead, pilus extension and retraction requires repeated rounds of pilin polymerization and depolymerization, both of which demand ATP hydrolysis [8,9]. In *P. aeruginosa*, the cytoplasmic ATPase PilB drives the assembly of pilin monomers into mature T4P [8,10], while the structurally related cytoplasmic ATPase PilT disassembles T4P back into pilin monomers [8,11,12]. Loss-of-function mutations in PilT result in the loss of twitching motility due to the inability of formed pilus fibers to retract [12]. The C-terminal half of the 117-kDa *P. aeruginosa* PilY1 protein shares sequence homology with the C-terminal domain (CTD) of the PilC proteins of pathogenic *Neisseria* species; in contrast, the N-terminal regions of the PilCs and PilY1 are divergent in sequence [13]. While the PilC proteins from *Neisseria* have been implicated in antagonizing pilus retraction by the pilus biogenesis ATPase PilT, the N-terminal domains of these proteins appear critical for host cell attachment [14,15]. Thus, we hypothesized that the conserved CTDs of PilY1 and PilC may play a common role in T4P

biogenesis rather than adhesion, and pursued a structural and functional analysis of the CTD from *Pseudomonas aeruginosa* PilY1.

2.3 RESULTS

2.3.1 PilY1 Exhibits a Modified β-Propeller Fold

Examination of the primary sequence of PilY1 from *P. aeruginosa* strain PAK revealed conservation between its C-terminal 550 residues and the same regions of the PilC proteins from *Neisseria*, and a predicted structural homology to the eight-bladed □-propeller fold exhibited by a range of proteins [16,17]. Thus, we overexpressed, purified and crystallized the PilY1 CTD (amino acids 614-1163) for examination by x-ray diffraction. Native diffraction data were collected to 2.1 Å resolution (Table I); however, attempts to determine the structure using existing β-propeller search models or by isomorphous replacement methods were not successful. PilY1 CTD contains only six methionine residues, which upon selenomethionine substitution failed to produce an adequate signal to support structure determination by anomalous dispersion [18]. To overcome this problem, a series of single leucine-to-methionine (L-M) substitutions were placed in the PilY1 CTD to provide additional sites for single wavelength anomalous dispersion (SAD) phasing (Supplemental Figures 2.1- 2.2). After several attempts, three L-M substitutions (at positions 712, 812, 823) were successfully combined, crystallized, and generated clear selenomethionine fluorescence signal upon examination in the x-ray beam. The structure was determined by SAD phasing using crystals containing nine total selenomethionine residues per protein monomer.

The structured 505 residues of the PilY1 CTD exhibit a seven-bladed modified β-propeller fold composed of 31 β-strands and 9 α-helices (Figure 2.1A; Supplemental Figures

2.1- 2.2; residues at the termini, as well as 713-721 and 1061-1068 were disordered and are not in the refined model). Blades I through IV are 4-stranded antiparallel β-sheets and align well with blades of a canonical β-propeller enzyme, quinohemoprotein alcohol dehydrogenase from *Comamonas testosteroni* (RCSB 1KB0; overall RMSD of 3.6 Å over 290 equivalent Cα positions with 15% sequence identity; Figure 2.1B) [16]. This β-propeller enzyme was identified by Phyre to align with the PilY1 predicted structure (E-value 0.014, 95% certainty) [16]. Blades V through VII of the PilY1 CTD, however, deviate from the standard β-propeller fold and align poorly with established β-propellers. Blade V contains a fifth strand (β20) that is shared with blade VI. Blade VI is composed of six strands, including β20, and maintains an insert containing a short helix and β-turn-β motif (α9, β26-27). Finally, blade VII is truncated and composed of three relatively short strands.

WD40 β-propeller proteins mediate protein-protein interactions via surface contacts at the propeller center [19]. Superposition of the PilY1 CTD structure onto that of the seven-bladed β-propeller WDR5, complexed with a lysine 4-containing histone H3 peptide, revealed an RMSD of 3.9 Å over 261 equivalent Cα positions sharing only 12% sequence identity [20]. Blades I-IV of the PilY1 CTD align well with the first four blades of WDR5, while the last three blades of each protein deviate more significantly in structure (Supplemental Figure 2.3). However, helices 4 and 7 of PilY1 appear to block the surface site used by WDR5 to interact with peptide [19]. Both helices are predicted to be conserved in the C-terminal domains of the related *Neisseria* PilC proteins (Supplemental Figure 2.2) [17]. These observations suggest that PilY1 and related pilus biogenesis factors do not mediate protein-protein interactions using the canonical WD40 surface-binding site.

2.3.2 PilY1 Contains a Unique Calcium Binding Loop

A strong $|F_o|-|F_c|$ electron density peak in the PilY1 CTD structure was interpreted as a calcium atom based on the observed coordination by three aspartic acid side chains (851, 855, 859), one asparagine side chain (853), one main-chain carbonyl oxygen of valine 857, and one water (Figure 2.2A; see also Supplemental Figure 2.1). The calcium binding observed in PilY1 is nearly identical to that seen in the canonical EF-hand Ca-binding motifs (Figure 2B; Supplemental Figure 2.4) [21]. PilY1 and EF hands both employ seven contacts to the bound calcium ion, including one from a water molecule and one bidentate contact via an acidic side chain. PilY1 is unique, however, in that it achieves this calcium chelation using a stretch of only nine amino acids (851-859) in a loop between two β -strands (β 13 and β 14) rather than the twelve residues between two α-helices typically observed in the EF-hands [21]. In addition, the carboxylic acid group of the bidentate Asp-859 residue is rotated nearly 90° with respect to the equivalent residue in EF-hand proteins [21]. Asp-859 forms a hydrogen bond with His-797, which is conserved in PilY1 proteins of known sequence. The calcium-chelating residues observed in the structure are conserved in the PilY1s of known sequence and in the related PilCs, with the exception that Asn-853 is replaced with an aspartic acid in the *Neisseria* proteins (Figure 2.2C; Supplemental Figure 2.2). This modified EF-hand motif is also present in PilY1 orthologues found in other bacteria that utilize T4P, including the human pathogen *Kingella kingae*. Thus, a novel calcium-binding site appears to be conserved in the C-terminal domains of pilus biogenesis proteins related to PilY1.

Measurement of calcium binding affinity using a fluorescence competition assay established that purified PilY1 CTD exhibits a K_d of 2.6 μM for calcium (Figure 2.2D), which is similar to the affinities reported for traditional EF-hand proteins [22]. Titration with increasing concentrations of magnesium chloride reveals that this cation does not bind to

PilY1. Mutation of the calcium chelating residue Asp-859 to alanine eliminates specific calcium binding by the protein (Figure 2.2D). Removal of calcium either by Chelex-100 or by mutating a chelating residue did not change the overall structure (as measured by circular dichroism spectropolarimetry; Supplemental Figure 2.6) or melting temperature (Supplemental Figure 2.7) of the PilY1 CTD [23]. Additional mutations D851A, N853, and D855A were made to PilY1, all of which eliminated calcium binding and did not affect the overall secondary structure (Figure Ad 2.1A-C, 2.2A-C). Thus, calcium binding appears not to play a role in the overall structure of the PilY1 C-terminal domain.

2.3.3 Calcium Binding and Release by PilY1 are Essential for Functional Pili

Expression of mutant versions of PilY1 in *P. aeruginosa* revealed that calcium binding and release are essential for pilus production and twitching motility. To examine the phenotypic consequences of altering the PilY1 calcium-binding site on T4P production and function, we engineered plasmid-encoded versions of full-length wild-type PilY1 and PilY1 carrying the D859A substitution. Both proteins were expressed to native levels in a *P. aeruginosa* strain in which the chromosomal *pilY1* gene was deleted (Supplemental Figure 2.8). The PilY1^{minus} strain is devoid of surface T4P, lacks measurable twitching motility, and is phenotypically indistinguishable from a non-piliated PilA^{minus} strain, which does not produce the major T4P subunit, pilin (Figures 2.3A-B). Complementation of the PilY1^{minus} strain with plasmid-expressed PilY1 restored twitching motility and pilus production to wild type levels (Figures 2.3A-B). In contrast, complementation of the PilY1^{minus} strain with full-length PilY1 D859A resulted in significantly less twitching motility ($p<0.001$) (Figure 2.3A). The level of surface T4P produced by the PilY1 D859A expressing strain was also dramatically reduced compared to wild type and likely accounts for the observed defect in twitching motility (Figure 2.3B).

PilY1 was previously shown to traffic to the surface T4P fraction [13] (Supplemental Figure 2.8), where it presumably functions through a direct association with the pilus fiber. To determine whether the defect in twitching observed with the D859A form of PilY1 was caused by disrupted pilus assembly/extension or increased pilus retraction, the PilY1 D859A mutant was expressed in a mutant strain lacking the PilT-retraction ATPase ($PilT^{minus}$, $PilY1^{minus}$ strain). These bacteria regained the ability to produce normal levels of T4P, and the mutant PilY1 protein was capable of trafficking to the sheared pilus fraction (Figures 2.3C-F). This result indicates that the loss of surface pili observed with the PilY1 D859A mutant is caused by PilT-mediated pilus retraction. In the presence of PilT, the D859A form of PilY1 is incapable of antagonizing PilT-mediated pilus retraction despite normal trafficking of the protein. We conclude that the calcium-binding site in the PilY1 CTD is necessary for normal pilus function by antagonizing the retractile activity of PilT.

We then created a mutation in full-length PilY1 designed to mimic calcium binding and to potentially render the protein calcium-insensitive. Specifically, a lysine residue was substituted for the bidentate calcium chelating Asp-859 residue (D859K). While a lysine residue is not equivalent to a divalent metal ion, modeling of the D859K substitution mutation indicates that the α-amino group of lysine would be expected to form a salt bridge with the two proximal aspartic acids at 851 and 855 (Supplemental Figure 9). Purified D859K PilY1 CTD does not bind calcium, and is not distinct in structure or melting temperature from the wild type CTD (Supplemental Figures 2.5- 2.7). When expressed to native levels in the *P. aeruginosa* $PilY1^{minus}$ strain (Supplemental Figure 2.8), the full-length PilY1 D859K mutant was significantly reduced for bacterial twitching motility ($p<0.001$) compared to the same strain expressing wild type PilY1 (Figure 2.3A). Interestingly, the level of surface pilus production in the PilY1 D859K expressing strain was equivalent to that of the wild type strain (Figure 2.3B), indicating that reduced fiber production does not account

for the twitching motility defect. PilY1 D859K was capable of trafficking to the surface T4P fraction when expressed in both a *pilY1* mutant background (Supplemental Figure 2.8) and a PilT^{minus}, PilY1^{minus} strain (Figures 2.3C-F). Thus, using the crystal structure as a guide, we produced a single-site mutation that dramatically alters pilus function without affecting pilus production. Based on these data, we conclude that the release of calcium by PilY1 is required for PilT-dependent fiber retraction and twitching motility.

Finally, we tested whether the calcium chelator EGTA impacts *P. aeruginosa* pilus production. We found that EGTA reduces the levels of surface pili present on bacteria expressing wild-type PilY1 while the non-retractile PilT^{minus} strain is blind to calcium chelation (Figure 2.4A). Similarly, the D859K form of PilY1 is insensitive to the effects of EGTA and supports the production of wild-type levels of surface pili (Figure 2.4A). These data show that the PilY1 D859K mutant, mimicking the calcium bound state of PilY1, has increased capacity to antagonize PilT-mediated pilus retraction. Taken together, these cell-based studies support the conclusion that both calcium binding and calcium release by the unique site in PilY1 are essential for the proper regulation of pilus retraction dynamics and twitching motility.

2.4 DISCUSSION

Based on the structural and functional data presented here, we propose that the PilY1 C-terminal domain exists in two critical states: calcium-bound, which inhibits PilT-mediated pilus retraction, and calcium-free, which does not inhibit PilT and allows pilus retraction to proceed. We further propose that the interconversion between these two states in wild-type PilY1 is required for the cycles of pilus extension and retraction necessary for

twitching motility (Figure 2.4B, *top*). The D859A mutant form of PilY1 appears to mimic the calcium-free state of the protein, and is not capable of antagonizing PilT-mediated retraction; thus, the equilibrium is shifted toward retraction, similar to that seen with the PilY1^{minus} strain (Figure 2.4B). Calcium chelation by EGTA also shifts the equilibrium toward retraction. In contrast, the D859K variant mimics the calcium-bound state, shifting the equilibrium toward pilus extension and producing an effect similar to that seen with the PilT^{minus} strain (Figure 2.4B). The relatively moderate 2 μM calcium binding affinity exhibited by PilY1 is in the range where cycles of calcium binding and release would be expected to be physiologically relevant. Thus, we conclude that PilY1 acts as a calcium-dependent regulator of the opposing forces responsible for T4P-mediated twitching motility. However, we stress that this is a functional hypothesis; the physical contacts between PilY1 and other factors necessary to achieve this regulation have yet to be elucidated. It is interesting to note that calcium binding by bacterial pseudopilins has recently been shown to be critical for functional type II secretion, a process believed to be analogous to T4P biogenesis and function [24]. Thus, calcium may play an important role in several aspects of pilus biogenesis and regulation.

Twitching motility mediated by PilY1's influence on the PilB/PilT oscillatory motor would be expected to be coordinated with the significant >100 pN retractile motion exerted by the system once target cell adhesion occurs [25,26]. Surface translocation by twitching motility likely involves relatively moderate affinity contacts between a surface and T4P [26]. For example, a disulfide loop in pilin, the major pilin subunit of the pilus fiber, has been proposed to be a point of contact between surfaces and T4P [27]. We propose that the cycles of pilus extension and retraction actuated by PilY1's C-terminal domain may control twitching motility involving these moderate affinity contacts. Once target host cell contact has been achieved, however, the T4P system would be expected to convert to a rapidly

retracting, PilT-dominated state in which nearly nN forces are exerted [28,29]. The function of this mode would be to quickly draw the bacterial cell into close contact with host tissue cells. It is tempting to speculate that PilY1 may serve as the switch between twitching and rapid retraction. The sequence divergent N-terminal domains of PilY1 orthologues are proposed to perform target cell-specific adhesion; once that is achieved, perhaps the conserved C-terminal domains switch to the calcium-free state to facilitate rapid PilT-mediated retraction [14,30,31].

The C-terminal domain of *P. aeruginosa* PilY1 shares significant sequence identity with the equivalent regions of the *Neisseria* PilC's (Figure 2.2C), and similar levels of identity in PilY1 homologues from other human, plant, and marine infectious bacteria [17]. We find that each PilY1 homologue contains a predicted calcium-binding site highly similar in sequence to that observed in the PilY1 C-terminal domain (see Supplemental Figure 2.2). Thus, calcium binding and release may play an equally important role in pilus biogenesis and motility in organisms that maintain a PilY1 homologue. Taken together, the structural and functional data we outline provide new insights into the complex functional regulation of the T4P essential to a range of human pathogenic bacteria.

2.5 METHODS

Structure Determination. PilY1 residues 615-1163 were cloned from genomic DNA from the PAK strain of *P. aeruginosa* (GenBank #EU234515), and overexpressed recombinantly in *E. coli*. The protein was purified using Ni-affinity and size-exclusion chromatography steps to >95% purity, and crystallized in 0.3 M sodium malonate (pH 6.5), 20% (w/v) PEG 3350, 50 mM DTT, 30 mM ammonium phosphate, and 4-8% trifluoroethanol. Residues 614-1163 of PilY1 contained only five methionine residues; as such, crystals containing selenomethionine-substituted protein failed to produce sufficient signal to allow structure

determination. L712M, L813M and L823M mutations were successfully generated, combined, expressed, purified and crystallized in PilY1 specimen sufficient for x-ray data collected. Diffraction data to 2.8 Å resolution were collected at the peak wavelength (0.979 Å) for selenium single-wavelength anomalous dispersion (SAD) phasing (Table 1), and indexed and scaled in space group C2 using HKL3000 [32,33]. Automated model building correctly built 30% of the final structure; complete building and refinement was accomplished using COOT and CNS, respectively [34,35]. Once the selenomethionine-substituted structure was refined at 2.8 Å resolution, it was used in molecular replacement to solve the 2.1 Å native structure, which was refined using COOT and CNS to the final statistics shown in Table 1 [34,35].

Calcium Binding and Biophysical Studies: Calcium was removed from purified PilY1 using Chelex-100 (BioRad) prior to biophysical studies [23]. A binding curve for Oregon Green® 488 BAPTA-5N was measured on a PHERAstar (BMGLabtech) at 488 nm and the K_d established at 10.1 μM. WT, D851A, N853A, D855A, D859A, and D859K PilY1 CTD was serial diluted 2 fold to calculate PilY1 CTD K_d for calcium binding, if applicable. For biophysical characterizations via circular dichroism spectropolarimetry, a wavelength scan from 195-260 was performed at 22 ^{o}C. Thermal denaturation protein samples were measured 210 nm at a range of 10 ^{o}C to 85 ^{o}C.

Isolation of Surface T4P: *P. aeruginosa* strains were spread on LB agar plates and grown until confluent. Bacteria were collected and suspended in 1 ml 0.15M NaCl/0.2% formaldehyde and vortexed vigorously for 1 minute to release surface T4P. Bacterial cells were removed by centrifugation at 12,000 x *g* for 5 minutes. T4P fractions were separated by SDS-PAGE (18% polyacrylamide) and pilin visualized by GelCode Blue stain (Pierce).

Twitching Motility: Bacteria were stab inoculated to the bottom of 100 mm tissue culture-treated plates containing 5 ml LB agar (1% w/v). Plates were incubated for 40 hours at 37°C

in a humidified incubator. Twitching motility was quantified by measuring the diameter of the subsurface zone of bacterial spread.

Western Blots: Whole cell lysates and T4P fractions were separated on 18% (pilin) or 7.5% (PilY1) SDS-polyacrylamide gels and transferred to nitrocellulose or PVDF membranes, respectively. Membranes were probed with PKL1 anti-pilin monoclonal antibody or anti-PilY1 CTD rabbit serum. Horseradish peroxidase-conjugated secondary antibodies were used for the detection of specific antibody-antigen complexes. Blots were developed with chemiluminescence reagents and visualized via autoradiography.

2.6 CREDITS

We thank Wladik Minor and Zbyszek Otwinowski for HKL3000 guidance, Joseph Lomino and Lisa Charlton of the Redinbo Laboratory for help with CD experiments, and Rebekah Potts and members of the Redinbo and Wolfgang groups for assistance with manuscript preparation. Supported by NIH grants AI078924 (M.R.R.) and AI069116 (M.C.W.), and a Howard Hughes Medical Institute Med-into-Grad Initiative Training Grant (K.A.C.).

2.7 FIGURE LEGENDS

Figure 2.1 Crystal structure of the *P. aeruginosa* PilY1 CTD. A. 2.1 Å resolution crystal structure of the *P. aeruginosa* PilY1 C-terminal domain, which begins at residue 644 and ends at 1148 and encompasses seven β-blades (I-VII; colored red, orange, yellow, green, blue, magenta and violet). **B.** Superposition of the seven-bladed PilY1 CTD β-propeller (red through violet) on the eight-bladed β-propeller of the quinohemoprotein alcohol dehydrogenase from *Comamonas testosteroni* (1KB0; grey).

Figure 2.2 PilY1 calcium-binding site. A. The PilY1 calcium binding site is composed of aspartic acids 851, 855 and 859, as well as asparagine 853, the main chain carbonyl oxygen of valine 857, and a water molecule (red sphere). Distances are in Å. **B.** Superposition of the nine-residue calcium-binding site of PilY1 (green) on the canonical twelve-residue site in human calmodulin (CaM; cyan). The calcium atoms (Ca) and water molecules (W) are depicted as spheres. Viewed in roughly the same orientation as 2A. **C.** Sequence conservation in the calcium binding sites of the PilY1 homologues PilC1 and PilC2 from *Neisseria meningitidis* (*N.men.*) and *N. gonorrhoeae* (*N.gon.*). **D.** The PilY1 CTD binds to calcium with a Kd of 2.6 μM (black), while the Asp-859-Ala mutant form of the CTD exhibits only non-specific calcium binding (grey). Error represents standard error of the mean.

Figure 2.3 The PilY1 calcium-binding site is essential for T4P production and function. A. Twitching motility of *P. aeruginosa* (wt), or a *pilY1* mutant expressing either empty vector (-), PilY1, or mutant versions of PilY1 (D859A or D859K). The twitching motility zones produced by bacteria expressing mutant PilY1 were significantly (*, $p < 0.001$) reduced compared to those of bacteria expressing wild type PilY1. **B.** Coomassie Blue-stained gel

of pilin isolated from the bacterial surface. **C-F**. Abolishing T4P retraction allows conditional localization of PilY1 to the bacterial surface. **C.** Coomassie-stained gel of pilin isolated from the bacterial surface. **D**. Western blot of T4P-containing surface fractions probed with PilY1-specific antiserum. **E.** Western blot of whole cell lysates probed with a pilin-specific antibody. **F.** Western blot of whole cell lysates probed with a PilY1-specific antiserum.

Figure 2.4 Calcium chelation impacts T4P production. A. Pilus preparations from a *pilT* mutant or a *pilY1* mutant expressing either PilY1, or mutant versions of PilY1 grown in the presence (+) or absence (-) of the calcium chelator EGTA**. B.** Summary of the impact specific mutants have on pilus state. Wild-type PilY1 appears to balance extension and retraction to produce twitching motility (boxed), while gene deletions, PilY1 site mutants, and the calcium chelator EGTA all significantly disrupt the equilibrium between pilus extension and retraction.

2.8 SUPPLEMENTAL FIGURE LEGENDS

Supplemental Figure 2.1 Topology diagram of the *P. aeruginosa* PilY1 CTD fold showing the positions of secondary structural elements (strands as arrows, helices as cylinders), disordered regions (dotted lines), the calcium binding site (green sphere), and the locations of the seven leucine-to-methionine mutations examined during structure determination. Colored as shown in Figure 1A.

Supplemental Figure 2.2 Sequence alignment of the PilY1 CTDs from three *Pseudomonas* strains (PAK, the subject of this study; PA01, PA14) along with the PilC1's from two *Neisseria* strains, *N. meningitidis* (NEIME) and *N. gonorrhoeae*

(NEIGO). Secondary structure elements, disordered regions, the calcium binding site, and the leucine-to-methionine mutations are indicated as in Supplemental Figure 1.

Supplemental Figure 2.3 A. Seven-bladed β-propeller structure of WDR5 (purple) complexed with an H3 peptide containing lysine-4 (yellow). **B.** Seven-bladed β -propeller structure of the PilY1 CTD (cyan). **C.** Superposition of the β -propeller structures showing that the site employed by WDR5 for peptide binding is blocked by β helices 4 and 7 in PilY1.

Supplemental Figure 2.4 Comparison of the ligand-to-calcium atom distances in PilY1 and human calmodulin (CaM), as well as the sequences of the calcium binding sites in the two proteins.

Supplemental Figure 2.5 Calcium binding curve for purified *P. aeruginosa* PilY1 D859K C-terminal domain.

Supplemental Figure 2.6 Circular dichroism spectropolarimetry wavelength scans for purified *P. aeruginosa* PilY1 C-terminal domain proteins in the presence and absence of calcium.

Supplemental Figure 2.7 Melting temperature for purified *P. aeruginosa* PilY1 C-terminal domain proteins in different conditions as monitored by circular dichroism spectropolarimetry.

Supplemental figure 2.8 A-D. Modulation of calcium binding influences T4P production without altering pilin availability. **A.** Coomassie-stained gel of pilin isolated from the bacterial surface. **B**. Western blot of T4P-containing surface fractions probed with PilY1-

specific antiserum. **C.** Western blot of whole cell lysates probed with a pilin-specific antibody. **D.** Western blot of whole cell lysates probed with PilY1-specific antiserum.

Supplemental Figure 2.9 Model of the Asp-859-Lys (D859K) mutation in the PilY1 C-terminal domain calcium binding site.

2.9 ADDITIONAL FIGURE LEGENDS

Additional Figure 2.1 A-C Calcium binding curve for purified *P. aeruginosa* PilY1 **A**. D851A **B**. N853A, and **C**. D855A C-terminal domain.

Additional Figure 2.2 A-C Circular dichroism spectropolarimetry wavelength scans for purified *P. aeruginosa* PilY1 **A**. D851A, **B**. N853A, and **C**. D855A C-terminal domain proteins in the presence and absence of calcium.

Figure 2.1

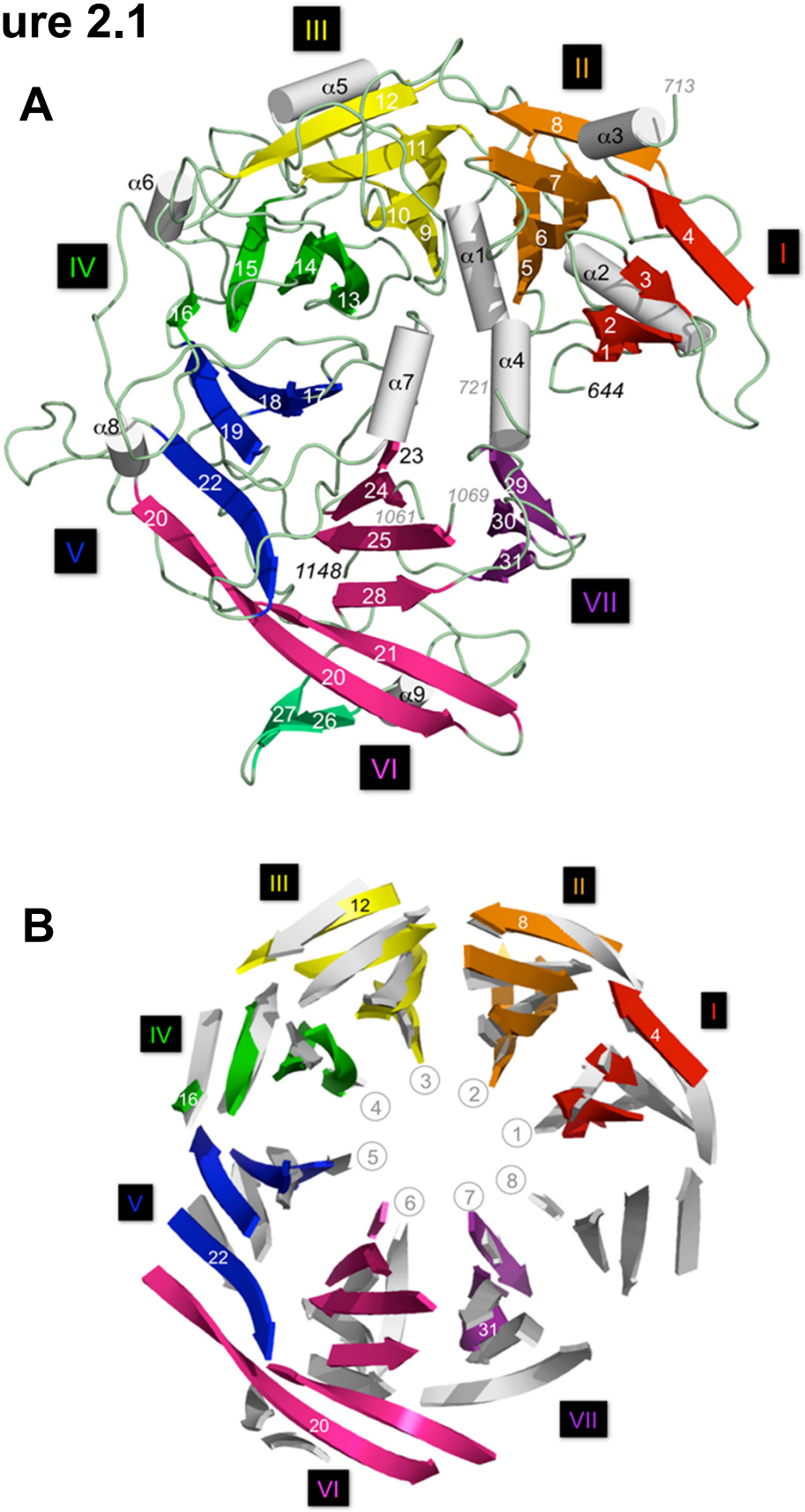
A
III
II
I
IV
V
VI
VII
α1
α2
α3
α4
α5
α6
α7
α8
α9
713
644
721
1069
1061
1148
B
III
II
I
IV
V
VI
VII

Figure 2.2

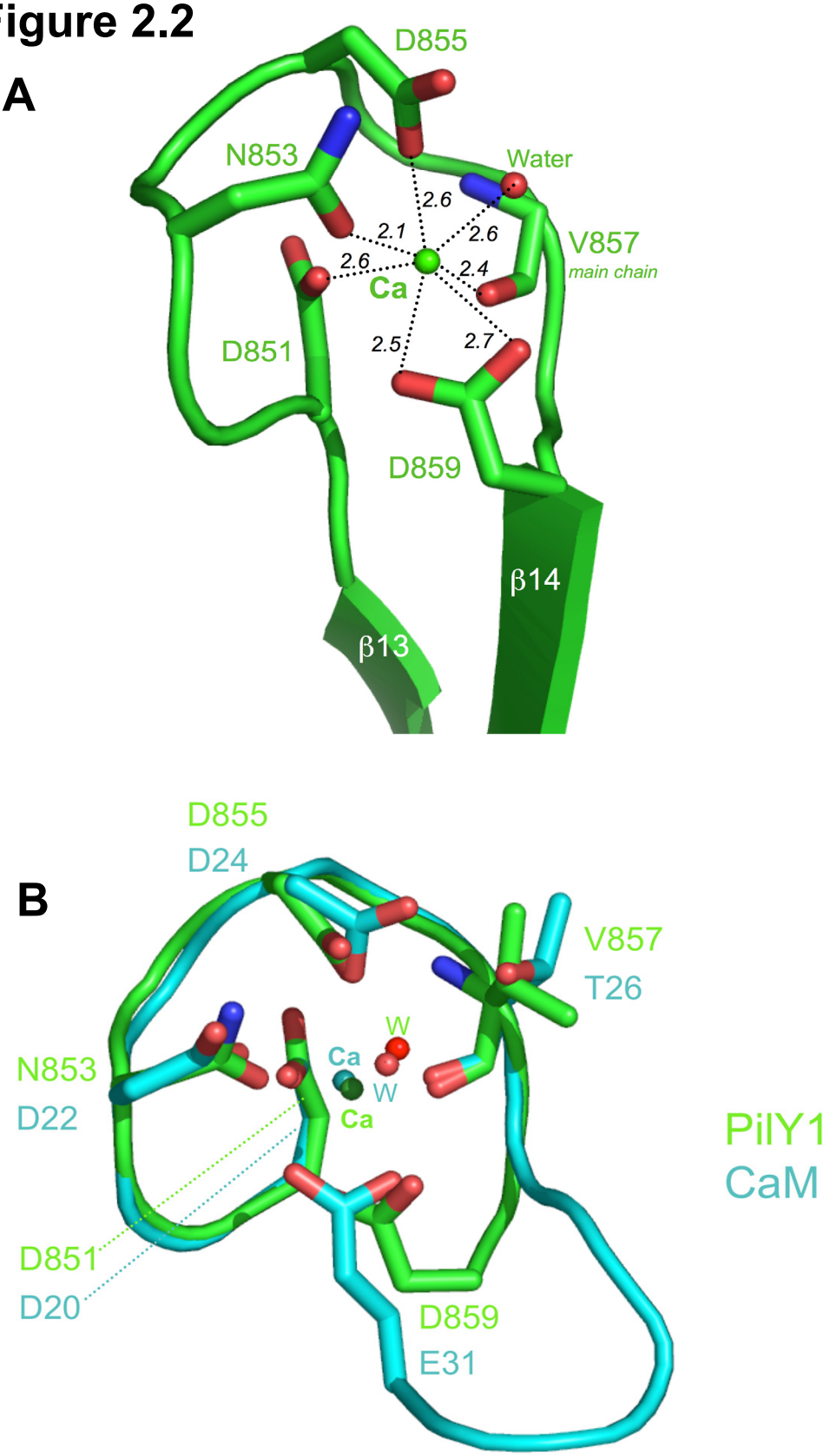
A
D855
N853
Water
2.6
2.1
2.6
2.6
2.4
V857
main chain
Ca
D851
2.5
2.7
D859
β14
β13
B
D855
D24
V857
T26
W
Ca
W
N853
D22
Ca
D851
D20
D859
E31
PilY1
CaM

Figure 2.2 contd.

C

P.aer. PilY1 *851-*DNNSDGVAD*-859*
N.men. PilC1 *728-*DKDLDGTVD*-736*
N.men. PilC2 *738-*DKDLDGTVD*-746*
N.gon. PilC1 *736-*DKDLDGTAD*-744*
N.gon. PilC2 *741-*DKDLDGTVD*-749*

D

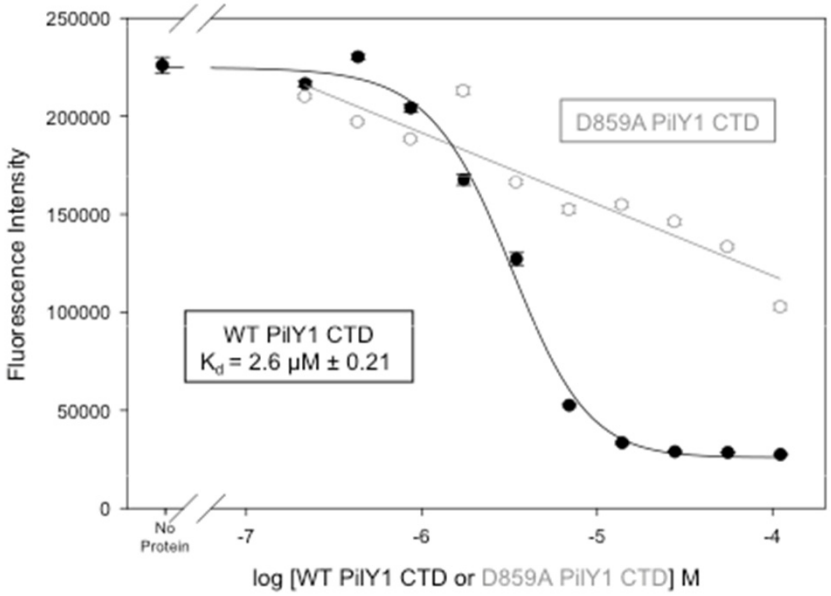

Figure 2.3

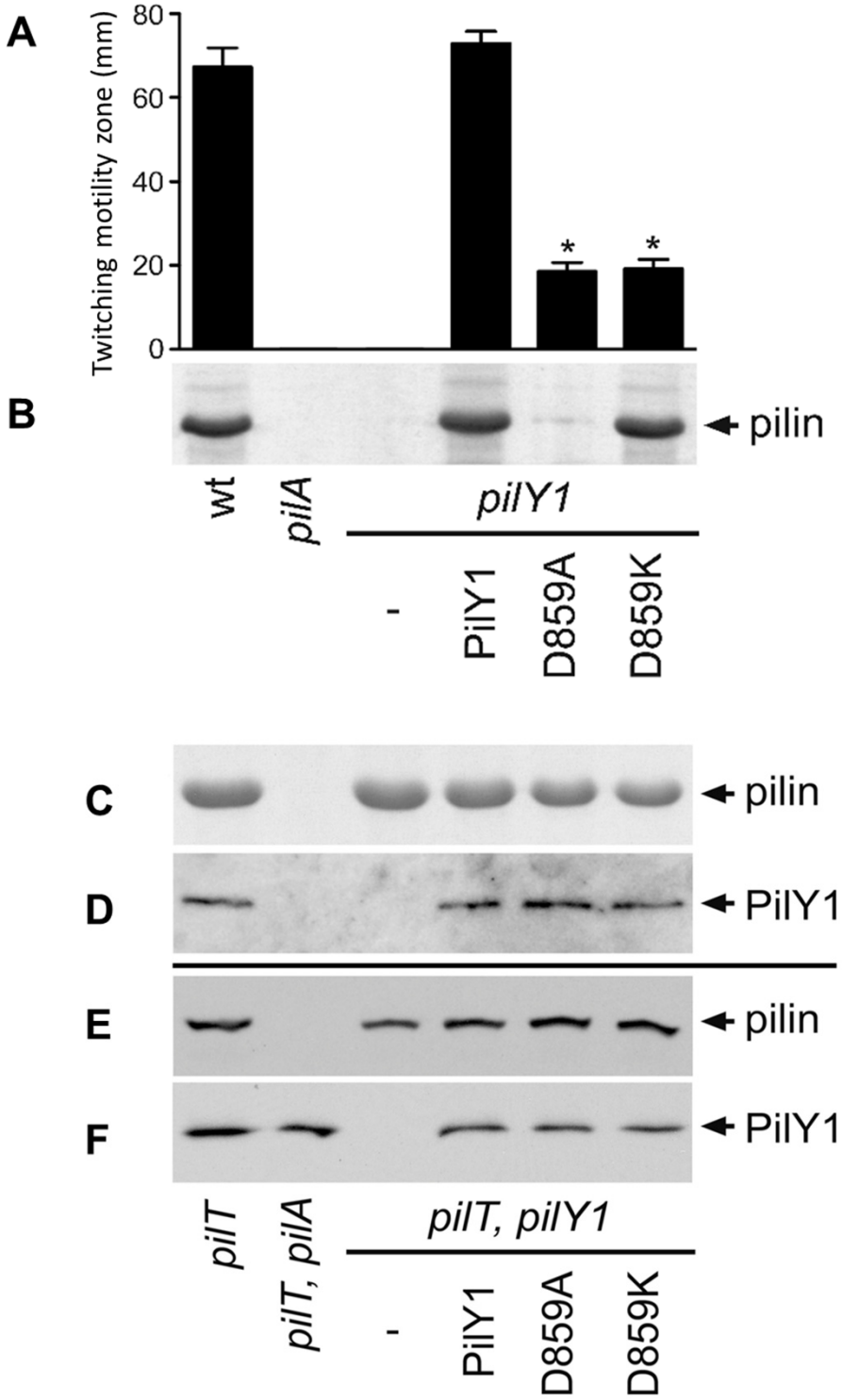
A
Twitching motility zone (mm)
80
60
40
20
0
*
*
B
pilin
wt
pilA
pilY1
-
PilY1
D859A
D859K
C
pilin
D
PilY1
E
pilin
F
PilY1
pilT
pilT, pilA
pilT, pilY1
-
PilY1
D859A
D859K

Figure 2.4

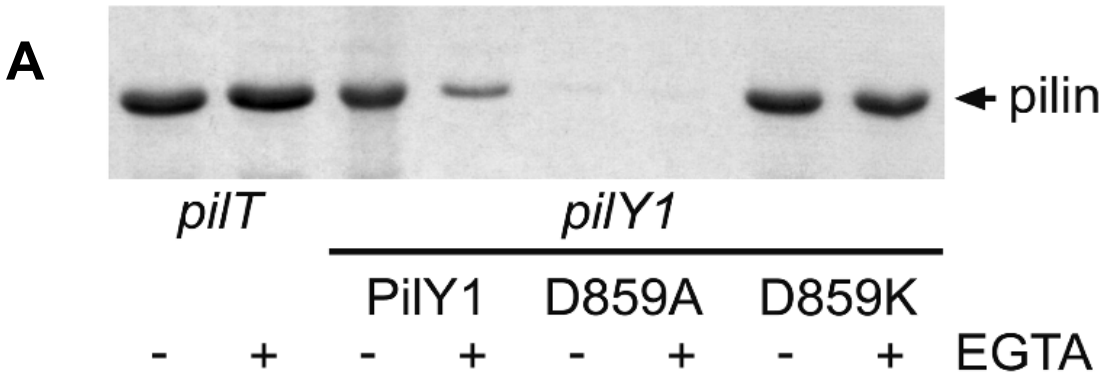
A
pilin
pilT
pilY1
PilY1
D859A
D859K
- + - + - + - + EGTA

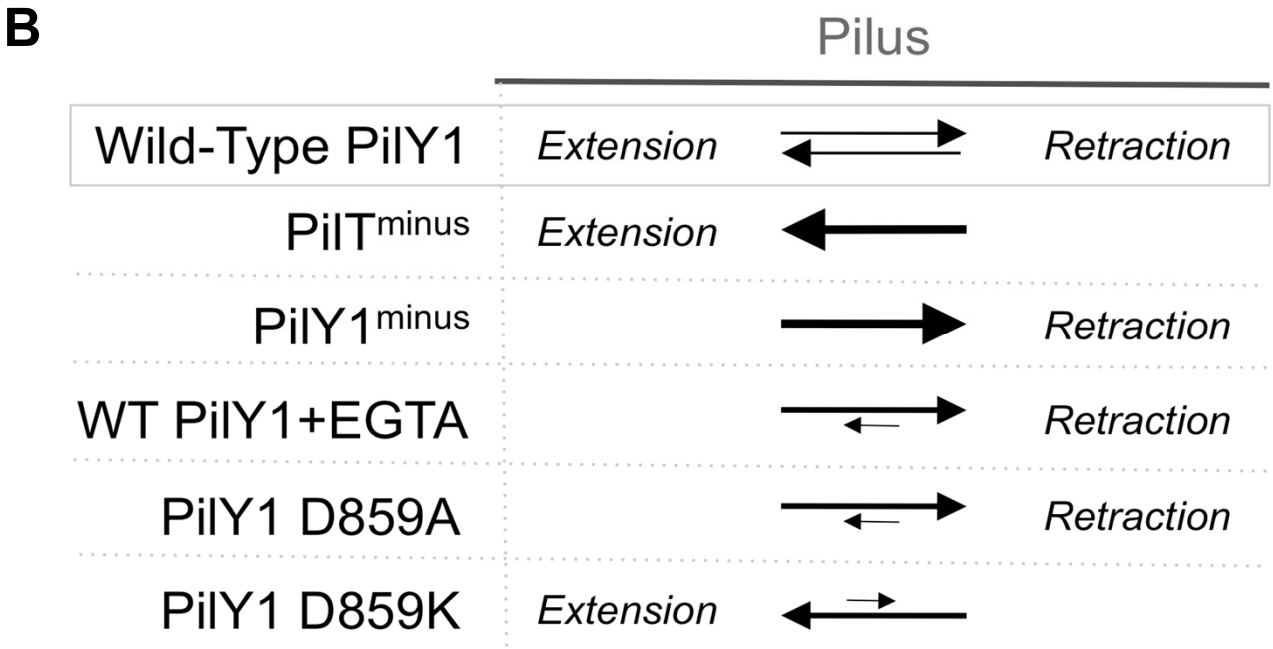
B
Pilus
Wild-Type PilY1
Extension
Retraction
PilT minus
Extension
PilY1 minus
Retraction
WT PilY1+EGTA
Retraction
PilY1 D859A
Retraction
PilY1 D859K
Extension

Supplemental Figure 2.1

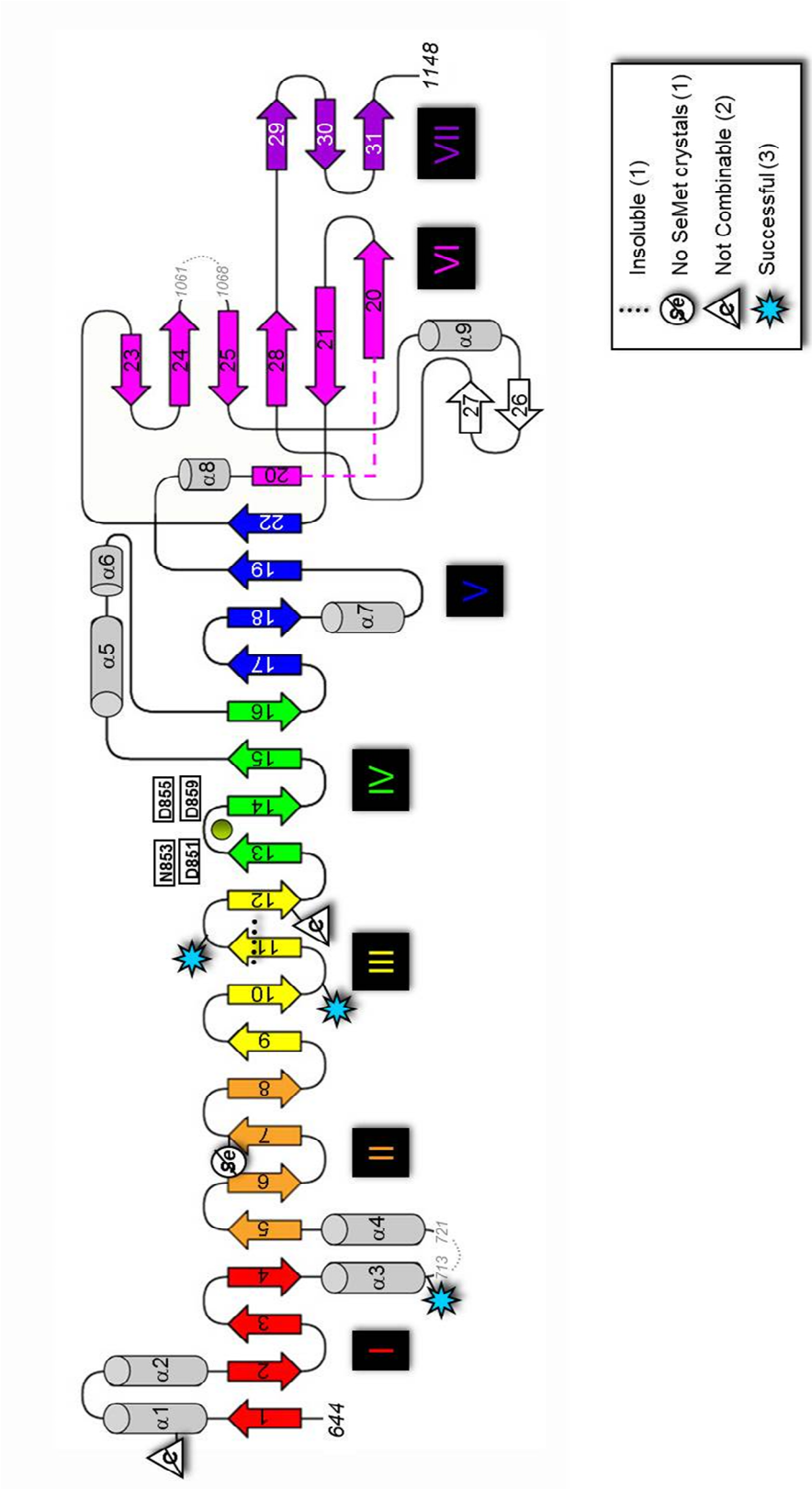

Supplemental Figure 2.2

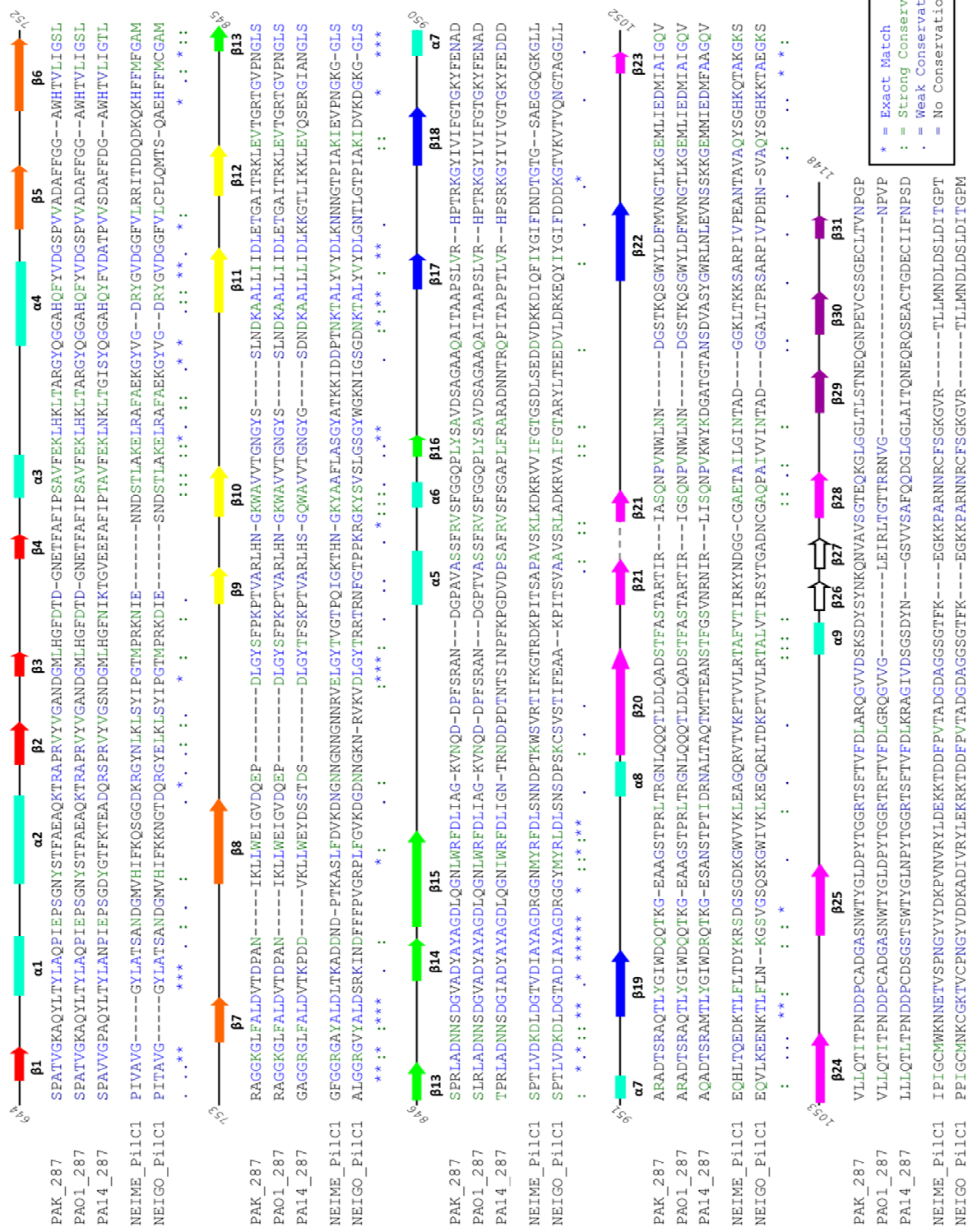

Supplemental Figure 2.3

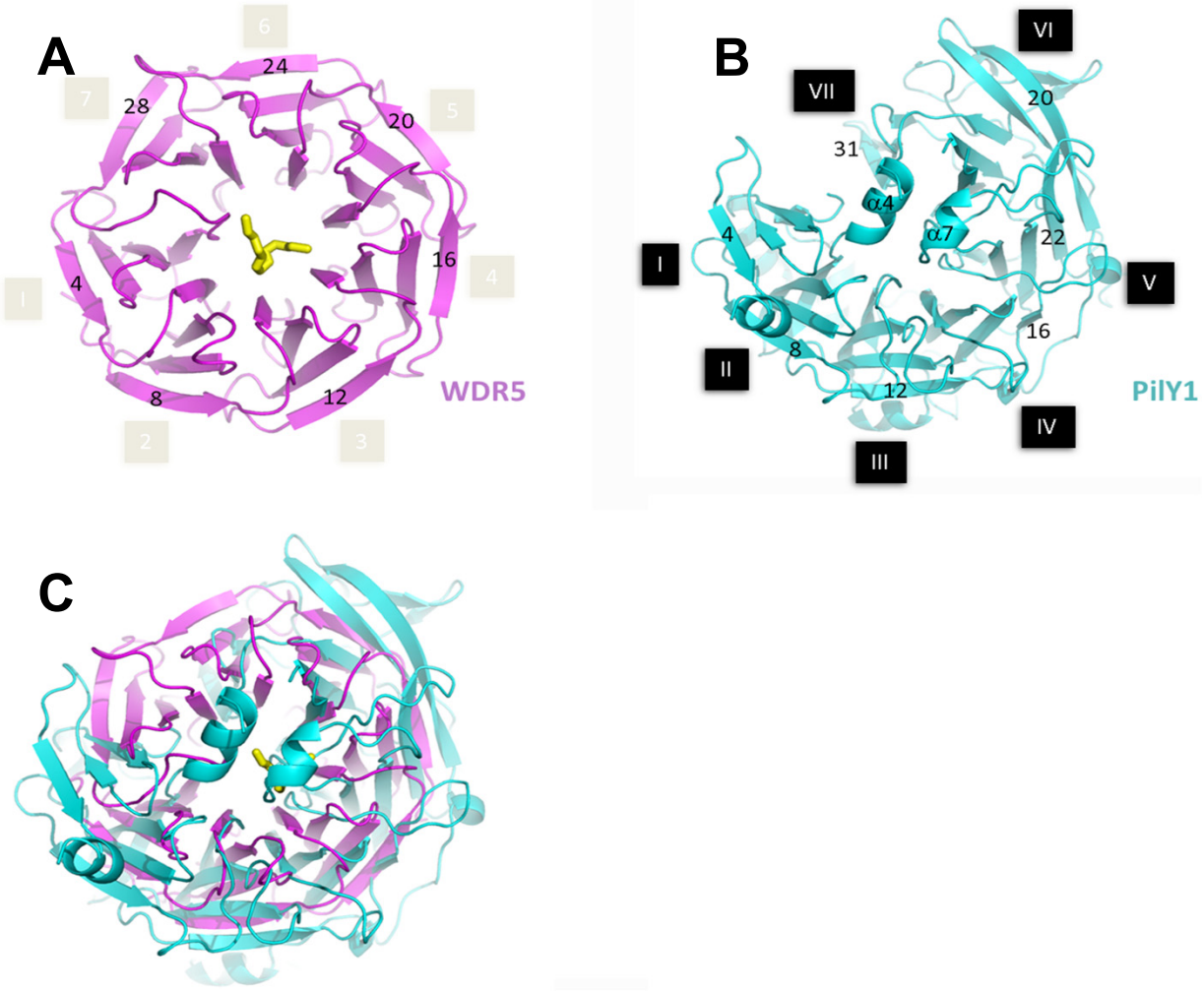

Supplemental Figure 2.4

PilY1 Structure	Distance to Ca (Å)	Distance to Ca (Å)	Calmodulin Structure
D851	2.6	2.4	D20
N853	2.1	2.6	D22
D855	2.6	2.4	D24
V857 O	2.4	2.4	T26 O
D859	2.5	2.4	E31
	2.7	2.4	
water	2.6	2.4	water

PilY1 *851*-DNNSDGVA---D-*859*
CaM *20*-DKDGDGTITTKE-*31*

Supplemental Figure 2.5

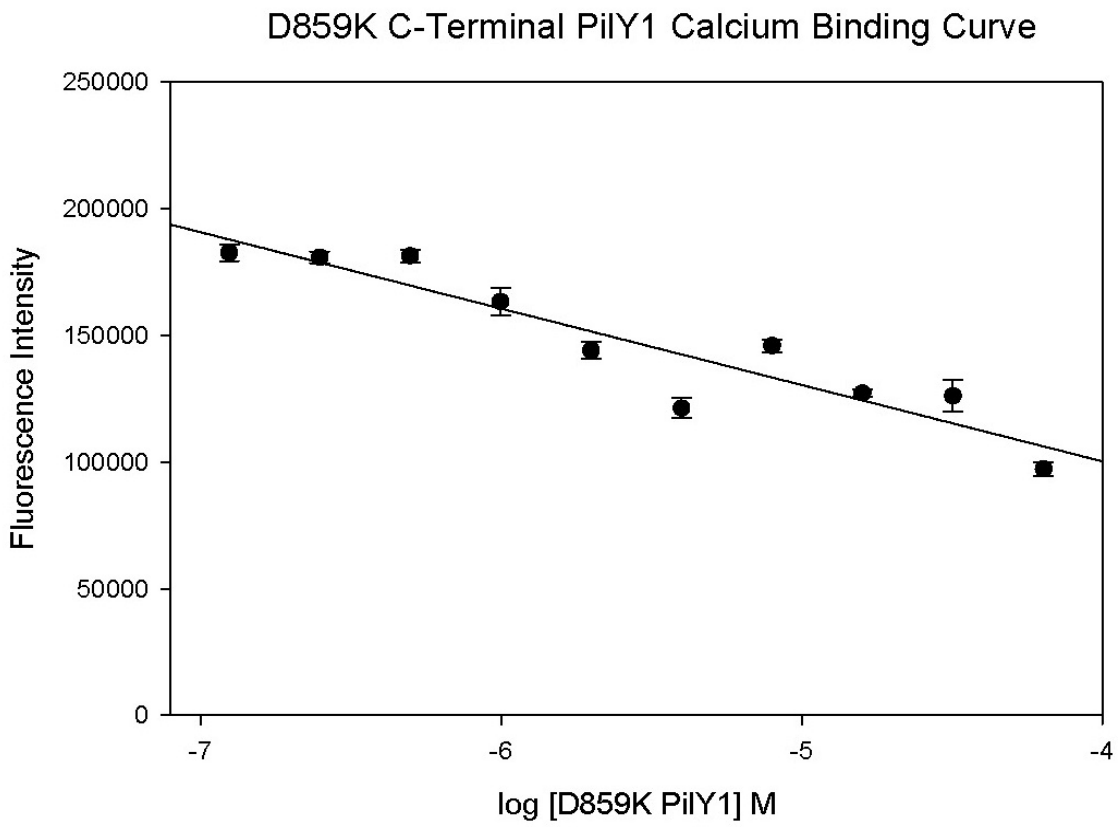

Supplemental Figure 2.6

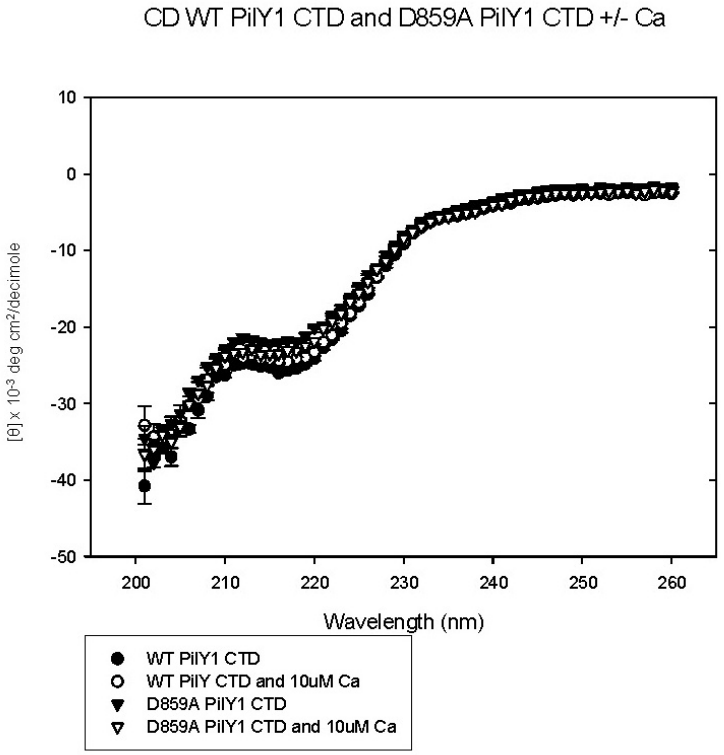

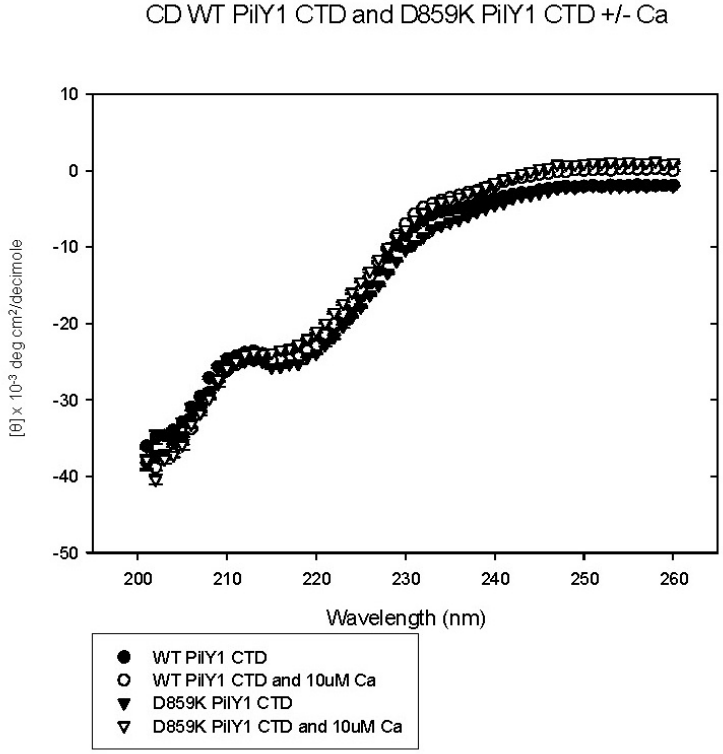

Supplemental Figure 2.7

Melting Temperature (T_m) Measured by CD for PilY1 CTD Proteins	
Protein	T_m (^oC)
WT PilY1 CTD	41.0 ± 0.3
WT PilY1 CTD plus 10μM Ca	41.9 ± 0.4
D859A PilY1 CTD plus 10μM Ca	43.5 ± 0.3
D859K PilY1 CTD plus 10μM Ca	43.4 ± 0.3

Supplemental Figure 2.8

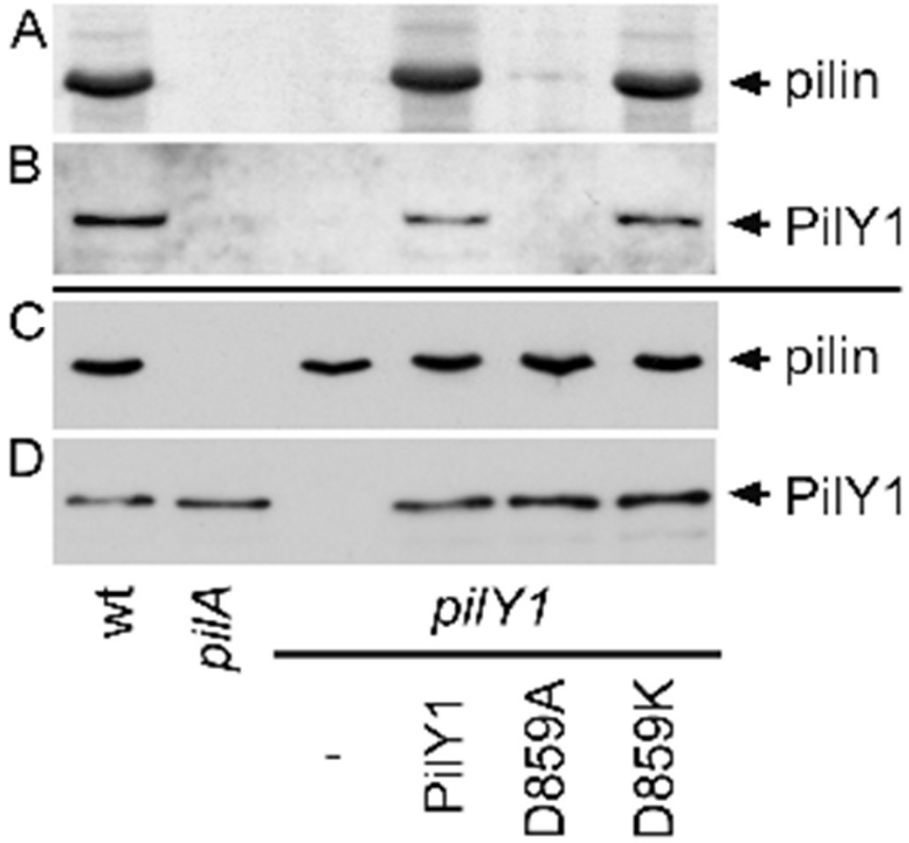

Supplemental Figure 2.9

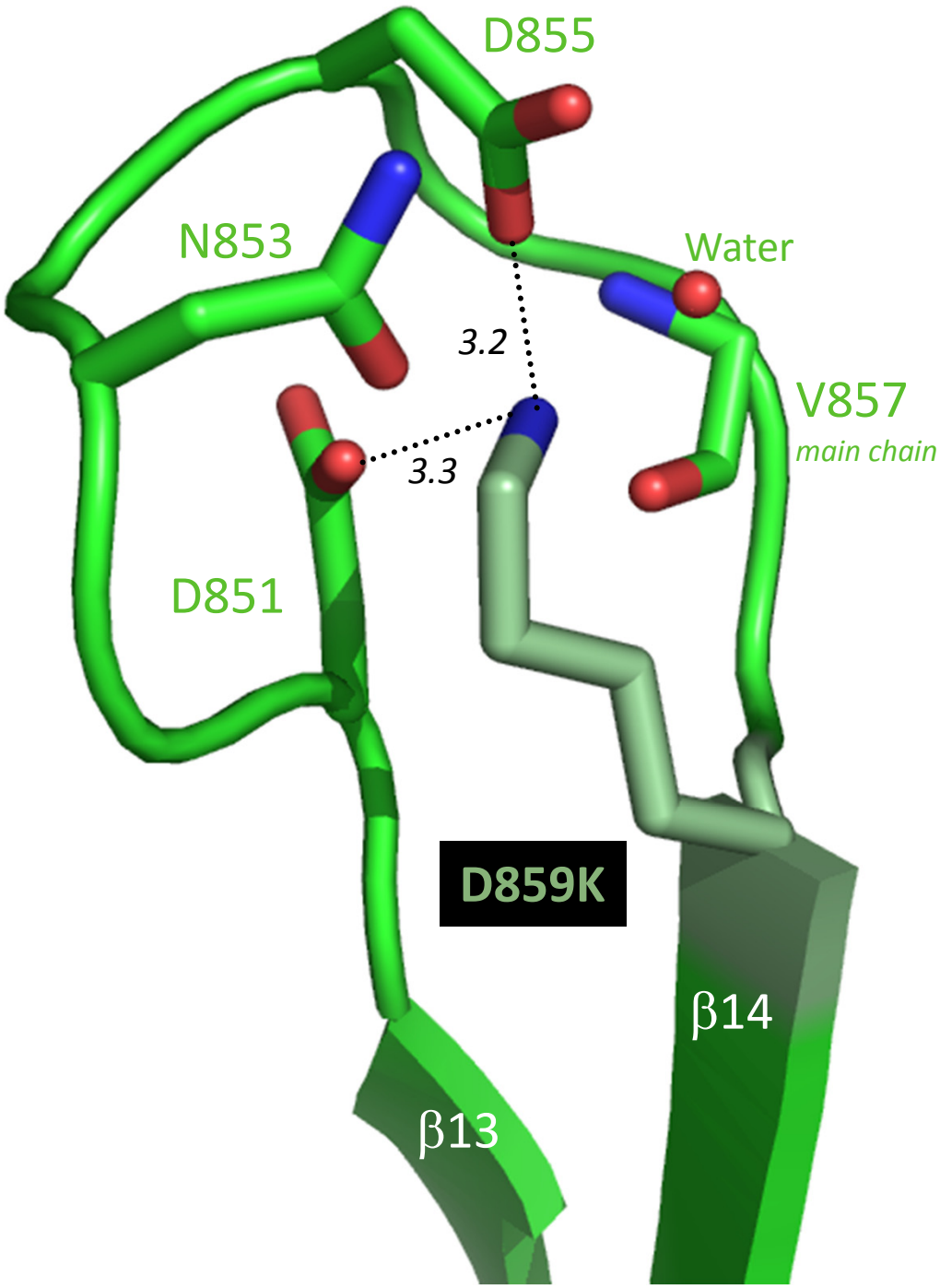

Additional Figure 2.1

A.

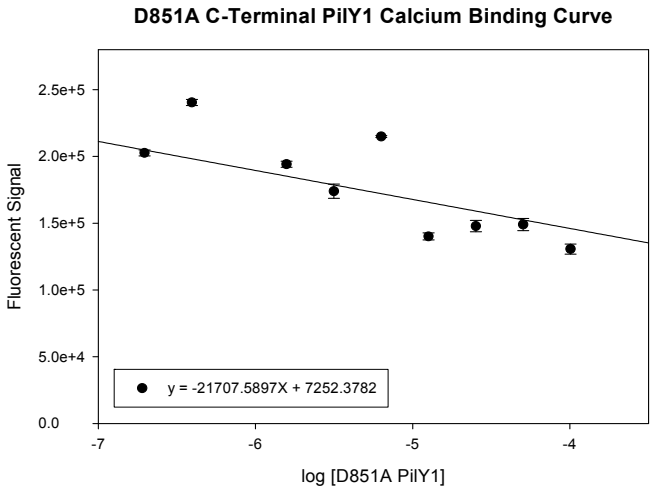

B.

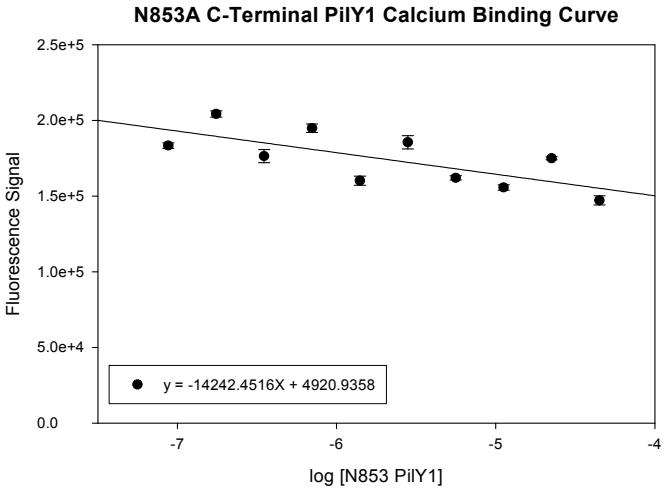

C.

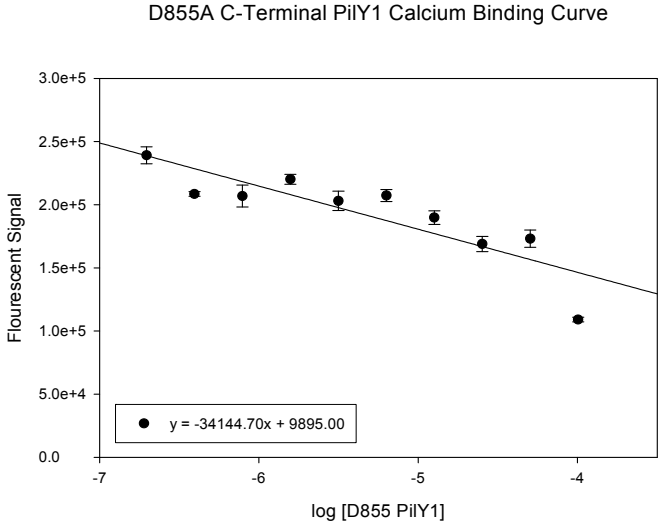

Additional Figure 2.2

A.

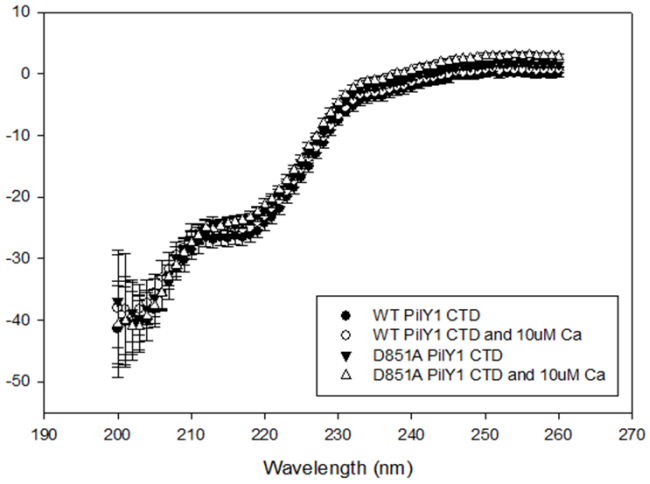

B.

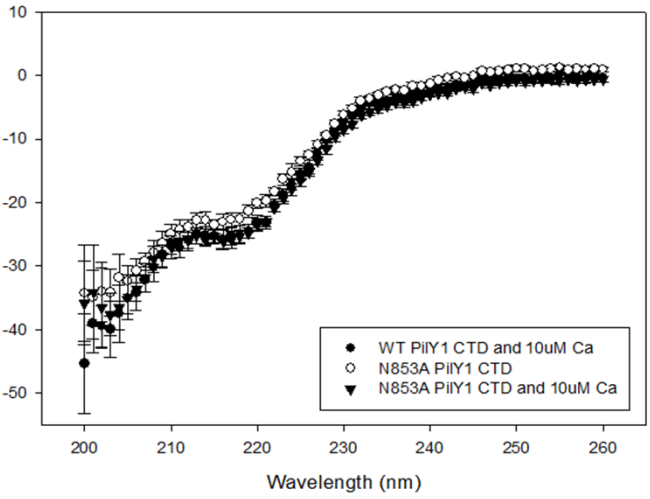

C.

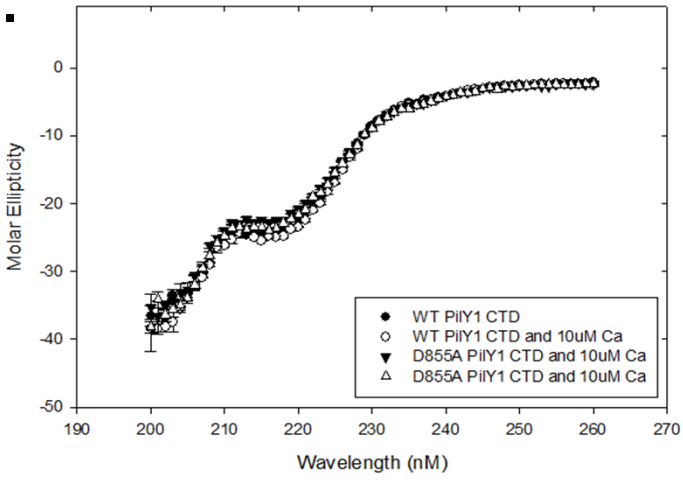

2.10 REFERENCES

1. Craig L, Li J (2008) Type IV pili: paradoxes in form and function. Curr Opin Struct Biol 18: 267-277.

2. Merz AJ, So M, Sheetz MP (2000) Pilus retraction powers bacterial twitching motility. Nature 407: 98-102.

3. Skerker JM, Berg HC (2001) Direct observation of extension and retraction of type IV pili. Proc Natl Acad Sci U S A 98: 6901-6904.

4. Wolfgang M, Lauer P, Park HS, Brossay L, Hebert J, et al. (1998) PilT mutations lead to simultaneous defects in competence for natural transformation and twitching motility in piliated Neisseria gonorrhoeae. Mol Microbiol 29: 321-330.

5. Comolli JC, Hauser AR, Waite L, Whitchurch CB, Mattick JS, et al. (1999) Pseudomonas aeruginosa gene products PilT and PilU are required for cytotoxicity in vitro and virulence in a mouse model of acute pneumonia. Infect Immun 67: 3625-3630.

6. Mattick JS (2002) Type IV pili and twitching motility. Annu Rev Microbiol 56: 289-314.

7. Tang H, Kays M, Prince A (1995) Role of Pseudomonas aeruginosa pili in acute pulmonary infection. Infect Immun 63: 1278-1285.

8. Chiang P, Sampaleanu LM, Ayers M, Pahuta M, Howell PL, et al. (2008) Functional role of conserved residues in the characteristic secretion NTPase motifs of the Pseudomonas aeruginosa type IV pilus motor proteins PilB, PilT and PilU. Microbiology 154: 114-126.

9. Jakovljevic V, Leonardy S, Hoppert M, Sogaard-Andersen L (2008) PilB and PilT are ATPases acting antagonistically in type IV pilus function in Myxococcus xanthus. J Bacteriol 190: 2411-2421.

10. Turner LR, Lara JC, Nunn DN, Lory S (1993) Mutations in the consensus ATP-binding sites of XcpR and PilB eliminate extracellular protein secretion and pilus biogenesis in Pseudomonas aeruginosa. Journal of bacteriology 175: 4962-4969.

11. Morand PC, Bille E, Morelle S, Eugene E, Beretti JL, et al. (2004) Type IV pilus retraction in pathogenic Neisseria is regulated by the PilC proteins. Embo J 23: 2009-2017.

12. Whitchurch CB, Hobbs M, Livingston SP, Krishnapillai V, Mattick JS (1991) Characterisation of a Pseudomonas aeruginosa twitching motility gene and evidence for a specialised protein export system widespread in eubacteria. Gene 101: 33-44.

13. Alm RA, Hallinan JP, Watson AA, Mattick JS (1996) Fimbrial biogenesis genes of Pseudomonas aeruginosa: pilW and pilX increase the similarity of type 4 fimbriae to the GSP protein-secretion systems and pilY1 encodes a gonococcal PilC homologue. Mol Microbiol 22: 161-173.

14. Rudel T, Scheurerpflug I, Meyer TF (1995) Neisseria PilC protein identified as type-4 pilus tip-located adhesin. Nature 373: 357-359.

15. Wolfgang M, Park HS, Hayes SF, van Putten JP, Koomey M (1998) Suppression of an absolute defect in type IV pilus biogenesis by loss-of-function mutations in pilT, a twitching motility gene in Neisseria gonorrhoeae. Proc Natl Acad Sci U S A 95: 14973-14978.

16. Kelley LA, Sternberg MJ (2009) Protein structure prediction on the Web: a case study using the Phyre server. Nat Protoc 4: 363-371.

17. Subramaniam S (1998) The Biology Workbench--a seamless database and analysis environment for the biologist. Proteins 32: 1-2.

18. Hendrickson WA, Horton JR, LeMaster DM (1990) Selenomethionyl proteins produced for analysis by multiwavelength anomalous diffraction (MAD): a vehicle for direct determination of three-dimensional structure. Embo J 9: 1665-1672.

19. Smith TF, Gaitatzes C, Saxena K, Neer EJ (1999) The WD repeat: a common architecture for diverse functions. Trends in Biochemical Sciences 24: 181-185.

20. Holm L, Kaariainen S, Rosenstrom P, Schenkel A (2008) Searching protein structure databases with DaliLite v.3. Bioinformatics 24: 2780-2781.

21. Chattopadhyaya R, Meador WE, Means AR, Quiocho FA (1992) Calmodulin structure refined at 1.7 A resolution. J Mol Biol 228: 1177-1192.

22. Weber C, Lee VD, Chazin WJ, Huang B (1994) High level expression in Escherichia coli and characterization of the EF-hand calcium-binding protein caltractin. J Biol Chem 269: 15795-15802.

23. Suzuki H, Pabst MJ, Johnston RB, Jr. (1985) Enhancement by Ca2+ or Mg2+ of catalytic activity of the superoxide-producing NADPH oxidase in membrane fractions of human neutrophils and monocytes. J Biol Chem 260: 3635-3639.

24. Korotkov KV, Gray MD, Kreger A, Turley S, Sandkvist M, et al. (2009) Calcium is essential for the major pseudopilin in the type 2 secretion system. J Biol Chem 284: 25466-25470.

25. Maier B, Potter L, So M, Long CD, Seifert HS, et al. (2002) Single pilus motor forces exceed 100 pN. Proc Natl Acad Sci U S A 99: 16012-16017.

26. Maier B, Koomey M, Sheetz MP (2004) A force-dependent switch reverses type IV pilus retraction. Proc Natl Acad Sci U S A 101: 10961-10966.

27. Farinha MA, Conway BD, Glasier LM, Ellert NW, Irvin RT, et al. (1994) Alteration of the pilin adhesin of Pseudomonas aeruginosa PAO results in normal pilus biogenesis but a loss of adherence to human pneumocyte cells and decreased virulence in mice. Infect Immun 62: 4118-4123.

28. Thomas W, Forero M, Yakovenko O, Nilsson L, Vicini P, et al. (2006) Catch-bond model derived from allostery explains force-activated bacterial adhesion. Biophys J 90: 753-764.

29. Sokurenko EV, Vogel V, Thomas WE (2008) Catch-bond mechanism of force-enhanced adhesion: counterintuitive, elusive, but ... widespread? Cell Host Microbe 4: 314-323.

30. Kirchner M, Heuer D, Meyer TF (2005) CD46-independent binding of neisserial type IV pili and the major pilus adhesin, PilC, to human epithelial cells. Infect Immun 73: 3072-3082.

31. Kallstrom H, Liszewski MK, Atkinson JP, Jonsson AB (1997) Membrane cofactor protein (MCP or CD46) is a cellular pilus receptor for pathogenic Neisseria. Mol Microbiol 25: 639-647.

32. Otwinowski Z, Minor W (1997) Processing of X-ray diffraction data collected in oscillation mode. Methods in Enzymology 276: 307-326.

33. Minor W, Cymborowski M, Otwinowski Z, Chruszcz M (2006) HKL-3000: the integration of data reduction and structure solution--from diffraction images to an initial model in minutes. Acta Crystallogr D Biol Crystallogr 62: 859-866.

34. Cowtan PEaK (2004) Coot: Model-Building Tools for Molecular Graphics. Acta Crystallographica Section D - Biological Crystallography 60: 2126-2132.

35. Brunger AT, Adams PD, Clore GM, DeLano WL, Gros P, et al. (1998) Crystallography & NMR system: A new software suite for macromolecular structure determination. Acta Crystallogr D Biol Crystallogr 54: 905-921.

CHAPTER 3

Pseudomonas aeruginosa PilY1 Binds Integrin in an RGD- and Calcium-Dependent Manner

Michael D. L. Johnson[1], Christopher K. Garrett[1], Jennifer E. Bond[2], Kimberly A. Coggan[3], Matthew C. Wolfgang[3,4], and Matthew R. Redinbo[1,3,5]*

1 Department of Biochemistry and Biophysics, University of North Carolina at Chapel Hill, Chapel Hill, North Carolina, United States of America, 2. Division of Plastic and Reconstructive Surgery, Department of Surgery, Duke University Medical Center, Durham, North Carolina, United States of America, 3. Department of Microbiology and Immunology, University of North Carolina at Chapel Hill, Chapel Hill, North Carolina, United States of America, 4. Cystic Fibrosis/Pulmonary Research and Treatment Center, University of North Carolina at Chapel Hill, Chapel Hill, North Carolina, United States of America, 5. Department of Chemistry, University of North Carolina at Chapel Hill, Chapel Hill, North Carolina, United States of America.

Pending approval from PLoSONE

Michael D. L. Johnson contributed to all figures found in this manuscript. He also contributed additional figures, not found in the text, that were not originally part of this manuscript.

3.1 SUMMARY

PilY1 is a type IV pilus (tfp)-associated protein from the opportunistic pathogen *Pseudomonas aeruginosa* that shares functional similarity with related proteins in infectious *Neisseria* and *Kingella* species. Previous data have shown that PilY1 acts as a calcium-dependent pilus biogenesis factor necessary for twitching motility with a specific calcium binding site located at amino acids 850-859 in the 1,163 residue protein. In addition to motility, PilY1 is also thought to play an important role in the adhesion of *P. aeruginosa* tfp to host epithelial cells. Here, we show that PilY1 contains an integrin binding arginine-glycine-aspartic acid (RGD) motif located at residues 619-621 in the PilY1 from the PAK strain of *P. aeruginosa*; this motif is conserved in the PilY1s from the other *P. aeruginosa* strains of known sequence. We demonstrate that purified PilY1 binds integrin *in vitro* in an RGD-dependent manner. Furthermore, we identify a second calcium binding site (amino acids 600-608) located ten residues upstream of the RGD. Eliminating calcium binding from this site using a D608A mutation abolished integrin binding; in contrast, a calcium binding mimic (D608K) preserved integrin binding. Finally, we show that the previously established PilY1 calcium binding site at 851-859 also impacts the protein's association with integrin. Taken together, these data indicate that PilY1 binds to integrin in an RGD- and calcium-dependent manner *in vitro*. As such, *P. aeruginosa* may employ these interactions to mediate host epithelial cell binding *in vivo*.

3.2 INTRODUCTION

Pseudomonas aeruginosa is a Gram-negative, opportunistic pathogen prevalent in immunocompromised patients, burn victims, and people with cystic fibrosis. *P. aeruginosa* can infect any part of the body, but typically targets the respiratory tissues, skin abrasions, and the urinary tract [1]. This pathogen accounted for ~11% of the hospital-acquired infections reported in the U.S in 2002 [2,3], and has also been shown to infect other mammalian species, as well as insects and plants [4,5]. *P. aeruginosa* uses a range of methods to resist the effects of antibiotics, including efflux pumps, adaptive mutagenesis, and protective biofilms [6,7,8]. As such, *Pseudomonas aeruginosa* presents a significant challenge to human health.

P. aeruginosa employs type IV pili (tfp) for twitching motility and infection. The precise mechanism of host cell attachment has remained unclear, although evidence exists that loops of the major pilus structural subunit PilA exposed at the tip of the pilus fiber bind to gangliosides GM1 and GM2 [9]. In contrast, some data indicate that several *P. aeruginosa* clinical isolates, as well as laboratory strains, do not employ GM1 and GM2 during host cell attachment [10,11]. As such, it has been proposed that other factors on the *Pseudomonas* tfp are involved in binding to target cells [12,13].

Recent studies have suggested that host cell integrin proteins play a role in *Pseudomonas* infection. Anti-integrin antibodies were shown to reduce *P. aeruginosa* attachment to host cells [14]. Specifically, antibodies to the αVβ5 integrin and αVβ3 integrin were effective at disrupting *P. aeruginosa* binding to host cells, with antibodies to αVβ5 integrin having the most pronounced effect [14]. Integrins are present on the epithelial cell surface of tissues infected by *P. aeruginosa*; indeed, αVβ5 integrin is highly expressed in the lungs [15]. The presence of *P. aeruginosa* has also been shown to increase the expression of integrin subunits αV, α5, and β1 in epithelial cells [16,17]. Integrins and integrin-like proteins are found widely in animals, plants, and insects, all targets of *P. aeruginosa*

infection [18]. Integrins are responsible for a range of cellular processes, including cell-cell attachment, cellular signaling, and angiogenesis [19]. The most common ligands for integrins are proteins that contain an arginine-glycine-aspartic acid (RGD) sequence, although other short peptides have also been found to mediate integrin-protein interactions (*e.g.*, leucine-aspartic acid-valine or LDV).

The PilC class of proteins in *Neisseria gonorrhoeae*, *Neisseria meningitidis*, and *Kingella kingae* have been characterized as tfp biogenesis factors and as proteins involved in adhering to target tissues [20,21,22]. Generally, PilC N-terminal regions are associated with adhesion domains, while the C-terminal domains regulate tfp biogenesis. *P. aeruginosa* PilY1 shares sequence homology with the C-terminal regions of the PilCs proteins, and this domain in PilY1 has been shown to be a calcium-mediated tfp biogenesis factor (Supplemental Table 3.1) [23]. Indeed, PilY1 is required for both twitching and swarming motility and adhesion to host cells [23,24,25]. The N-terminal domains of PilY1 and the PilCs share low sequence similarity, which might be expected if these domains are involved in target cell-specific activities. The target tissues of the *Neisseria* strains and *Kingella* are likely to be distinct from those targeted by *P. aeruginosa*. Here, we focus on putative regions of PilY1 involved in host cell attachment and we show that purified PilY1 binds to integrins in an RGD- and calcium-dependent manner *in vitro*.

3.3 RESULTS

3.3.1 PilY1 Contains a Conserved Integrin Binding Motif

Given the importance of the tfp associated PilY1 protein in host tissue adherence and the ability of antibodies targeting the RGD binding domains of αVβ5 and αVβ3 integrins to reduce interactions between *P. aeruginosa* and host cells, we examined PilY1's sequence to locate possible integrin binding motifs (RGD or LDV) [14,25]. PilY1 was found to contain a conserved RGD motif (Figure 3.1A, B). No other type IV pilus proteins or known surface

proteins in *P. aeruginosa* contained an RGD or other putative integrin binding sequence [26,27]. One RGD motif was found in each of the PilY1s of *P. aeruginosa* strains of known sequence. For example, in the PilY1 from *P. aeruginosa strain K* (PAK), the RGD is located at residues 619-621; however, in the PAO1 *P. aeruginosa* strain PilY1, the RGD is at 657-659 (Figure 3.1B). Based on these observations, we hypothesized that PilY1 binds to integrin in an RGD-dependent manner.

3.3.2 PilY1 Binds Integrin in an RGD-Dependent Manner

To test the hypothesis that PilY1's RGD motif mediates contacts with integrins, we created a purified form of PilY1 that starts at amino acid 532 and extends to C-terminus of the protein (residue 1163) and tested the ability of 532-1163 PilY1 to bind to αVβ5 using an integrin binding assay. Titration of increasing concentrations of 532-1163 PilY1 showed that mid-nanomolar concentrations of this purified protein binds specifically to αVβ5 (Figure 3.2A). Next, we employed synthetic RGDS and GRADSP peptides to compete with PilY1 binding to αVβ5 integrin. We found that that the RGDS peptide significantly reduced PilY1 binding to αVβ5 integrin ($p<0.10$), while the GRADSP control peptide had no effect (Figure 3.2B). Because previous reports also indicated that PAK binding to host cells can be reduced by using an anti-αVβ3 integrin antibody, we also examined PilY1 binding to αVβ3. We found that purified 532-1163 PilY1 binds to αVβ3 integrin in an RGD-dependent manner, although with a lower apparent affinity than observed with αVβ5 integrin (Figure 3.2C) [14]. We therefore used αVβ5 as the primary integrin of this study. Finally, we tested two RGD mutants of 532-1163 PilY1, D621A (RGA) and Δ619-621 (ΔRGD), for their ability to bind to αVβ5 integrin *in vitro*. Deleting the RGD residues or mutating the aspartic acid residue at position 621 to alanine significantly reduced the association of PilY1 with αVβ5 integrin (Figure 3.2D). Importantly, these mutations did not alter the global secondary structure or the melting temperature of purified 532-1163 PilY1 (Figure 3.2E, Supplemental Table 3.2).

Taken together, these data indicate that *P. aeruginosa* PilY1 binds to integrins *in vitro* in an RGD-dependent manner.

3.3.3 PilY1 has a Second Calcium Binding Site

A second potential calcium binding site was noted in the sequence of *P. aeruginosa* PilY1 between residues 600 and 608, which is in close proximity to the RGD motif (619-621) described above (Figure 3.1A). Recall that a calcium binding site at residues 851-859 in PilY1 was shown in previous work to be critical to tfp biogenesis and twitching motility [23]. The sequences of the two calcium binding sites are closely related (Figure 3.3A), and the putative 600-608 site is conserved in PilY1s of known sequence (Figure 3.1B). Indeed, in the *P. aeruginosa* PilY1 sequences examined, this second potential calcium binding site was always found 8-10 residues upstream of the conserved RGD motif (Figure 3.1B). To test the 600-608 site's ability to bind calcium in purified 532-1163 PilY1, we eliminated the previously published calcium binding site using either a D859A or D859K mutation [23], and measured calcium binding. The D859A and D859K forms of 532-1163 PilY1 exhibited K_d's for calcium binding of 412 and 266 nM, respectively (Figure 3.3B). Thus, the 600-608 site appeared to bind calcium. We next created corresponding mutations (D608A, D608K) in the 532-1163 PilY1 construct, and found that these variants bound calcium with 2.3-2.4 μM affinity, similar to that reported previously for the 851-859 PilY1 site (Figure 3.3C) [23]. Finally, we created a D608A/D859A double-mutant form of 532-1163 PilY1 and compared its calcium binding to wild-type 532-1163 PilY1. We found that the double-mutant exhibited only non-specific calcium binding, while wild-type 532-1163 PilY1 associated with calcium with a 700 nM affinity (Figure 3.3D). The variant forms of 532-1163 PilY1 examined *in vitro* in these studies maintained an overall wild-type fold and melting temperature, indicating that these changes did not alter the stability of the proteins (Supplemental Figure 3.1A-E; Supplemental Table 3.2). To further confirm that our 532-1163 construct of PilY1 contained

two calcium binding sites, we used isothermal titration calorimetry. Indeed, with wild type PilY1, we observed a binding site N value of 1.61 indicating that there were two calcium binding sites (Additional Figure 3.1A). However, when we used the D608A mutation, we observed an N value of .946 indicating that one calcium binding site remained (Additional Figure 3.1B).

Finally, mutations in the RGD sequence adjacent to the 600-608 site did not alter calcium binding by these purified forms of 532-1163 PilY1 (Supplemental Figure 3.2A). Taken together, these observations support the conclusion that purified 532-1163 PilY1 contains two calcium binding sites, the previously characterized one at 851-859 and a newly identified one at 600-608 that is ten residues N-terminal to PilY1's RGD motif.

3.3.4 PilY1 Binds Integrin in a Calcium Dependent Manner

Because the 600-608 calcium binding site in PilY1 is close in sequence to the RGD motif, we next sought to examine whether calcium binding impacted the association between 532-1163 PilY1 and integrin. We found that D859A, D859K, and D608K mutant forms of 532-1163 PilY1 exhibit wild-type or only slightly reduced binding to αVβ5; in contrast, the D608A mutant of purified PilY1 was significantly inhibited in its binding to this integrin (Figure 3.4A). Thus, eliminating the charged D608 side chain proximal to the RGD motif impacted PilY1's interaction with αVβ5. We then examined double mutant forms of 532-1163 PilY1 and found that the two calcium binding sites interacted functionally with respect to integrin binding (Figure 3.4B). For example, the D608A/D859A variant of 532-1163 PilY1 shows nearly wild-type levels of αVβ5 binding (Figure 3.4B); recall that the D608A form of PilY1 exhibited little integrin binding *in vitro* (Figure 3.4A). Thus, D859A appears to act as a dominant positive over the D608A mutation. Similarly, the D608K/D859A PilY1 shows increased integrin binding relatively to wild-type (Figure 3.4B). In contrast, adding the D859K mutation to either D608A or D608K in PilY1 had no impact on

integrin binding relative to the 608 mutants alone (Figure 3.4B). Taken together, these data suggest that both calcium binding sites in PilY1 impact integrin binding *in vitro*. Note that the single- and double-mutants considered here did not bind calcium (Supplemental Figure 3.2B), and exhibited wild-type CD spectra and melting temperatures (Supplemental Figure 3.1A-E, Supplemental Table 3.2), indicating that the overall structure of these purified proteins was not altered.

The crystal structure of the C-terminal domain of PilY1 does not contain the 600-621 region; as such, it is not known whether the two calcium binding sites are in close structural proximity. However, it is possible that they interact physically, and that the functional impact of one upon the other is via the swapping of an aspartic acid from one site (*e.g.,* D851 or D855) into the other site (600-608). To test this hypothesis, we created two triple mutant forms of 532-1163 PilY1, D608A/D851A/D859A and D608A/D855A/D859A, and one quadruple mutant form, D608A/D851A/D855A/D859A. Both triple mutants and the quadruple mutant show wild type levels of binding (Supplemental Figure 3.3). Thus, we conclude that an interaction between the two calcium binding sites in PilY1 is not primarily associated with aspartic acids in one site helping to coordinate calcium in the other site. Additionally, to test whether the D608A/D859A mutation created an unknown secondary integrin binding site, consequently, leading to wild type binding, we mutated the RGD motif aspartic acid to alanine and tested integrin binding. Similarly to the D621A (RGA) single mutation, a mutation to the RGD motif in the D608A/D859A severely reduced binding (Additional Figure 3.2). However, taken together, these data indicated that a functional interaction between the two calcium binding sites in PilY1 impacts the ability of the RGD motif in this protein to bind to integrins *in vitro*.

3.4 DISCUSSION

P. aeruginosa is an established and increasingly antibiotic resistant pathogen that predominantly infects patients with compromised defense mechanisms. Toward this end, we sought to understand how *P. aeruginosa* binds to host cells, a necessary first step in infection. We focused on the type IV pilus-associated protein PilY1, which is involved in bacterial motility and is related in sequence to factors in other bacteria required for host cell binding. We show that PilY1 contains an integrin binding RGD motif that mediates contact between purified PilY1 and integrin proteins *in vitro*. Additionally, we show that PilY1 contains two calcium binding sites and that each site impacts the protein's ability to associate with integrin (Figure 3.4C). Both the calcium binding sites and the RGD motif are conserved in all PilY1 sequences from *P. aeruginosa* strains reported to date (Figure 3.1B).

It was not anticipated that the PilY1 calcium binding sites, particularly the one distal (851-859) to the RGD sequence, would impact integrin binding. In fact, D859A can be seen as a dominant positive with respect to integrin binding (Figure 3.4C). For example, while the D608A mutant form of PilY1 is significantly reduced in integrin binding, combining it with D859A to create a D608A/D859A double-mutant produces a protein that is capable of binding to integrin (Figure 3.4B). Further, a D608K/D859A double-mutant exhibits higher integrin binding than either single mutant or the wild-type protein (Figure 3.4B). In spite of these *in vitro* data, however, the molecular contacts involved in these effects are not clear, in part because the region between residues 600 and 643 in PilY1 has not been elucidated structurally. It is tempting to speculate that a physical association exists between the two calcium binding sites that impacts RGD presentation for integrin binding. Such speculation is supported by the data outlined here, but remains speculation until future studies to examine the structure of this region of PilY1 are complete.

One hypothesis on how calcium binding plays a role in RGD-mediated binding is based on a putative calcium binding site in the αVβ3 structure (Additional Figure 3.3A).

αVβ3 integrin has eight known calcium/manganese binding sites identified by the crystal structures and one putative consensus aspartic acid - x - aspartic acid - x - aspartic acid - glycine (DxDxDG) calcium binding site in a loop region of the αV subunit [28,29]. This putative DxDxDG site is located 3.0 Å away from the phenylalanine-tyrosine-tryptophan (FYW) residues in αV subunit that are used to mediate RGD substrate binding (Additional Figure 3.3B) [29,30]. The αVβ3 structure shows the binding to an RGD peptide, not to a protein substrate, and thus is small enough to fit in the groove between the FYW and the putative consensus calcium binding domain. Although this putative consensus calcium binding site in integrin does not have metal bound in either structure, the site could still be playing a role in the local area dynamics if the protein substrate either contributes charge or eases the steric burden that this unbound calcium binding site could be imposing to prevent binding.

When the 532-1163 construct of PilY1 is modeled using I-TASSER, and the top generated .pdb is aligned with the RGD of the integrin structure, the unbound 600-608 PilY1 calcium binding site is 6.0 Å from the putative consensus DxDxDG calcium binding domain in the αV subunit (Additional Figure 3.3C) [29,30,31,32]. It is unlikely that the 600-608 site in PilY1 is donating calcium to the new putative integrin calcium binding site as when PilY1 has no calcium to donate (i.e. the D608K or D608K/D859A mutations), integrin binding still occurs. However, there are four aspartic acids in the 600-608 calcium binding site that could lead to dynamic repelling motion from each other without the metal present. Thus, it is enticing to speculate that the bound 600-608 PilY1 calcium binding site could be easing a steric hindrance otherwise caused by the unbound 600-608 calcium binding site of PilY1 in respect to PilY1 binding to integrin or at the very least providing room for the putative integrin calcium binding site to move away from the FYW to facilitate binding.

Also of note, the aspartic acid in the RGD peptide in the αVβ3 structure is 2.7 Å away from the manganese in the structure (Additional Figure 3.3C) [29]. This measurement

is consistent with previous distance measurements of calcium bond lengths to the chelating residue. [23]. As measured in this study, there is a high binding affinity for PilY1 to αVβ5 (Figure 3.2A). This high affinity could be contributed by the proximity of the aspartic acid in the substrate RGD as it helps to coordinate the metal. This observation could also explain why the aspartic acid being mutated to alanine causes a significant reduction in overall substrate:integrin binding but in the literature, a mutation to glutamic acid yields binding at wild type levels (Figure 3.2B) [33].

Integrins and integrin-like proteins are present in plants, insects, and the animal kingdom. They are up-regulated during cellular stress and recovery [34,35,36]; indeed, the presence of *P. aeruginosa* itself up-regulates the expression levels of the αV integrin subunit [16]. In addition, integrins are established targets for bacterial pathogens. *Bordetella pertussis* protein pertactin, containing two RGD motifs, has been shown to adhere to Chinese hamster ovary cells in an RGD-dependent manner [37,38]. Pertactin is a member of the auto-transporter family, many of which contain RGD motifs mediating adherence to integrins [39]. However, there are conflicting data on whether auto-transporter RGDs are relevant in mouse models of infection [40]. Still, other *in vitro* and *in vivo* studies have shown that the following bacteria bind integrin in an RGD-dependent manner: *Pyrenophora tritici-repentis* (a wheat pathogen), *Mycoplasma conjunctivae* (sheep pathogen), and the mammalian pathogens *Klebsiella pneumoniae* and *Helicobacter pylori* [41,42,43,44]. Integrins are also known targets for viral pathogens. Proteins in hepatitis C virus, coxsackievirus A9, human herpes virus 8, Epstein-Barr virus, and adenovirus bind to host cells in an RGD dependent manner [45,46,47,48,49]. In summary, integrins have the potential to be important target proteins for PilY1-mediated attachment of *P. aeruginosa*.

Interestingly, calcium has also been shown to play a vital role in host RGD substrate:integrin binding events (Table 3.1). Calcium binding helps in the folding of the blood clotting factor fibrinogen, and it protects against cleavage and degradation of the

hemostasis protein von Wildenbrand factor and the elastin scaffold protein fibrillin (Table 3.1) [50,51,52,53]. Some integrin substrates, such as thrombospondin, use cooperative calcium binding at multiple sites to facilitate integrin binding, while calcium increases adhesion in tenascin, vitronectin, and osteopontin to target integrins (Table 3.1) [54,55,56,57,58] . Thus, there is precedent for calcium regulation of RGD-mediated contacts with integrins.

PilY1 is an established pilus biogenesis factor [23] and has been implicated in *P. aeruginosa* adhesion to host cells by functional studies [25] and due to its homology to the PilCs adhesin proteins of *Neisseria* [59]. Here, we provide evidence that PilY1 serves as an adhesin that binds to integrins in an RGD-dependent manner. Furthermore, we show that integrin binding is regulated by two distinct calcium binding sites in PilY1. These data provide an *in vitro* advance in our understanding of PilY1 structure and function. It will be of interest to determine in future studies whether PilY1 and integrins are involved in *P. aeruginosa* attachment to host cells *in vivo*.

3.5 METHODS

PilY1 constructs and protein purification

Site-directed mutagenesis was performed to produce D608A, D608K, D621A, Δ619-621, D859A, D859K, D608A/D859A, D608A/D859K, D608K/D859A, D608K/D859K, D608A/D621A/D859A, D608A/D851A/D859A, D608A/D855A/D859A, and D608A/D851A/D855A/D859A mutants in a pDONR vector containing PilY1. Amino acids 532-1163 were cloned out of the pDONR vector for entry into pMCSG7 for protein expression. Vectors were transformed into BL21 Gold (Stratagene) on ampicillin plates overnight and a single colony was used to inoculate a 100mL LB flask overnight containing 50μM/mL ampicillin. Cell cultures were centrifuged at 3000 x g and the supernatant was discarded. The resultant pellet was used to inoculate a 1.5 L shaker flask of Terrific Broth

with 50µL of antifoam (Sigma-Aldrich) and 50µg/mL ampicillin. Cells were grown at 37 ^{o}C until OD_{600} reached 0.6-0.8. Temperature was reduced to 18 ^{o}C and protein expression was induced with 0.5 mM IPTG. Cells were grown overnight and harvested by centrifugation 6000 x g at for 15 minutes at 4 ^{o}C, and pellets were stored at -80 ^{o}C.

Cells pellets were thawed using buffer consisting of 25 mM HEPES pH 7.5, 150 mM NaCl, 10 mM imidazole, 5% glycerol, DNase and protease inhibitor tablets (Roche). Cells were sonicated and cell lysate was separated into soluble and insoluble fractions using high-speed centrifugation. The soluble fraction was filtered then nickel purified, buffer exchanged, and separated using an S200 gel filtration column on an ÄKTAxpress™ (GE HealthCare). If necessary, protein and storage buffers were chelated by Chelex-100 to remove bound calcium (Bio-Rad Laboratories). Purified proteins were concentrated to ~100 µM, frozen, and stored at -80 ^{o}C.

Integrin binding assay

Costar EIA/RIA stripwell high binding plates were coated with either 2 µg of purified αVβ5 integrin or 2 µg of purified αVβ3 integrin (Millipore) for the experimental wells, or the molar equivalent of BSA for the control wells, at 100 µL in 100 mM sodium bicarbonate buffer pH 9.6 (Abcam) for 16 hours at 4^{o}C. Plates were washed 1 x with 300 µL of PBS. Wells were then blocked with 1% BSA in PBS for one hour at room temperature. Plates were washed 1 x with PBS and 100µg/mL of PilY1 (Wild Type, D621A, Δ619-621, D608A, D608K, D859A, D859K, D608A/D859A, D608A/D859K, D608K/D859A, D608K/D859K, D608A/D621A/D859A, D608A/D851A/D859A, D608A/D855A/D859A, or D608A/D851A/D855A/D859A) in binding buffer (50 mM Tris pH 7.8, 100 mM NaCl 2mM $CaCl_2$, 1 mM $MgCl_2$, 1 mM $MnCl_2$, and 0.1% Triton) was added to each well including the BSA control wells for 6 hours at 16 ^{o}C with or without RGDS peptide (inhibitor), GRADSP peptide (control), or no peptide. Plates were then washed 3 x with PBST (0.1% Tween-20)

and 3 x with PBS before adding rabbit αPilY1 polyclonal antibody 1:500 per well in 1% BSA in PBS overnight for 16 hours at 4^{o}C. Plates were then washed 3 times with PBST and 3 x with PBS before adding the Alexa fluor 488 f(ab')$_2$ fragment goat anti-rabbit (Invitrogen) 1:5000 in 1% BSA in PBS protected from light at room temperature for 1 hour. Plates were then washed 3 x with PBST, 3 x with PBS, then dried. Plates were read on a PHERAstar (BMG LabTech). The experimental and control well averages and standard error of the mean (SEM) were calculated, and then the control average was subtracted from the experimental values and the errors were compounded using the equation$\sqrt{((experimental\ SEM)^2 + (control\ SEM)^2)}$.

Calcium binding assay

A binding curve for Oregon Green® 488 BAPTA-5N, hexapotassium salt (Invitrogen) in 25 mM HEPES pH 7.5, 150mM NaCl, and 5% glycerol was measured on a PHERAstar (BMGLabtech) at 488 nm. With 20 μM Oregon Green and 2 μM CaCl2, PilY1 constructs were serial diluted 1.5-3 fold from ~100 μM to ~1 nM to obtain an EC50 which was then used to calculate the respective PilY1 K_d for calcium as described previously[23].

Isothermal titration calorimetry

Chelated 532-1163 wild type or D608A PilY1 protein was brought to 20 μM and $CaCl_2$ was brought to 300 μM in chelated 25 mM HEPES pH 7.5, 150mM NaCl, and 5% glycerol. Machine temperature was set to 23^{o}C and after the first injection, there were 19 equal injections. ITC measurements were carried out on an Auto-iTC$_{200}$ (MicroCal/GE Healthcare).

Circular dichroism and thermal denaturation

Protein samples were buffer exchanged into chelated 10 mM $K_xH_xPO_4$ 50 mM NaF pH 7.7 buffer and brought to 5μM with or without the addition of $CaCl_2$. A wavelength scan from 200-260 λ was performed on a Circular Dichroism Spectrometer 62 DS (Aviv) at 16 ^oC with a 10 second averaging time. Melting temperatures were measures at λ 214 from 3 ^oC to 95 ^oC at one degree increments with a 10 second averaging time.

Structure images

All images of PilY1 and αVβ5 were created using The PyMOL Molecular Graphics System, Version 1.2r3pre, Schrödinger, LLC.

3.6 CREDITS

Supported by an NIH Predoctoral Fellowship (MJ) and by NIH grant AI78924 (MR).

3.7 FIGURE LEGENDS

Figure 3.1 *P. aeruginosa* PilY1 strains contain conserved integrin binding residues RGD and conserved putative calcium binding site. (a) A bar representation of PilY1. The consensus c-terminal pilus biogenesis domain is in blue and the green represents the n-terminal addition to the previously examined construct. Calcium binding motifs are highlighted in yellow and the RGD is highlighted in orange. (b) Five varying strains of *P. aeruginosa* PilY1 were aligned using the biology workbench server [26,27]. Blue residues and an "*" corresponds to identical residues throughout the 5 strains, green residues and a ":" correspond to highly conserved residues, and navy residues and a "." corresponds to mildly conserved residues (e.g. alanine and leucine). Reference numbers are for PAK_287 PilY1 (the strain used in this study).

Figure 3.2 Purified PilY1 binds to integrin in an RGD dependent manner. (a) PilY1 was titrated onto a solid phase binding assay keeping the concentration of αVβ5 integrin constant at 2μg/mL. The curve was fit to the ligand binding, one site saturation equation f = Bmax*abs(x)/(K_d + abs(x)) with an r^2 = 0 .98. The K_d was calculated at 164nM ±38. (b-d) Wild type PilY1 was established as a reference point and the value all measurements were compared to. (b) RGDS inhibitor peptide or GRADSP control peptide were added in 2, 100, and 250 fold molar excess to PilY1. "*" corresponds to p<.1 compared to PilY1 binding to αVβ5 integrin. (c) PilY1 was added with or without 50 fold molar excess of the inhibitor RGDS peptide to 2μg/mL of αVβ3 integrin. "**" corresponds to p<.02 compared to PilY1 binding to αVβ3 integrin. (d) ΔRGD (Δ619-621) or D621A mutations of PilY1 were added to 2μg/mL of αVβ5 integrin. "***" corresponds to p<.01 compared to PilY1 binding to αVβ5 integrin. (e) Molar ellipticity values were calculated for the respective wavelength scans and compared.

Figure 3.3 PilY1 has two functional calcium binding sites. (a) An alignment of the two calcium binding sites in PilY1 was done as performed for figure 2. Calcium coordinating residues are underlined. (b) D608A, D859A, (c) wild type and D608A/D859A, and (d) D608K were modeled to a one-site competition (D608A, D859A, D608K, and wild type), or linear line (D608A/D859A). Error represents standard error of the mean.

Figure 3.4. Calcium binding sites play a role in PilY1's ability binds to integrin. (a) D608A, D608K, D859A, D859K (b) D608A/D859A, D608A/D859K, D608K/D859A, and D608K/D859K mutations of PilY1 were added to αVβ5 integrin as seen in figure 2B. "*" corresponds to $p<.01$ compared to wild type PilY1 binding to αVβ5 integrin and "**" corresponds to $p<.1$ as compared to wild type PilY1 binding to αVβ5 integrin. (c) represents the model of the calcium binding effects on PilY1 binding to integrin. D to A mutations represent mutations in the final aspartic acid of the calcium binding site.

Table 3.1. Calcium effects on RGD binding proteins

3.8 SUPPLEMENTAL FIGURE LEGENDS

Supplemental Table 3.1 *P. aeruginosa* PilY1 is homologous to PilC family of bacterial adhesin and pilus biogenesis proteins. PilY1 was individually aligned to *K. Kingae* (Kk) PilC1 and PilC2, *N. gonorrhea* (Ng) PilC1 and PilC2, and *N. meningitidis* (Nm) PilC1 and PilC2 using http://blast.ncbi.nlm.nih.gov/. C-terminal homology indicates residues that are similar (e.g. leucine and isoleucine) while c-terminal identity corresponds to identical residues. Strains used for each protein are as follows: ACF19883 for *Kingella kingae* PilC1,

ACF19886.1 for *Kingella kingae* PilC2, O05924_NEIME for *Neisseria meningitidis* PilC1 O05925_NEIME for *Neisseria meningitidis* PilC2, O05923_NEIGO for *Neisseria gonorrhea* PilC1, and Q51019_NEIGO for *Neisseria gonorrhea* PilC2.

Supplemental Figure 3.1A-E Circular dichroism for calcium binding mutants. Molar ellipticity values were calculated for the respective wavelength scans and compared.

Supplemental Figure 3.2 RGD and calcium binding site mutations binding curves. (a) ΔRGD and R619A were modeled to one-site binding. (b) Double calcium binding site mutants D608A/D859K, D608K/D859A, and D608K/D859K. Error represents standard error of the mean

Supplemental Table 3.2 Melting temperatures (T_M) for mutations of PilY1. Proteins were scanned at 214 nm after an initial CD scan. T_Ms were calculated using the standard three parameter sigmoidal fit.

Supplemental Figure 3.3 Mutational effects on PilY1:Integrin binding. As in Figure 2b-d, Wild type PilY1 was established as a reference point and D608A/D851A/D859A, D608A/D855A/D859A, and D608A/D851A/D855A/D859A were measured for integrin binding.

3.9 ADDITIONAL FIGURE LEGENDS

Additional Figure 3.1 Isothermal titration calorimetry PilY1. (a) Wild type or (b) D608A PilY1 in the 532-1163. The top panel of each section consists of µcal/sec and the bottom panel is Kcal/Mole of Injectant.

Additional Figure 3.2 Mutational effects on PilY1:Integrin binding. As in Figure 2b-d, Wild type PilY1 was established as a reference point and D608A/D621A/D859A was measured for integrin binding.

Additional Figure 3.3 The structure of αVβ3 integrin bound to RGD peptide PDB ID 1L5G. (a) The αV subunit is highlighted in red, the β5 subunit is highlighted in green, and the RGD peptide is highlighted in blue. (b) Same coloring as in A. with the DxDxDG calcium binding domain in the αV subunit in magenta and the phenylalanine-tyrosine-tryptophan in cyan. All measurements are in angstroms unless otherwise noted. (c) Same coloring as in A and B with the PilY1 modled RGD in purple and the PilY1 modeled 600-608 calcium binding loop in hot pink. Mn is labeled in green. The αV residue D150 is italicized.

Figure 3.1

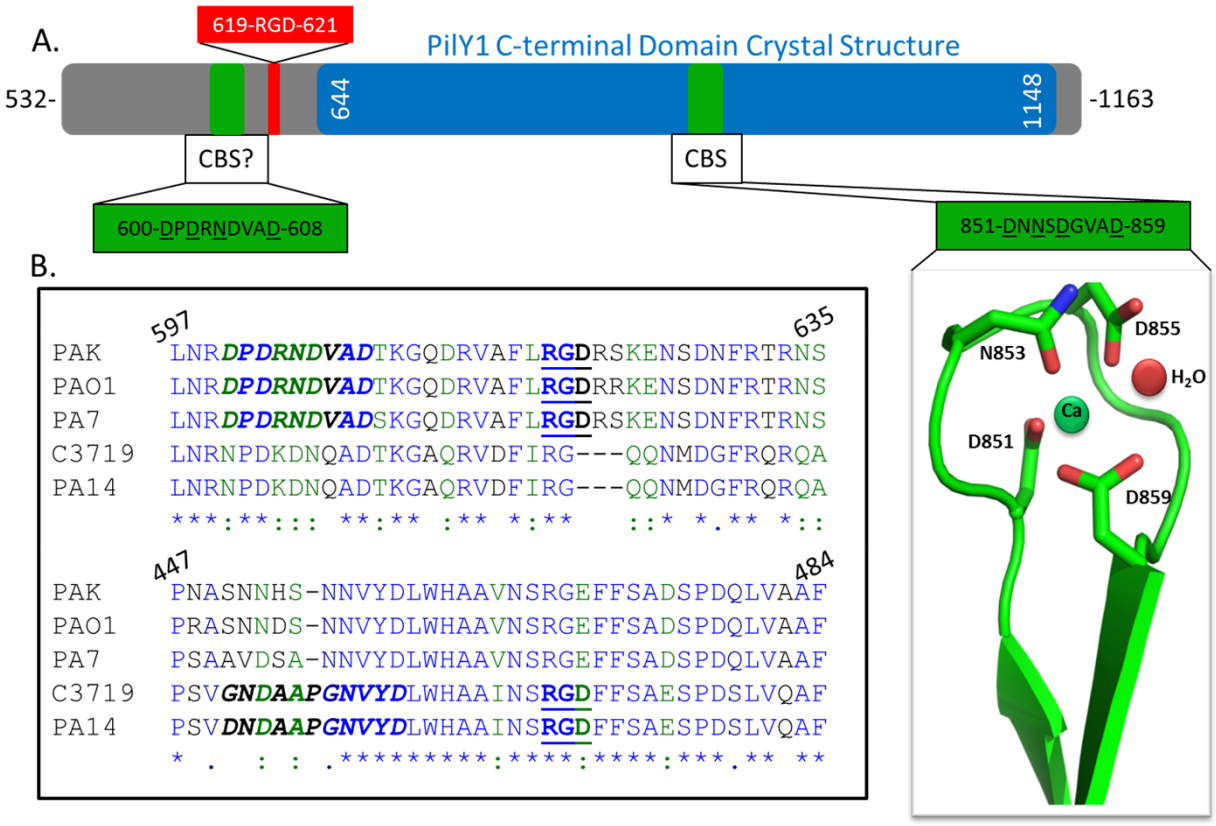
A.
619-RGD-621
PilY1 C-terminal Domain Crystal Structure
532-
644
1148
-1163
CBS?
CBS
600-DPDRNDVAD-608
851-DNNSDGVAD-859
B.
597
635
PAK LNRDPDRNDVADTKGQDRVAFLRGDRSKENSDNFRTRNS
PAO1 LNRDPDRNDVADTKGQDRVAFLRGDRRKENSDNFRTRNS
PA7 LNRDPDRNDVADSKGQDRVAFLRGDRSKENSDNFRTRNS
C3719 LNRNPDKDNQADTKGAQRVDFIRG---QQNMDGFRQRQA
PA14 LNRNPDKDNQADTKGAQRVDFIRG---QQNMDGFRQRQA
447
484
PAK PNASNNHS-NNVYDLWHAAVNSRGEFFSADSPDQLVAAF
PAO1 PRASNNDS-NNVYDLWHAAVNSRGEFFSADSPDQLVAAF
PA7 PSAAVDSA-NNVYDLWHAAVNSRGEFFSADSPDQLVAAF
C3719 PSVGNDAAPGNVYDLWHAAINSRGDFFSAESPDSLVQAF
PA14 PSVDNDAAPGNVYDLWHAAINSRGDFFSAESPDSLVQAF
N853
D855
H2O
Ca
D851
D859

Figure 3.2

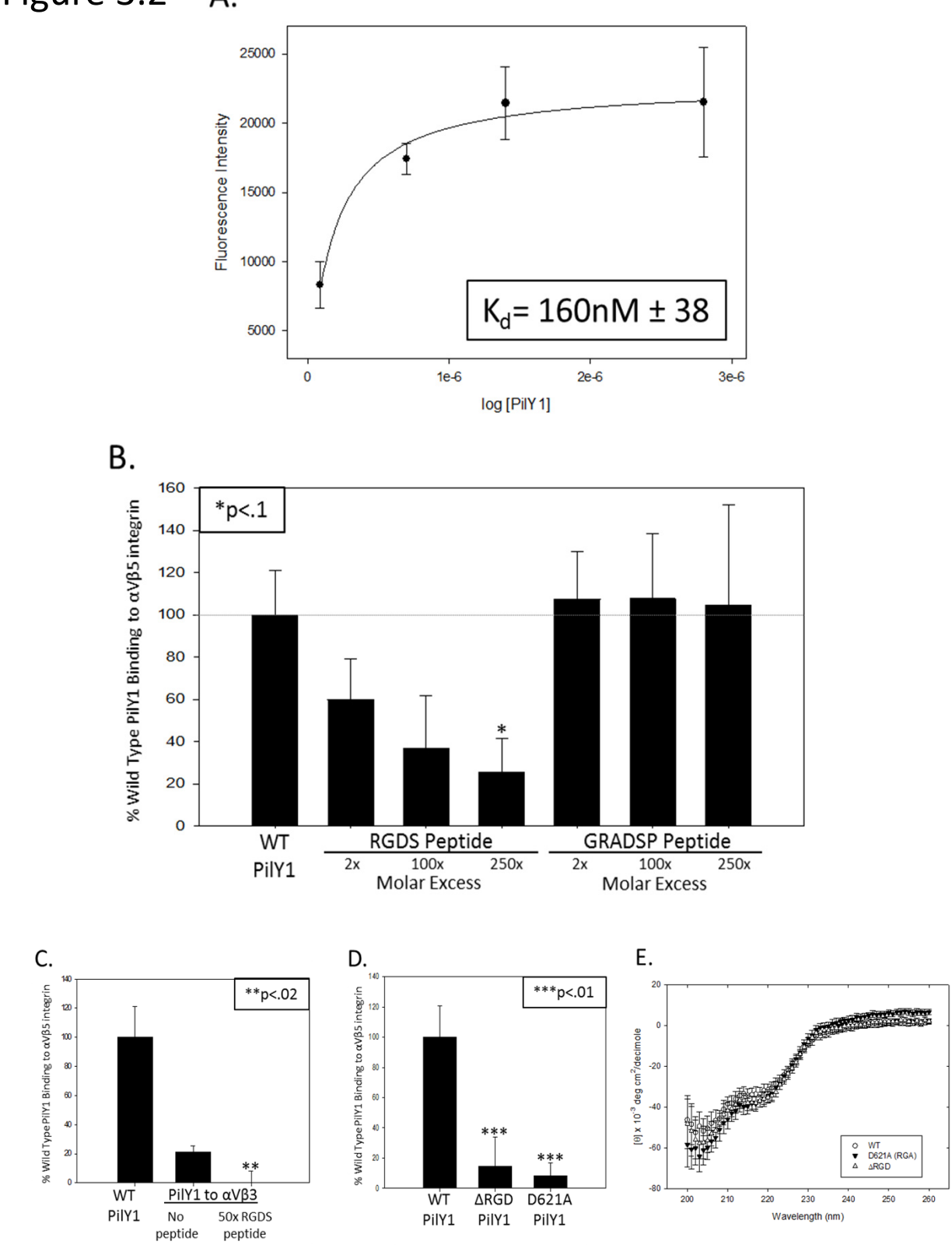
A.
Fluorescence Intensity
25000
20000
15000
10000
5000
0
1e-6
2e-6
3e-6
log [PilY1]
K_d= 160nM ± 38
B.
% Wild Type PilY1 Binding to αVβ5 integrin
*p<.1
160
140
120
100
80
60
40
20
0
*
WT PilY1
RGDS Peptide
2x
100x
250x
Molar Excess
GRADSP Peptide
2x
100x
250x
Molar Excess
C.
% Wild Type PilY1 Binding to αVβ5 integrin
**p<.02
**
WT PilY1
PilY1 to αVβ3
No peptide
50x RGDS peptide
D.
% Wild Type PilY1 Binding to αVβ5 integrin
***p<.01
***
***
WT PilY1
ΔRGD PilY1
D621A PilY1
E.
[θ] x 10^-3 deg cm^2/decimole
20
0
-20
-40
-60
-80
200
210
220
230
240
250
260
Wavelength (nm)
WT
D621A (RGA)
ΔRGD

Figure 3.3

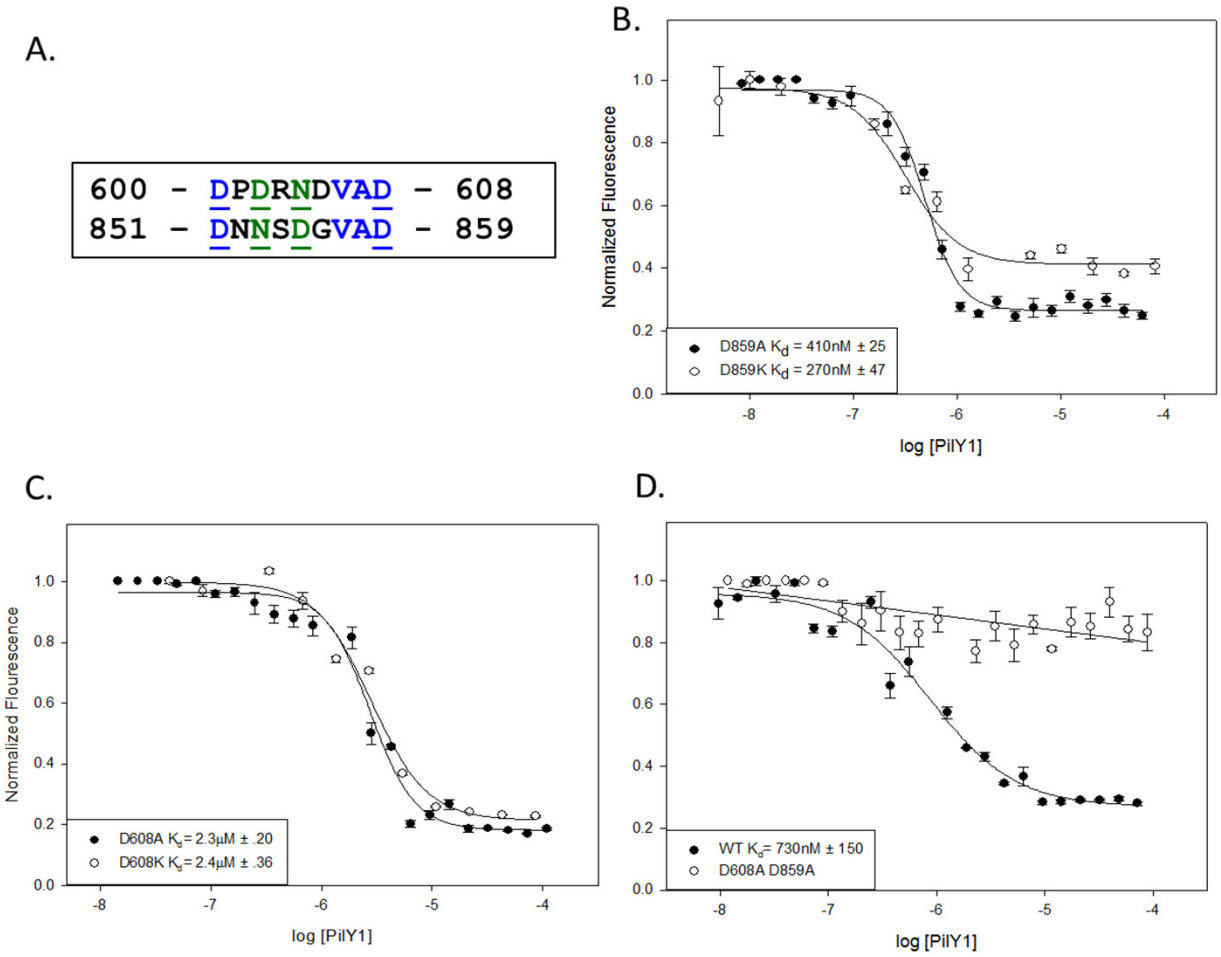
A.
600 - DPDRNDVAD - 608
851 - DNNSDGVAD - 859
B.
Normalized Fluorescence
D859A Kd = 410nM ± 25
D859K Kd = 270nM ± 47
log [PilY1]
C.
Normalized Flourescence
D608A Kd = 2.3µM ± .20
D608K Kd = 2.4µM ± .36
log [PilY1]
D.
WT Kd = 730nM ± 150
D608A D859A
log [PilY1]

Figure 3.4

A.

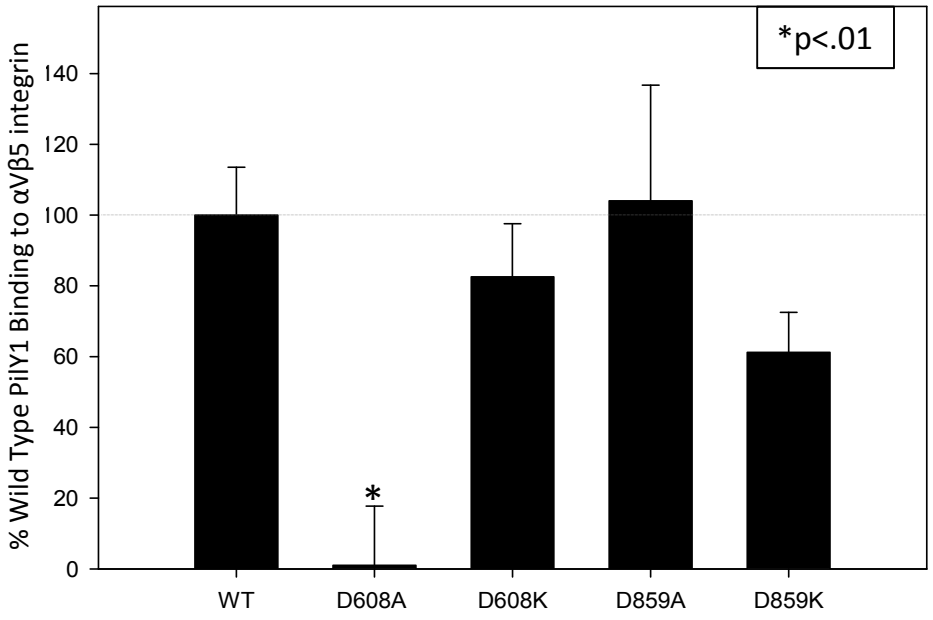
*p<.01
% Wild Type PilY1 Binding to αVβ5 integrin
0
20
40
60
80
100
120
140
*
WT
D608A
D608K
D859A
D859K

B.

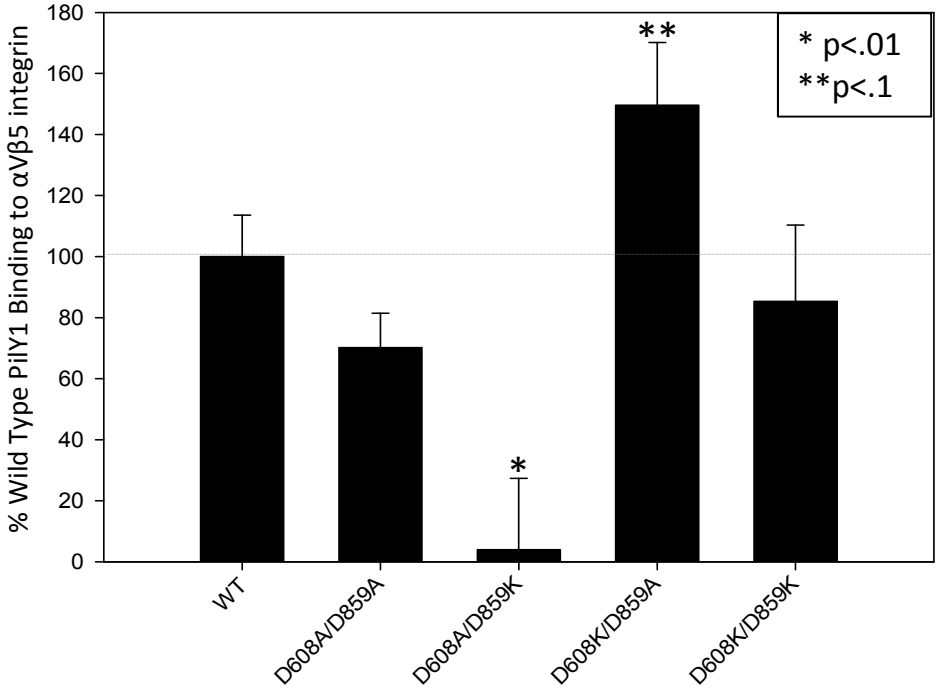
* p<.01
**p<.1
% Wild Type PilY1 Binding to αVβ5 integrin
0
20
40
60
80
100
120
140
160
180
**
*
WT
D608A/D859A
D608A/D859K
D608K/D859A
D608K/D859K

Figure 3.4 contd.

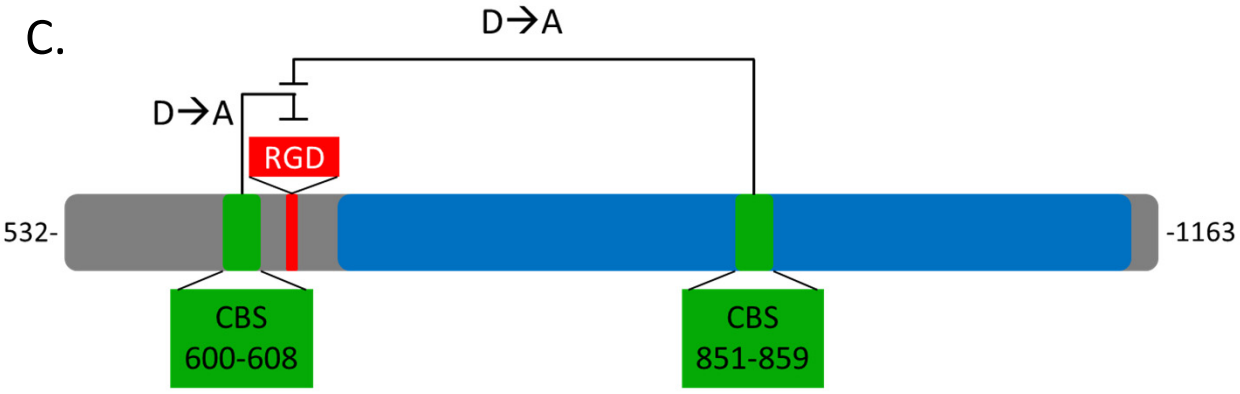

Table 3.1

Protein	Binds calcium	Known calcium binding effects	RGD binding integrin target(s) [17]
vWF [52]	unknown	impedes unfolding/protect from cleavage	αVβ3 and αIIbβ3
Thrombospondin [53]	yes	needed for integrin binding	αVβ3 and αIIbβ3
Fibronectin [49]	yes	unknown	αVβ3, αIIbβ3, αVβ6, αVβ1, α5β1, and α8β1
Osteopontin [55, 56]	yes	increased cell adhesion	αVβ3, αVβ5, αVβ6, αVβ1, α5β1, and α8β1
Fibrinogen [50, 52]	yes	affects folding	αVβ3 and αIIbβ3
Fibrillin [51]	yes	helps avoid degradation	αVβ3
Tenascin [57]	unknown	activates cell-adhesion	αVβ3 and α8β1
Vitronectin [54]	unknown	increased cell adhesion	αVβ3, αVβ5, α8β1 and αIIbβ3

Supplemental Table 3.1

Protein (residues used)	PilY1 alignment residues	C-terminal homology	C-terminal identity
Kingella kingae PilC1 (620-1129)	621-1066	40%	25%
Kingella kingae PilC2 (890-1455)	532-1120	39%	24%
Neisseria meningitidis PilC1 (470-910)	595-1085	40%	27%
Neisseria meningitidis PilC2 (486-833)	595-947	45%	30%
Neisseria gonorrhea PilC1 (506-852)	622-998	42%	28%
Neisseria gonorrhea PilC2 (508-859)	622-1000	44%	30%

Supplemental Table 3.2

PilY1 Protein	T_M (°C)
Wild Type	45.8 ± .2
Chelated Wild Type	44.8 ± .2
D621A (RGA)	44.9 ± .3
Δ619-621	46.0 ± .3
D608A	44.9 ± .1
Chelated D608A	45.1 ± .2
D608K	45.5 ± .3
Chelated D608K	46.0 ± .4
D859A	46.1 ± .2
Chelated D859A	45.3 ± .4
D859K	41.8 ± .3
Chelated D859K	43.2 ± .2
D608A/D859A	44.4 ± .4
Chelated D608A/D859A	45.0 ± .3

Supplemental Figure 3.1

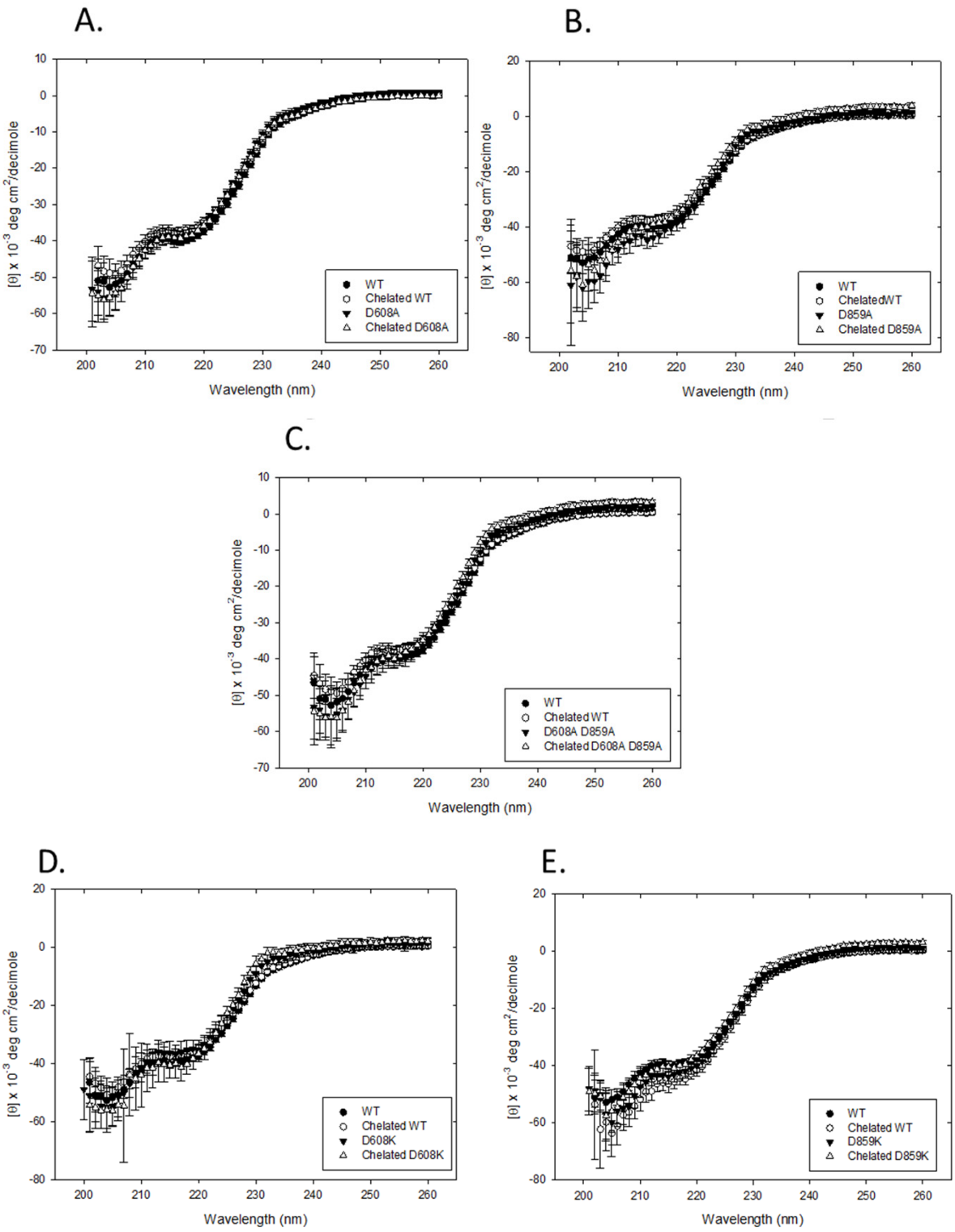

Supplemental Figure 3.2

A.

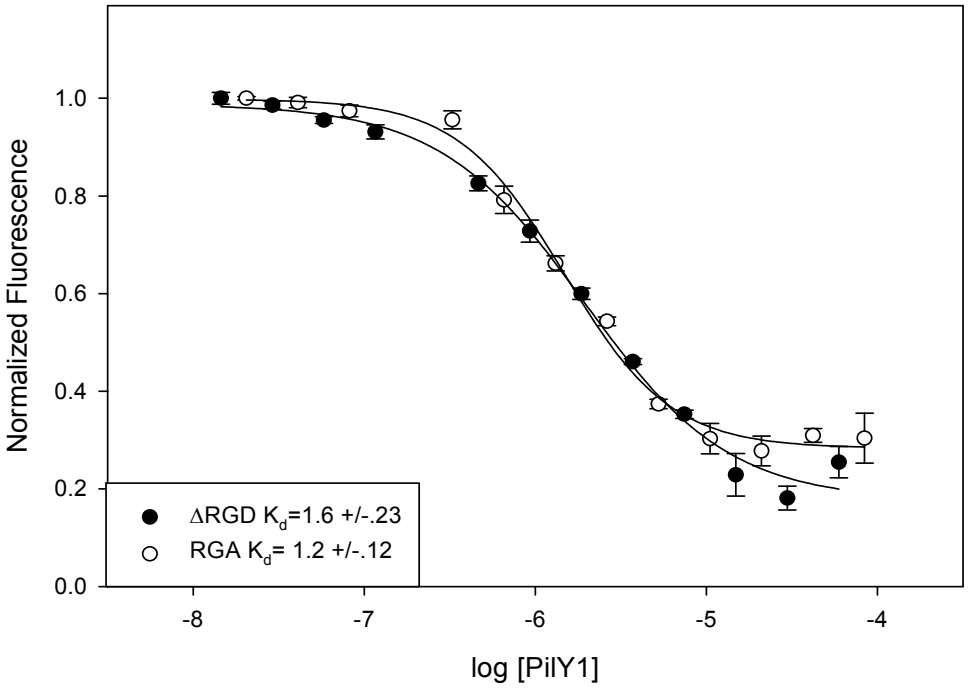

B.

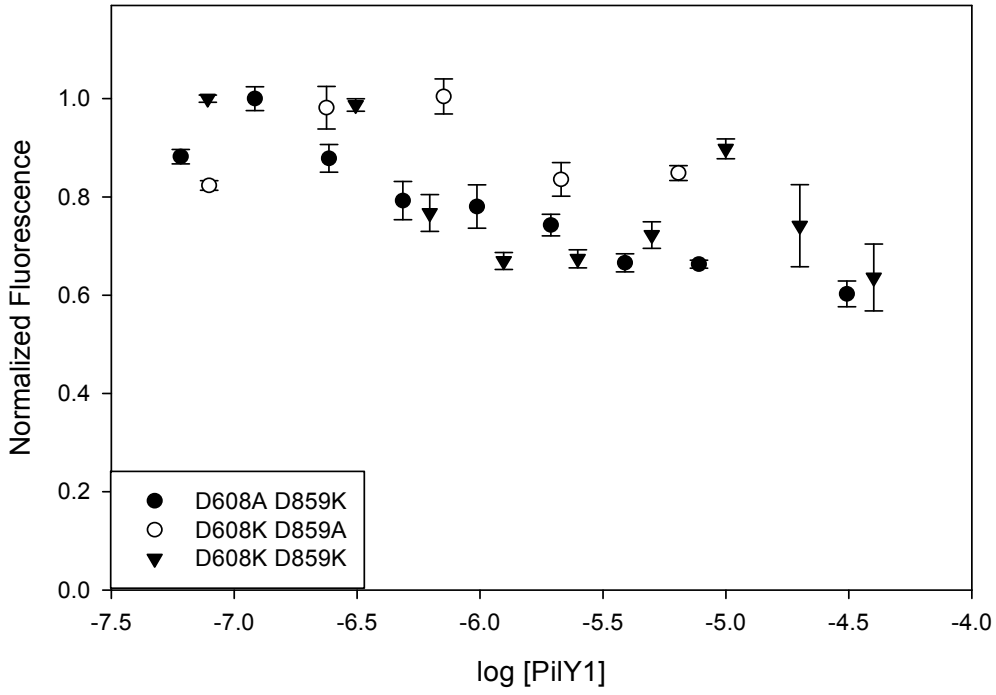

Supplemental Figure 3.3

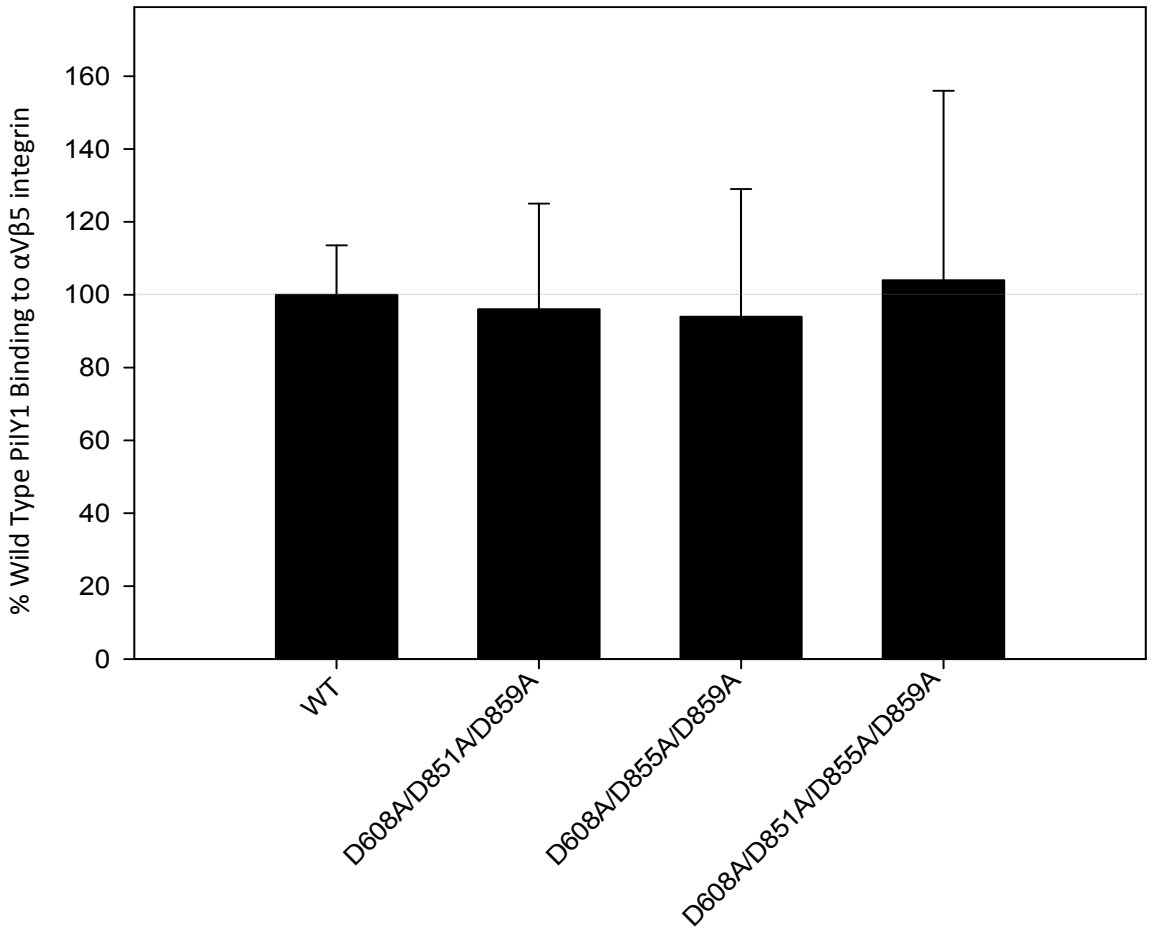

Additional Figure 3.1A

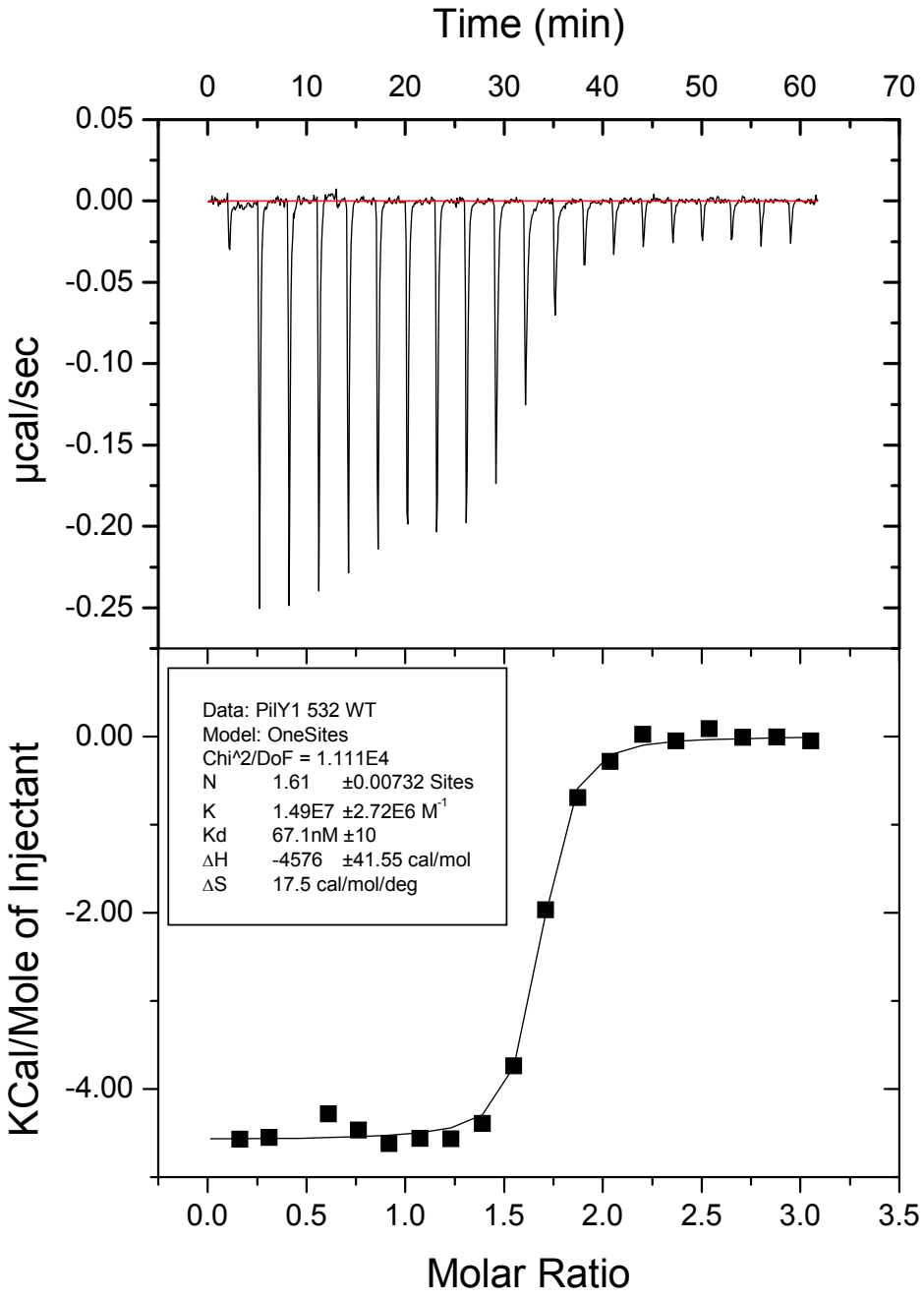

Additional Figure 3.1B

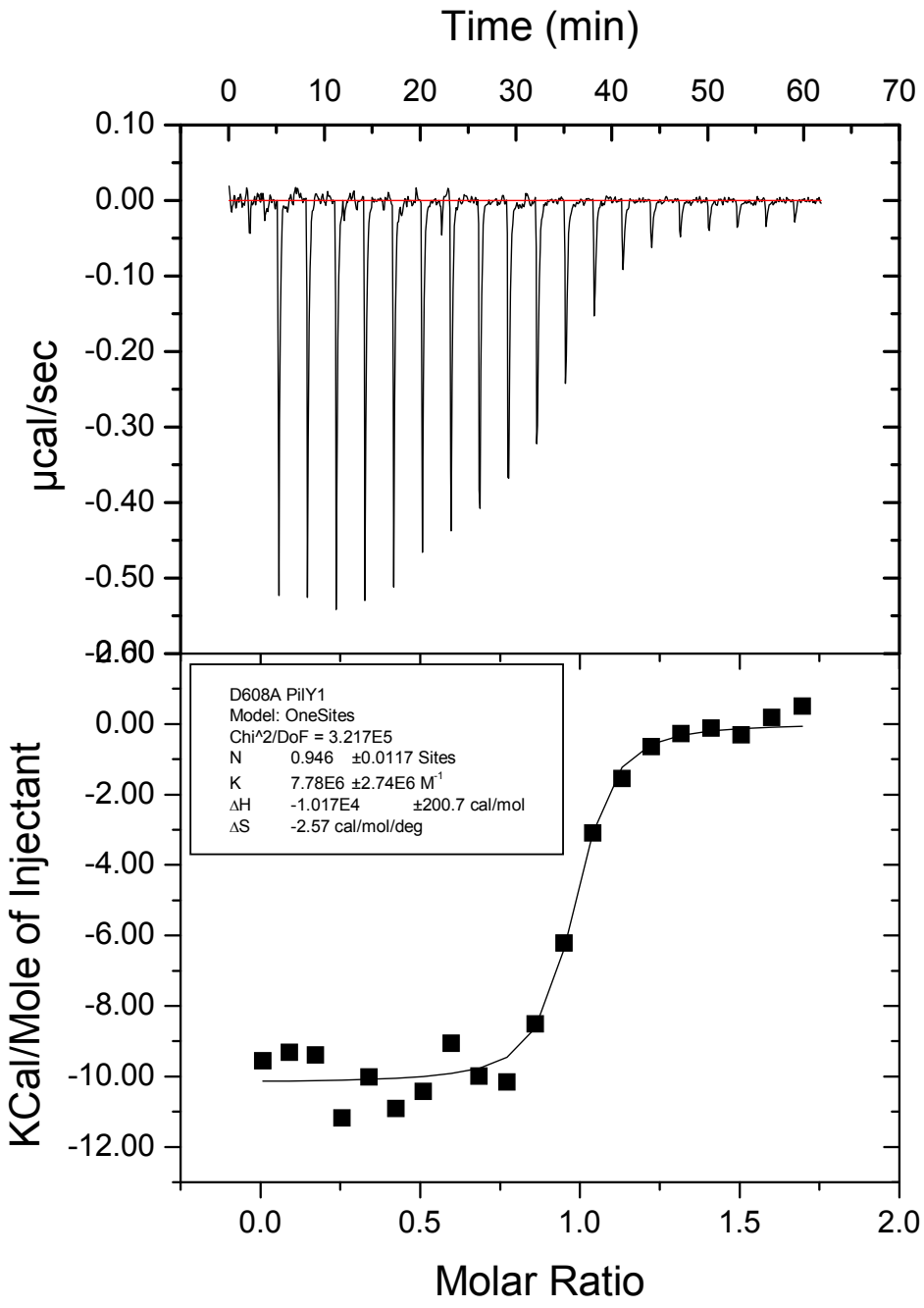

Additional Figure 3.2

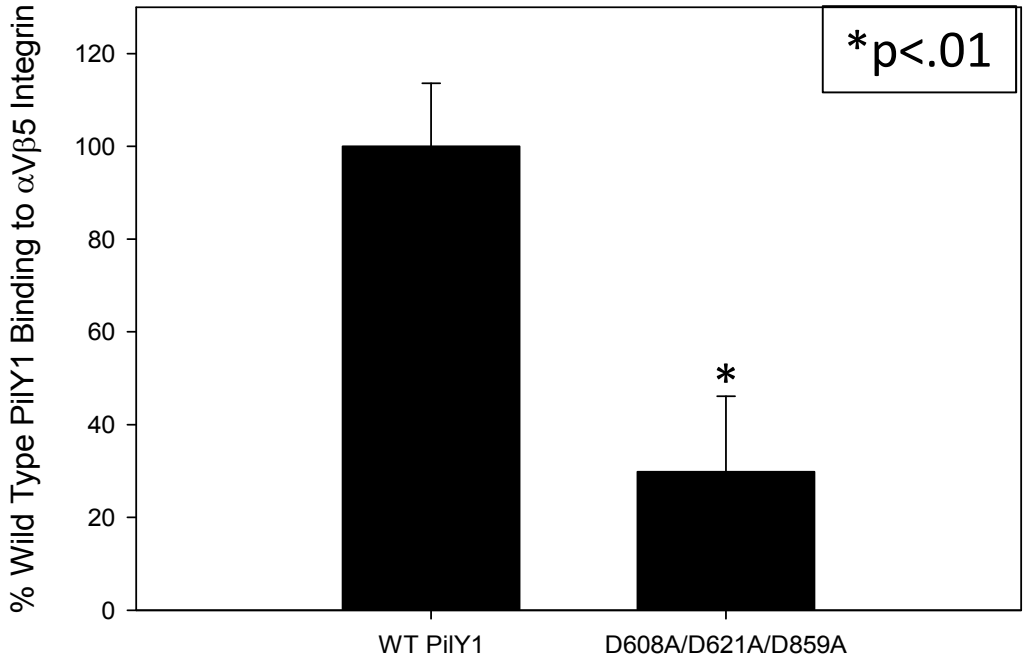

Additional Figure 3.3A

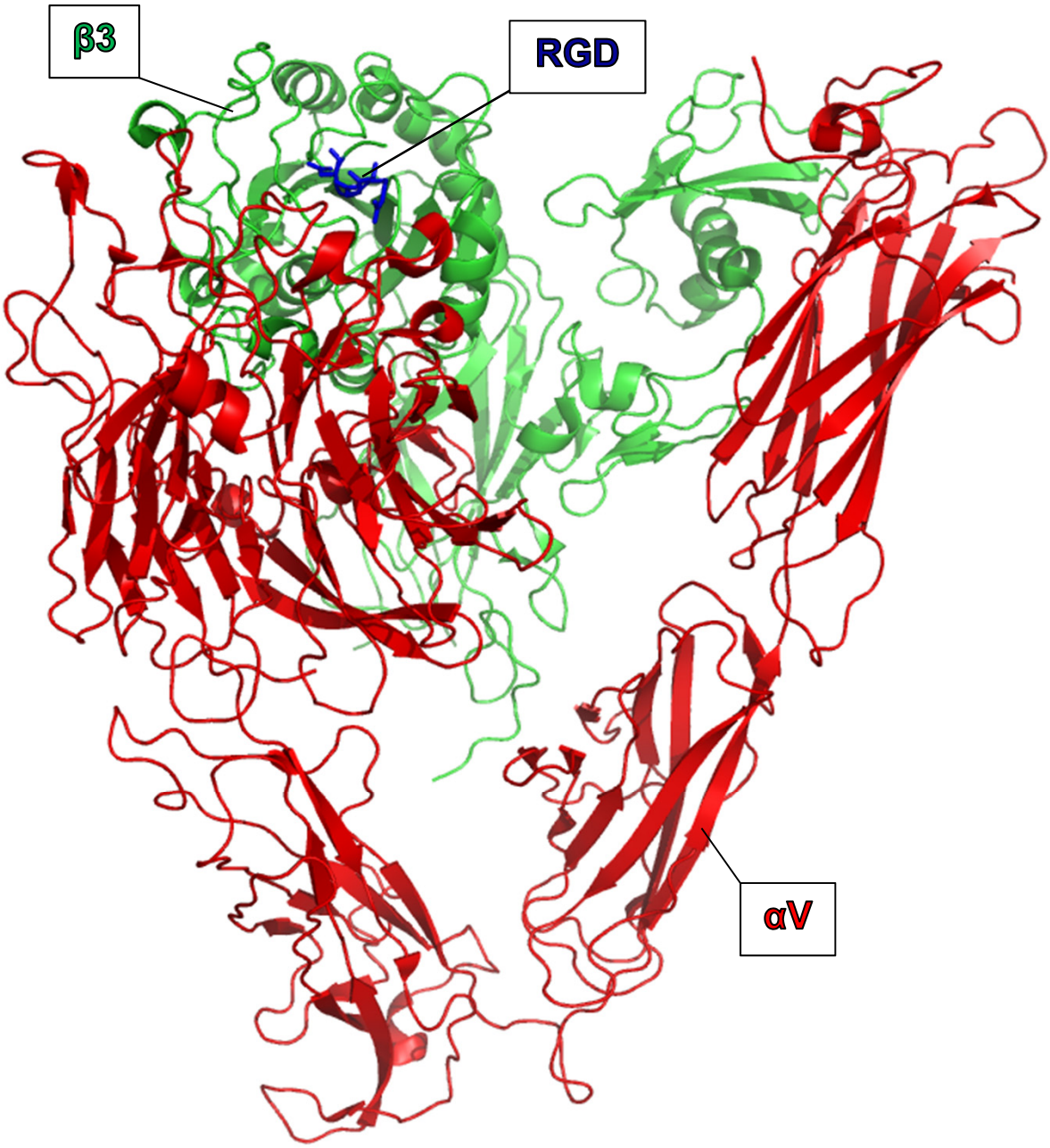

Additional Figure 3.3B

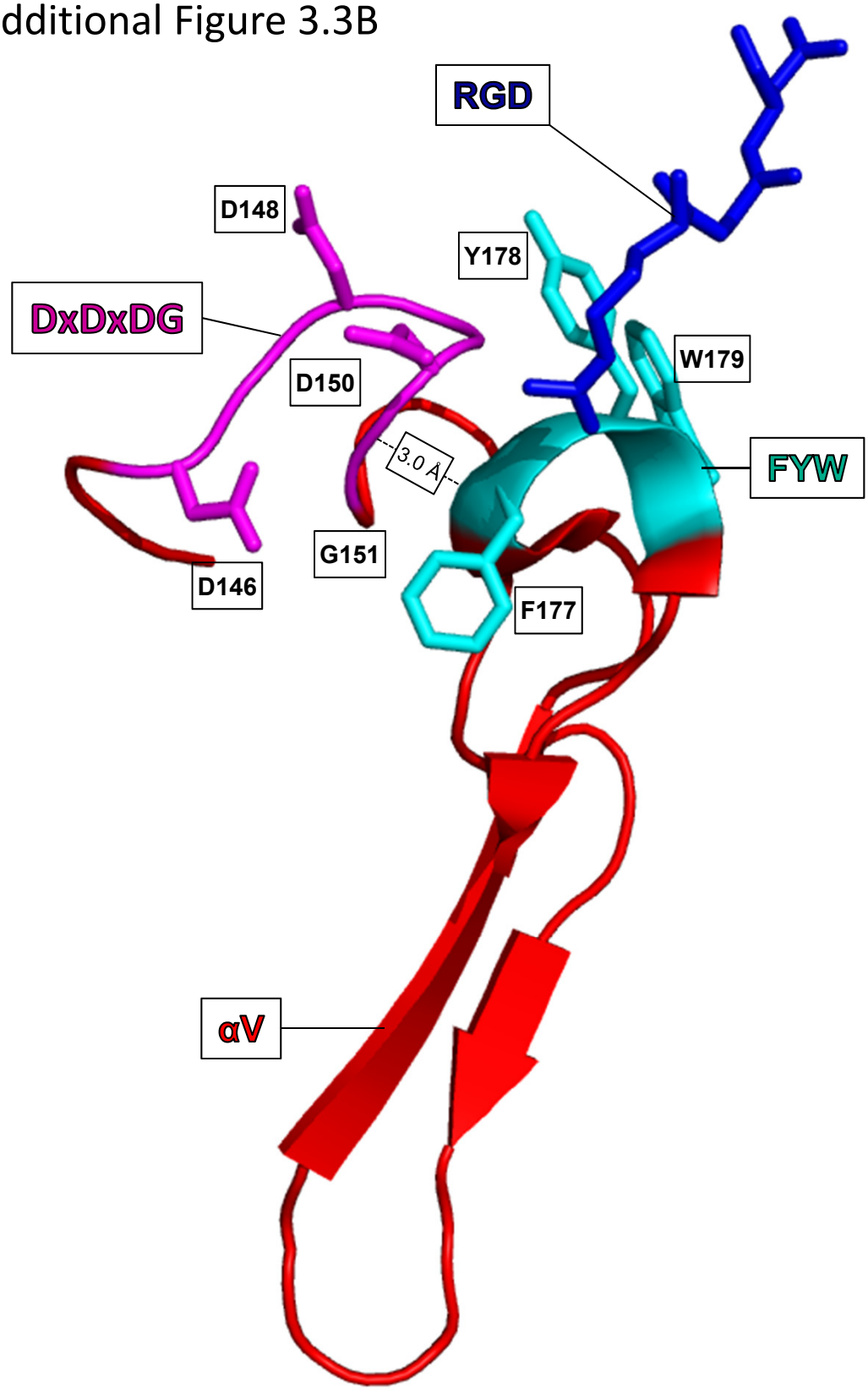

Additional Figure 3.3C

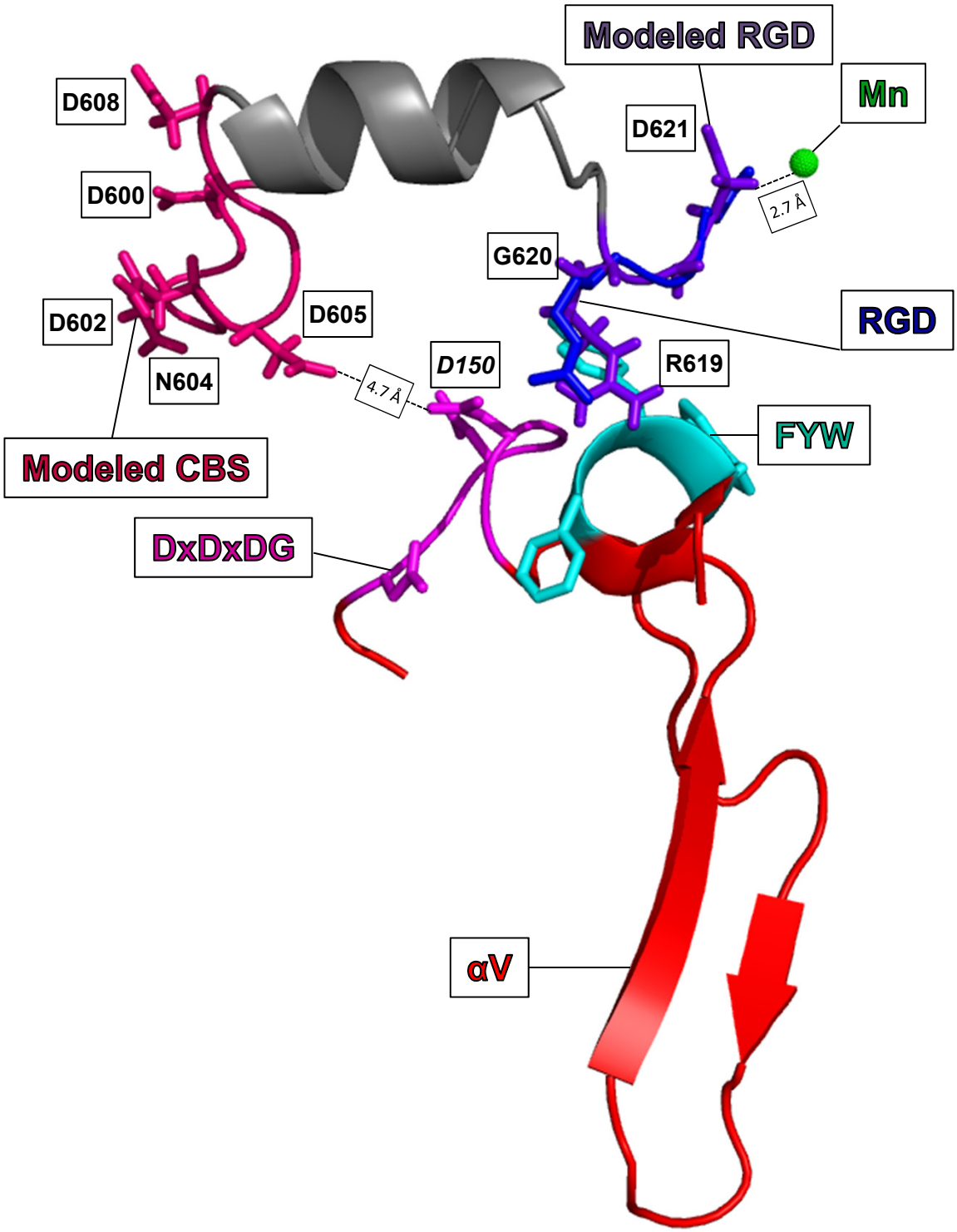

3.10 References

1. Richards MJ, Edwards JR, Culver DH, Gaynes RP (1999) Nosocomial infections in pediatric intensive care units in the United States. National Nosocomial Infections Surveillance System. Pediatrics 103: e39.

2. Klevens RM, Edwards JR, Richards CL, Jr., Horan TC, Gaynes RP, et al. (2007) Estimating health care-associated infections and deaths in U.S. hospitals, 2002. Public Health Rep 122: 160-166.

3. Schaberg DR, Culver DH, Gaynes RP (1991) Major trends in the microbial etiology of nosocomial infection. Am J Med 91: 72S-75S.

4. Apidianakis Y, Rahme LG (2009) Drosophila melanogaster as a model host for studying Pseudomonas aeruginosa infection. Nat Protoc 4: 1285-1294.

5. Starkey M, Rahme LG (2009) Modeling Pseudomonas aeruginosa pathogenesis in plant hosts. Nat Protoc 4: 117-124.

6. Hoiby N, Ciofu O, Bjarnsholt T (2010) Pseudomonas aeruginosa biofilms in cystic fibrosis. Future Microbiol 5: 1663-1674.

7. Mah TF, O'Toole GA (2001) Mechanisms of biofilm resistance to antimicrobial agents. Trends Microbiol 9: 34-39.

8. Poole K (2004) Efflux-mediated multiresistance in Gram-negative bacteria. Clin Microbiol Infect 10: 12-26.

9. Craig L, Pique ME, Tainer JA (2004) Type IV pilus structure and bacterial pathogenicity. Nat Rev Microbiol 2: 363-378.

10. Schroeder TH, Zaidi T, Pier GB (2001) Lack of adherence of clinical isolates of Pseudomonas aeruginosa to asialo-GM(1) on epithelial cells. Infect Immun 69: 719-729.

11. Emam A, Yu AR, Park HJ, Mahfoud R, Kus J, et al. (2006) Laboratory and clinical Pseudomonas aeruginosa strains do not bind glycosphingolipids in vitro or during type IV pili-mediated initial host cell attachment. Microbiology 152: 2789-2799.

12. Azghani AO, Idell S, Bains M, Hancock RE (2002) Pseudomonas aeruginosa outer membrane protein F is an adhesin in bacterial binding to lung epithelial cells in culture. Microb Pathog 33: 109-114.

13. Lillehoj EP, Kim BT, Kim KC (2002) Identification of Pseudomonas aeruginosa flagellin as an adhesin for Muc1 mucin. Am J Physiol Lung Cell Mol Physiol 282: L751-756.

14. Leroy-Dudal J, Gagniere H, Cossard E, Carreiras F, Di Martino P (2004) Role of alphavbeta5 integrins and vitronectin in Pseudomonas aeruginosa PAK interaction with A549 respiratory cells. Microbes Infect 6: 875-881.

15. Goldman MJ, Wilson JM (1995) Expression of alpha v beta 5 integrin is necessary for efficient adenovirus-mediated gene transfer in the human airway. J Virol 69: 5951-5958.

16. Gravelle S, Barnes R, Hawdon N, Shewchuk L, Eibl J, et al. (2010) Up-regulation of integrin expression in lung adenocarcinoma cells caused by bacterial infection: in vitro study. Innate Immun 16: 14-26.

17. Humphries JD, Byron A, Humphries MJ (2006) Integrin ligands at a glance. Journal of cell science 119: 3901-3903.

18. Swatzell LJ, Edelmann RE, Makaroff CA, Kiss JZ (1999) Integrin-like proteins are localized to plasma membrane fractions, not plastids, in Arabidopsis. Plant Cell Physiol 40: 173-183.

19. Sheppard D (2004) Roles of alphav integrins in vascular biology and pulmonary pathology. Curr Opin Cell Biol 16: 552-557.

20. Nassif X, Beretti JL, Lowy J, Stenberg P, O'Gaora P, et al. (1994) Roles of pilin and PilC in adhesion of Neisseria meningitidis to human epithelial and endothelial cells. Proc Natl Acad Sci U S A 91: 3769-3773.

21. Kallstrom H, Liszewski MK, Atkinson JP, Jonsson AB (1997) Membrane cofactor protein (MCP or CD46) is a cellular pilus receptor for pathogenic Neisseria. Mol Microbiol 25: 639-647.

22. Kirchner M, Heuer D, Meyer TF (2005) CD46-independent binding of neisserial type IV pili and the major pilus adhesin, PilC, to human epithelial cells. Infect Immun 73: 3072-3082.

23. Orans J, Johnson MD, Coggan KA, Sperlazza JR, Heiniger RW, et al. (2010) Crystal structure analysis reveals Pseudomonas PilY1 as an essential calcium-dependent regulator of bacterial surface motility. Proc Natl Acad Sci U S A 107: 1065-1070.

24. Kuchma SL, Ballok AE, Merritt JH, Hammond JH, Lu W, et al. (2010) Cyclic-di-GMP-mediated repression of swarming motility by Pseudomonas aeruginosa: the pilY1 gene and its impact on surface-associated behaviors. Journal of bacteriology 192: 2950-2964.

25. Heiniger RW, Winther-Larsen HC, Pickles RJ, Koomey M, Wolfgang MC (2010) Infection of human mucosal tissue by Pseudomonas aeruginosa requires sequential and mutually dependent virulence factors and a novel pilus-associated adhesin. Cell Microbiol 12: 1158-1173.

26. Higgins DG, Bleasby AJ, Fuchs R (1992) CLUSTAL V: improved software for multiple sequence alignment. Comput Appl Biosci 8: 189-191.

27. Thompson JD, Higgins DG, Gibson TJ (1994) CLUSTAL W: improving the sensitivity of progressive multiple sequence alignment through sequence weighting, position-specific gap penalties and weight matrix choice. Nucleic Acids Res 22: 4673-4680.

28. Xiong JP, Stehle T, Diefenbach B, Zhang R, Dunker R, et al. (2001) Crystal structure of the extracellular segment of integrin alpha Vbeta3. Science 294: 339-345.

29. Xiong JP, Stehle T, Zhang R, Joachimiak A, Frech M, et al. (2002) Crystal structure of the extracellular segment of integrin alpha Vbeta3 in complex with an Arg-Gly-Asp ligand. Science 296: 151-155.

30. Rigden DJ, Galperin MY (2004) The DxDxDG motif for calcium binding: multiple structural contexts and implications for evolution. J Mol Biol 343: 971-984.

31. Roy A, Kucukural A, Zhang Y (2010) I-TASSER: a unified platform for automated protein structure and function prediction. Nat Protoc 5: 725-738.

32. Zhang Y (2008) I-TASSER server for protein 3D structure prediction. BMC Bioinformatics 9: 40.

33. Rothwangl KB, Rong L (2009) Analysis of a conserved RGE/RGD motif in HCV E2 in mediating entry. Virol J 6: 12.

34. Cass DL, Bullard KM, Sylvester KG, Yang EY, Sheppard D, et al. (1998) Epidermal integrin expression is upregulated rapidly in human fetal wound repair. J Pediatr Surg 33: 312-316.

35. Pilewski JM, Latoche JD, Arcasoy SM, Albelda SM (1997) Expression of integrin cell adhesion receptors during human airway epithelial repair in vivo. Am J Physiol 273: L256-263.

36. Saalbach A, Haupt B, Pierer M, Haustein UF, Herrmann K (1997) In vitro analysis of adhesion molecule expression and gel contraction of human granulation fibroblasts. Wound Repair Regen 5: 69-76.

37. Leininger E, Roberts M, Kenimer JG, Charles IG, Fairweather N, et al. (1991) Pertactin, an Arg-Gly-Asp-containing Bordetella pertussis surface protein that promotes adherence of mammalian cells. Proc Natl Acad Sci U S A 88: 345-349.

38. Leininger E, Ewanowich CA, Bhargava A, Peppler MS, Kenimer JG, et al. (1992) Comparative roles of the Arg-Gly-Asp sequence present in the Bordetella pertussis adhesins pertactin and filamentous hemagglutinin. Infect Immun 60: 2380-2385.

39. Henderson IR, Navarro-Garcia F, Nataro JP (1998) The great escape: structure and function of the autotransporter proteins. Trends Microbiol 6: 370-378.

40. Julio SM, Inatsuka CS, Mazar J, Dieterich C, Relman DA, et al. (2009) Natural-host animal models indicate functional interchangeability between the filamentous haemagglutinins of Bordetella pertussis and Bordetella bronchiseptica and reveal a role for the mature C-terminal domain, but not the RGD motif, during infection. Mol Microbiol 71: 1574-1590.

41. Manning VA, Hamilton SM, Karplus PA, Ciuffetti LM (2008) The Arg-Gly-Asp-containing, solvent-exposed loop of Ptr ToxA is required for internalization. Mol Plant Microbe Interact 21: 315-325.

42. Huang YJ, Wu CC, Chen MC, Fung CP, Peng HL (2006) Characterization of the type 3 fimbriae with different MrkD adhesins: possible role of the MrkD containing an RGD motif. Biochem Biophys Res Commun 350: 537-542.

43. Zimmermann L, Peterhans E, Frey J (2010) RGD motif of lipoprotein T, involved in adhesion of Mycoplasma conjunctivae to lamb synovial tissue cells. Journal of bacteriology 192: 3773-3779.

44. Conradi J, Huber S, Gaus K, Mertink F, Royo Gracia S, et al. (2011) Cyclic RGD peptides interfere with binding of the Helicobacter pylori protein CagL to integrins alpha(V)beta (3) and alpha (5)beta (1). Amino Acids.

45. Nemerow GR, Stewart PL (1999) Role of alpha(v) integrins in adenovirus cell entry and gene delivery. Microbiol Mol Biol Rev 63: 725-734.

46. Wang FZ, Akula SM, Sharma-Walia N, Zeng L, Chandran B (2003) Human herpesvirus 8 envelope glycoprotein B mediates cell adhesion via its RGD sequence. J Virol 77: 3131-3147.

47. Xiao J, Palefsky JM, Herrera R, Berline J, Tugizov SM (2008) The Epstein-Barr virus BMRF-2 protein facilitates virus attachment to oral epithelial cells. Virology 370: 430-442.

48. Chintakuntlawar AV, Zhou X, Rajaiya J, Chodosh J (2010) Viral capsid is a pathogen-associated molecular pattern in adenovirus keratitis. PLoS Pathog 6: e1000841.

49. Harvala H, Kalimo H, Stanway G, Hyypia T (2003) Pathogenesis of coxsackievirus A9 in mice: role of the viral arginine-glycine-aspartic acid motif. J Gen Virol 84: 2375-2379.

50. Amphlett GW, Hrinda ME (1983) The binding of calcium to human fibronectin. Biochem Biophys Res Commun 111: 1045-1053.

51. Mihalyi E (2004) Review of some unusual effects of calcium binding to fibrinogen. Biophys Chem 112: 131-140.

52. Reinhardt DP, Ono RN, Sakai LY (1997) Calcium stabilizes fibrillin-1 against proteolytic degradation. J Biol Chem 272: 1231-1236.

53. Harfenist EJ, Packham MA, Kinlough-Rathbone RL, Cattaneo M, Mustard JF (1987) Effect of calcium ion concentration on the ability of fibrinogen and von Willebrand factor to support the ADP-induced aggregation of human platelets. Blood 70: 827-831.

54. Lawler J, Weinstein R, Hynes RO (1988) Cell attachment to thrombospondin: the role of ARG-GLY-ASP, calcium, and integrin receptors. J Cell Biol 107: 2351-2361.

55. Fusi FM, Bernocchi N, Ferrari A, Bronson RA (1996) Is vitronectin the velcro that binds the gametes together? Mol Hum Reprod 2: 859-866.

56. He B, Mirza M, Weber GF (2006) An osteopontin splice variant induces anchorage independence in human breast cancer cells. Oncogene 25: 2192-2202.

57. Singh K, Deonarine D, Shanmugam V, Senger DR, Mukherjee AB, et al. (1993) Calcium-binding properties of osteopontin derived from non-osteogenic sources. J Biochem 114: 702-707.

58. Slater M, Murphy CR, Barden JA (2002) Tenascin, E-cadherin and P2X calcium channel receptor expression is increased during rat blastocyst implantation. Histochem J 34: 13-19.

59. Mattick JS (2002) Type IV pili and twitching motility. Annu Rev Microbiol 56: 289-314.

Chapter 4

Kingella kingae PilC1 and PilC2

4.1 Introduction

Kingella kingae is an anaerobic Gram-negative emerging pathogen mostly involved in pediatric infections such as endocarditis, osteomyelitis, septic arthritis, and bacteremia [1]. These infections are initiated by attachment of surface bacterial fibers called type IV pili (tfp) to host cells. Tfp are essential for a surface walking movement called twitching motility, a process necessary for infection. Recently PilY1, in the opportunistic pathogen *Pseudomonas aeruginosa* was shown to use calcium to modulate tfp extension and retraction [2]. PilY1 has homologs in numerous other bacteria, such as PilC1 and PilC2 in *Neisseria meningitidis*, *Neisseria gonorrhoeae*, and *K. kingae*. In addition to pilus extension and retraction, PilCs in *N. meningitidis*, *N. gonorrhoeae*, and *K. kingae* are the organism's respective adhesion proteins [3,4,5]. Presented here are *in vitro* studies examining the calcium binding properties of the tfp associated proteins PilC1 and PilC2 in *K. kingae*.

4.2 Methods

PilC constructs and protein purification

Numerous constructs for PilC1 and PilC2 were examined in various cell lines and vectors (Table 4.1). The constructs discussed below produced protein *in vitro*.

PilC1 residues 739-1047 were cloned from a pUC vector containing full length PilC1 into a pMCSG9 LIC HIS MBP vector. Site-directed mutagenesis was performed to produce D930A and D930K mutations. Resultant vectors were transformed into BL21 RIPL cells

(Stratagene) ampicillin, tetracycline, streptomycin, and chloramphenicol plates overnight and a single colony was used to inoculate a 100 mL Luria Broth (LB) flask overnight containing 50 µg/mL ampicillin, 25 µg/mL tetracycline, 50 µg/mL streptomycin, and 50 µg/mL of chloramphenicol. Cell cultures were centrifuged at 3000 x g and the supernatant was discarded. The resultant pellet was used to inoculate a 1.5 L shaker flask of Terrific Broth (TB) with 50µL of antifoam (Sigma-Aldrich), 50 µg/mL ampicillin, 25 µg/mL tetracycline, 50 µg/mL streptomycin, and 50 µg/mL chloramphenicol. Cells were grown at 37 ^{o}C until OD_{600} reached 0.6-0.8. Temperature was reduced to 18 ^{o}C and protein expression was induced with 0.2 mM IPTG. Cells were grown overnight and harvested by centrifugation 6000 x g at for 15 minutes at 4 ^{o}C, and pellets were stored at -80 ^{o}C.

Thawed PilC1 pellets were suspended in loading buffer (50 mM sodium phosphate pH 7.6, 500 mM NaCl, 25 mM imidazole) supplemented with 0.5 mM EDTA, 0.1% Triton X-100, 1 mM PMSF, one tablet of a protease inhibitor cocktail (Roche) and 1 ug/ml lysozyme. After 1 hour of gently stirring on ice, the cells were sonicated on ice for 1 min and the lysate was centrifuged at 45,000 × g for 90 min at 4 ^{o}C. Using an ÄKTAxpress™ (GE HealthCare), protein from the filtered soluble fraction was nickel purified (Elution buffer consisted of 50 mM sodium phosphate pH 7.6, 500 mM NaCl, 500 mM imidazole) and purified on an S200 gel filtration column in the final buffer 20 mM Tris-HCl pH 7.5, 250 mM NaCl, 2 mM DTT, 5% Glycerol. Non-degraded protein was then TEV cleaved overnight in a stationary 15 or 50 mL tube (Figure 4.1A). TEV cleaved protein was then flowed over Nickel using S200 buffer with 25 mM imidazole, collected, then purified again over an S200 gel filtration column into S200 buffer (Figure 4.1B). Protein containing fractions were concentrated, flash frozen in liquid nitrogen and stored at -80 ^{o}C.

PilC2 residues 868-1502 (C-terminal fragment) were cloned from genomic *K. kingae* DNA into a pMCSG7 LIC HIS vector. Site-directed mutagenesis was performed to produce D1125A, D1125K, D1444A, and D1444K. Resultant vectors were transformed into BL21

Gold cells (Stratagene) on ampicillin plates overnight and a single colony was used to inoculate a 100mL LB flask overnight containing 50 µg/mL ampicillin. Cell cultures were treated as seen above except they were induces with 0.5 mM IPTG.

Cells pellets were thawed using buffer consisting of 10 mM Tris pH 7.8 and 50 mM NaCl as the common buffer base with 10 mM imidazole, DNase and protease inhibitor tablets (Roche). Cells were sonicated and cell lysate was separated into soluble and insoluble fractions using high-speed centrifugation. The soluble fraction was filtered then nickel purified, buffer exchanged, and separated using an S200 gel filtration column on an ÄKTAxpress™ (GE HealthCare). If necessary, protein and storage buffers were chelated by Chelex-100 to remove bound calcium (Bio-Rad Laboratories). Purified proteins were concentrated to ~100 µM, frozen, and stored at -80 ^{o}C.

Calcium binding assay

A binding curve for Oregon Green® 488 BAPTA-5N, hexapotassium salt (Invitrogen) in 10 mM Tris pH 7.8 and 50mM NaCl was measured on a PHERAstar (BMGLabtech) at 488 nm. With 20 µM Oregon Green and 2 µM CaCl2, 868-1502 PilC2 constructs were serial diluted 1.5-3 fold from ~100 µM to ~1 nM to obtain an EC50 which was then used to calculate the respective K_d for calcium as described previously [2].

Circular dichroism and thermal denaturation

Protein samples were exchanged into chelated 10 mM $K_xH_xPO_4$ 50 mM NaF pH 7.7 buffer and brought to 5 µM with or without the addition of 20 µM $CaCl_2$. A wavelength scan from 200-260 λ was performed on a Circular Dichroism Spectrometer 62 DS (Aviv) at 16 ^{o}C with a 10 second averaging time. Melting temperatures were measures at 214 λ from 3 ^{o}C to 95 ^{o}C at one degree increments with a 10 second averaging time.

4.3 Results

4.3.1 *Kingella kingae* PilC1 and PilC2 Protein Homology

An NIH BLAST alignment demonstrates that *Kingella kingae* PilC1 and PilC2 share a moderate sequence homology in contrast to PilC1 and PilC2 of *N. meningitidis* and *N. gonorrhoeae*, which are almost identical [6,7]. Clustal alignment ofthe C-terminal regions of PilC1 and PilC2 show that both are more similar to C-terminal *P. aeruginosa* PilY1 than they are to each other (Figure 4.2A and 4.3A) [6,7]. For example, the C-terminal domain of PilC1 and PilC2 have a 23% / 40% and 22% / 37% identity / similarity to *P. aeruginosa* PilY1, respectively.

4.3.2 PilC1 and PilC2 Calcium Binding

K. kingae PilC1 contains a putative calcium binding site located between residues 922-930 that resembles the sequence of the 851-859 site in *P. aeruginosa*, PilY1 (Figure 4.2B). The PilC1-MBP-739-1047 yield was not high enough post-TEV cleavage to conduct a calcium binding assay, so fusion protein was used for these assays. PilC1 exhibited a 530 nM affinity for calcium, which is within the affinity range of previous calcium-binding sites, thus confirming that PilC1 binds calcium (Figure 4.4) [Chapter 3 and 5] [2].

The C-terminal region of PilC2 did not contain the PilY1-like calcium binding domain; however, upon closer inspection, PilC2 had two putative calmodulin-like calcium binding sites at 1114-1125 and 1433-1444 (Figure 4.3B) [8]. Purified PilC2 bound calcium with a K_d of 5.5 μM (Figure 4.5A). Mutations in the predicted penultimate calcium binding residues were then introduced in an attempt to determine if one or both of these sites bound calcium. Mutations to the most calmodulin-like site (D1444A and D1444K) eliminated binding of calcium, indicating that only the 1433-1444 site bound calcium (Figure 4.5A). A mutation to the predicted penultimate calcium binding residue (D1125K) in the 1114-1125 site confirmed this hypothesis by binding calcium to wild type levels (Figure 4.5B, 4.5C).

To determine if the mutations to the 1433-1444 site eliminated calcium binding by disrupting protein structure, a wavelength scan of wild type and the D1444A mutation proteins was performed. There were no significant differences in the spectra of the two forms of PilC2 (Figure 4.6A). Also, there was no significant difference between the melting temperature of wild type and the D1444A mutant (Figure 4.6B). Taken together, these results indicate that mutating the calcium binding residues did not cause a global structural change or destabilize the protein.

4.3.3 PilC2 Crystal Trials

C-terminal PilC2 had a similar CD spectra and predicted β-propeller fold as C-terminal fragment of PilY1. To determine more about the PilC class of proteins, C-terminal PilC2 was entered into crystal trails in an attempt to solve the protein's structure (Figure 4.7) [2,9,10]. C-terminal PilC2 was mono-dispersed at concentrations up to 15 mg/mL according to dynamic light scattering (performed in the UNC Macromolecular Interactions Facility) (Figure 4.8). Therefore, C-terminal PilC2 in 10 mM Tris pH 7.8 and 50 mM NaCl was examined crystal trials at 7.5 mg/mL after optimal protein concentration was determined by a Qiagen prescreen. Screening PilC2 with Classics, classics lite, PEG I, PEG II, PEGrx, SaltRx, PEG/ION did not yield any significant results to date.

4.4 Figure Legends

Table 4.1 List of *K. kingae* PilC1 and PilC2 constructs made

Figure 4.1 SDS PAGE gel of PilC1 739-1047 *K. kingae* in LIC-HIS-MBP expression (a) before TEV cleavage and (b) after cleavage.

Figure 4.2 Homology of PilC1. (a). Homology of the C-terminal regions if *K. kingae* PilC1 and *P. aeruginosa* PilY1 (b). Homology of the C-terminal calcium binding site in *K. kingae* PilC1

Figure 4.3 Homology of PilC2. (a). Homology of the C-terminal regions if *K. kingae* PilC2 and *P. aeruginosa* PilY1 (b). Homology of two putative C-terminal calcium binding sites in *K. kingae* PilC2 and calmodulin's consensus calcium binding site.

Figure 4.4 *K. kingae* PilC1 binds calcium.

Figure 4.5 *K. kingae* PilC2 has one functional calcium binding site. (a) A wild type binding curve was tested in concert with two mutants (D1444A and D1444K) to determine if one, both or none of the putative calcium binding sites were real. (b) An additional mutant was made to test the remaining putative calcium binding site. (c) Homology showing that there is one confirmed C-terminal calcium binding sites in *K. kingae* PilC2 and calmodulin's consensus calcium binding site.

Figure 4.6 Stability of PilC2 D1444A mutants via (a) a circular dichroism wavelength scan and (b) and by determining the thermal melting temperature.

Figure 4.7 Comparison of C-terminal PilC2 and 532-1163 *P. aeruginosa* PilY1 by circular dichroism wavelength scan.

Figure 4.8 Dynamic light scattering of C-terminal PilC2 at (a) 10 mg/ml and (b) 15 mg/ml

Table 4.1

	Construct	BL21	BL21 RIPL
	Kk PilC1		
1	34-465	-	-
2	521-1047	-	-
3	540-end	-	-
4	739-1047	-	-
5	739-1047 MPB	-	+
6	540-1047	-	-
7	822-1022 CPD	-	-
8	848-1022 CPD	-	-
9	822-1042 CPD	-	-
10	848-1042 CPD	-	-
	Kk PilC2		
1	36-840	-	-
2	868-1502	++++	N/A

Figure 4.1

A.

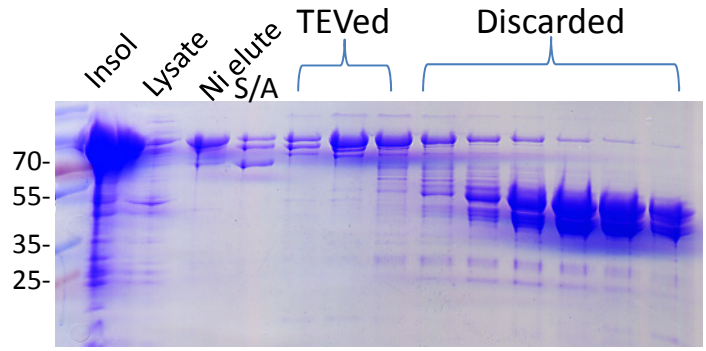
Insol
Lysate
Ni elute
S/A
TEVed
Discarded
70-
55-
35-
25-

B.

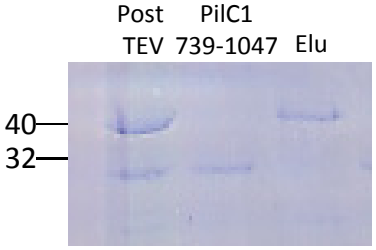
Post
TEV
PilC1
739-1047
Elu
40
32

Figure 4.2

A.

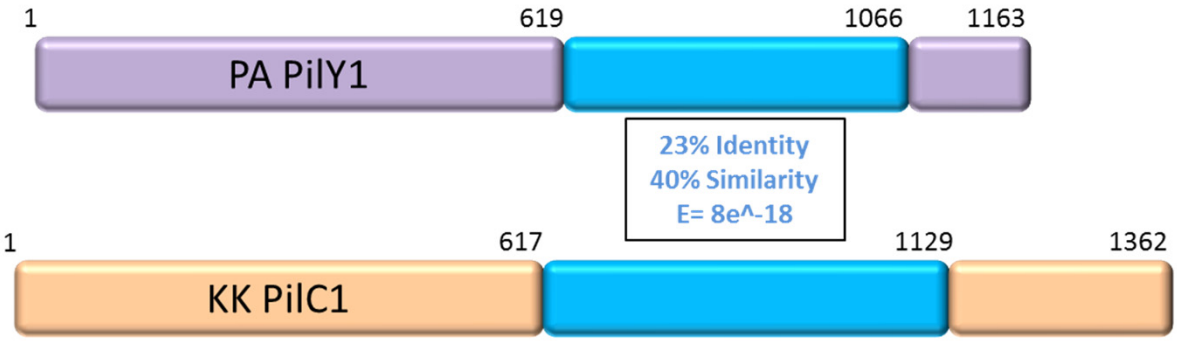

B.

***P. aeruginosa* PilY1 (851-859)**	D-N-N-S-D-G-V-A-D
***K. kingae* PilC1 (922-930)**	D-V-N-R-D-G-V-Y-D
N. gonorrhoeae PilC1	D-K-D-L-D-G-T-V-D
N. meningitidis PilC1	D-K-D-L-D-G-T-V-D
Consensus	D-Z-N-Z-D-G-O-V-O
	D I

Z: any amino acid
O: Oxygen containing amino acid

Figure 4.3

A.

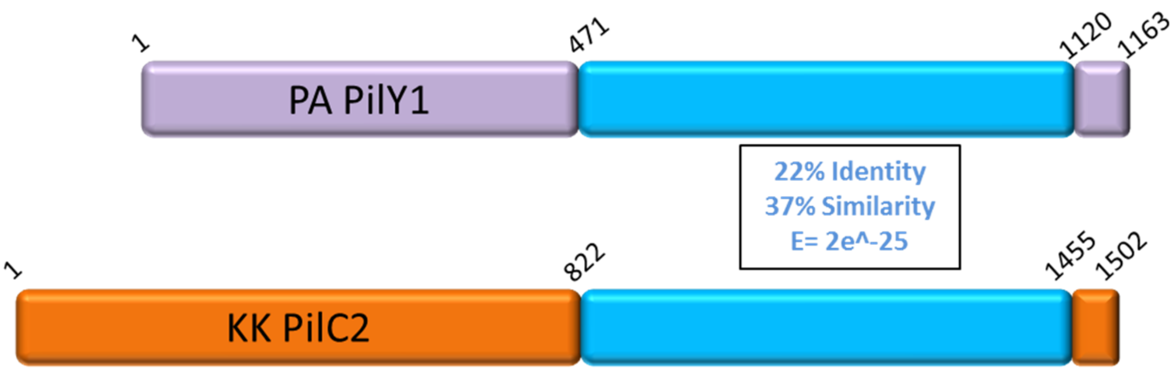

B.

PilC2	**1114**	**–**	**D**LT**N**PT**D**LTES**D**	**–**	**1125**
	1433	**–**	**D**T**N**G**D**GKFTEA**D**	**–**	**1444**
CaM	**20**	**–**	**D**K**D**G**D**GTITTK**E**	**–**	**31**

Figure 4.4

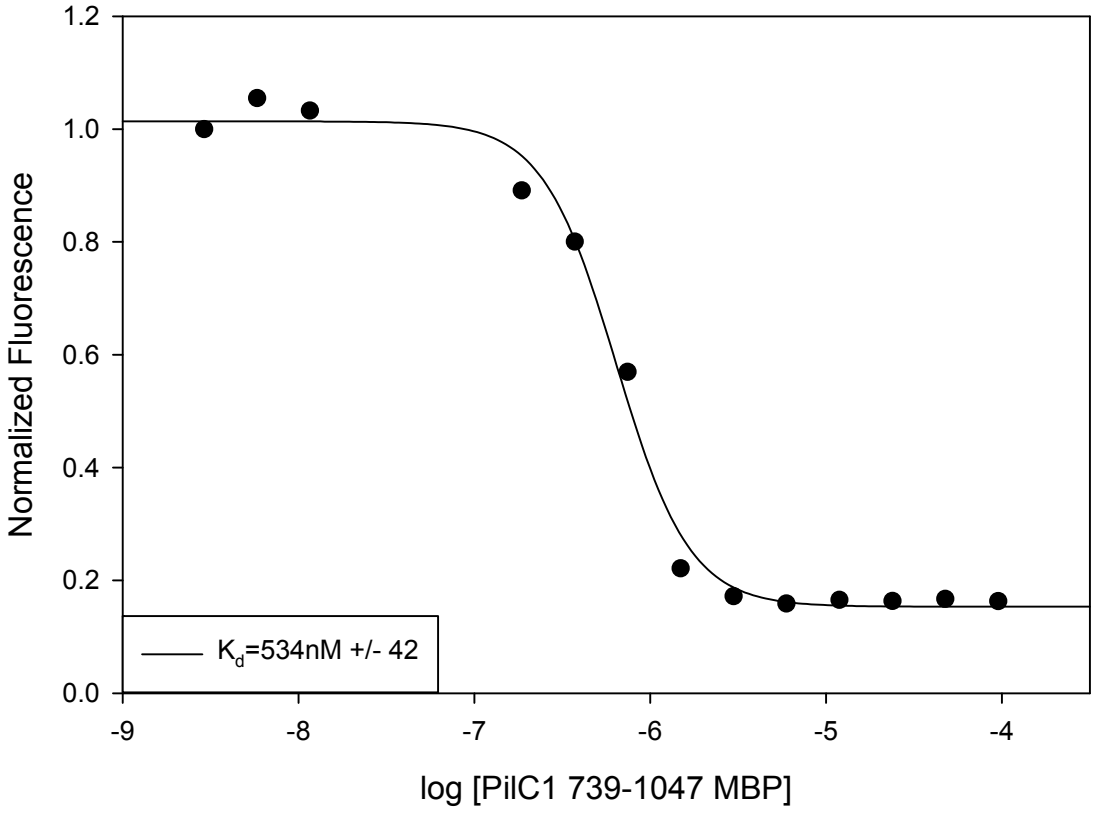
1.2
1.0
0.8
0.6
0.4
0.2
0.0
Normalized Fluorescence
-9
-8
-7
-6
-5
-4
log [PilC1 739-1047 MBP]
K$_d$=534nM +/- 42

Figure 4.5

A.

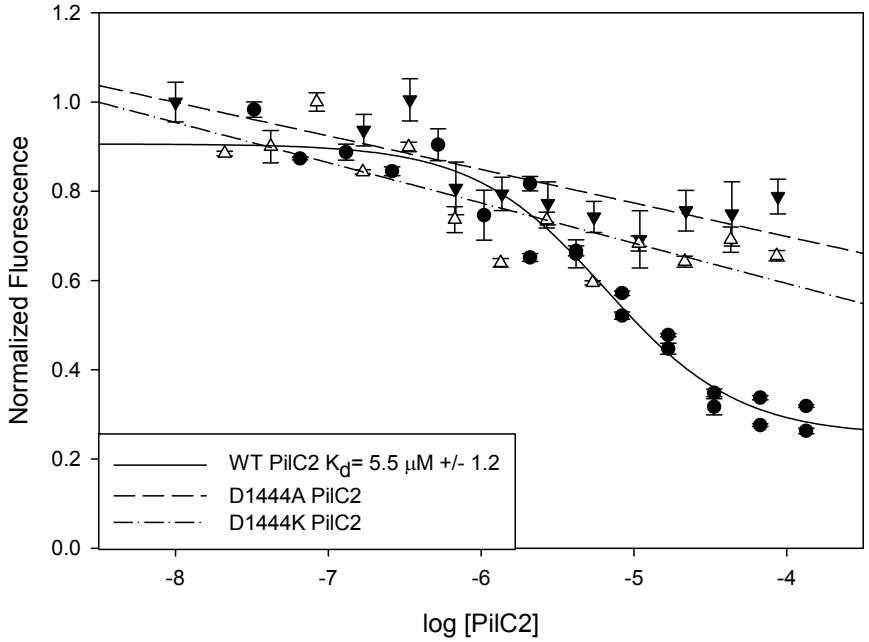

B.

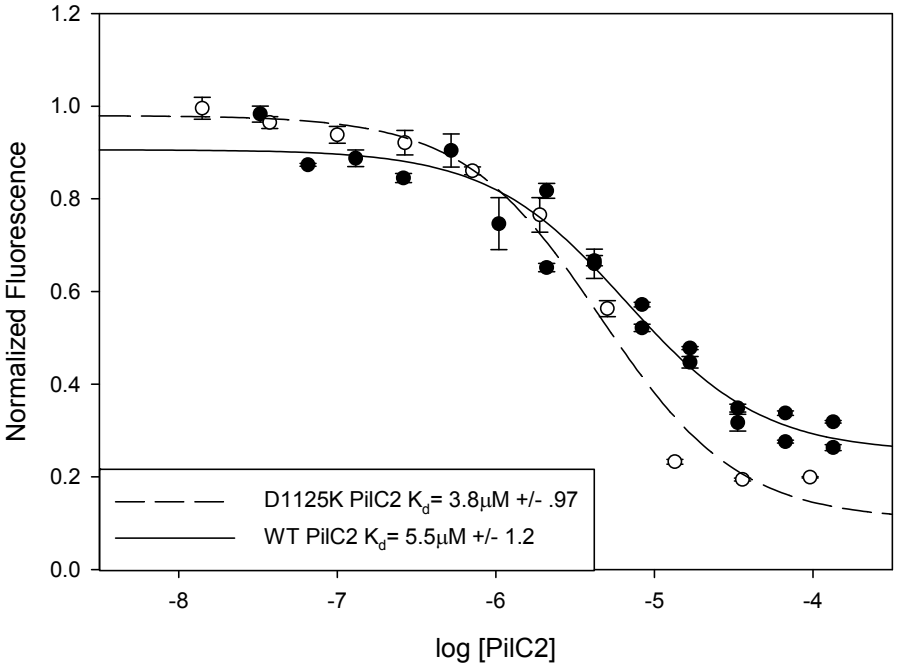

C.

PilC2	**1114**	–	**D**	L	T	**N**	P	T	**D**	L	T	E	S	**D**	–	**1125**
	1433	–	**D**	T	**N**	G	**D**	G	K	F	T	E	A	**D**	–	**1444**
CaM	**20**	–	**D**	K	**D**	G	**D**	G	T	I	T	T	K	**E**	–	**31**

Figure 4.6

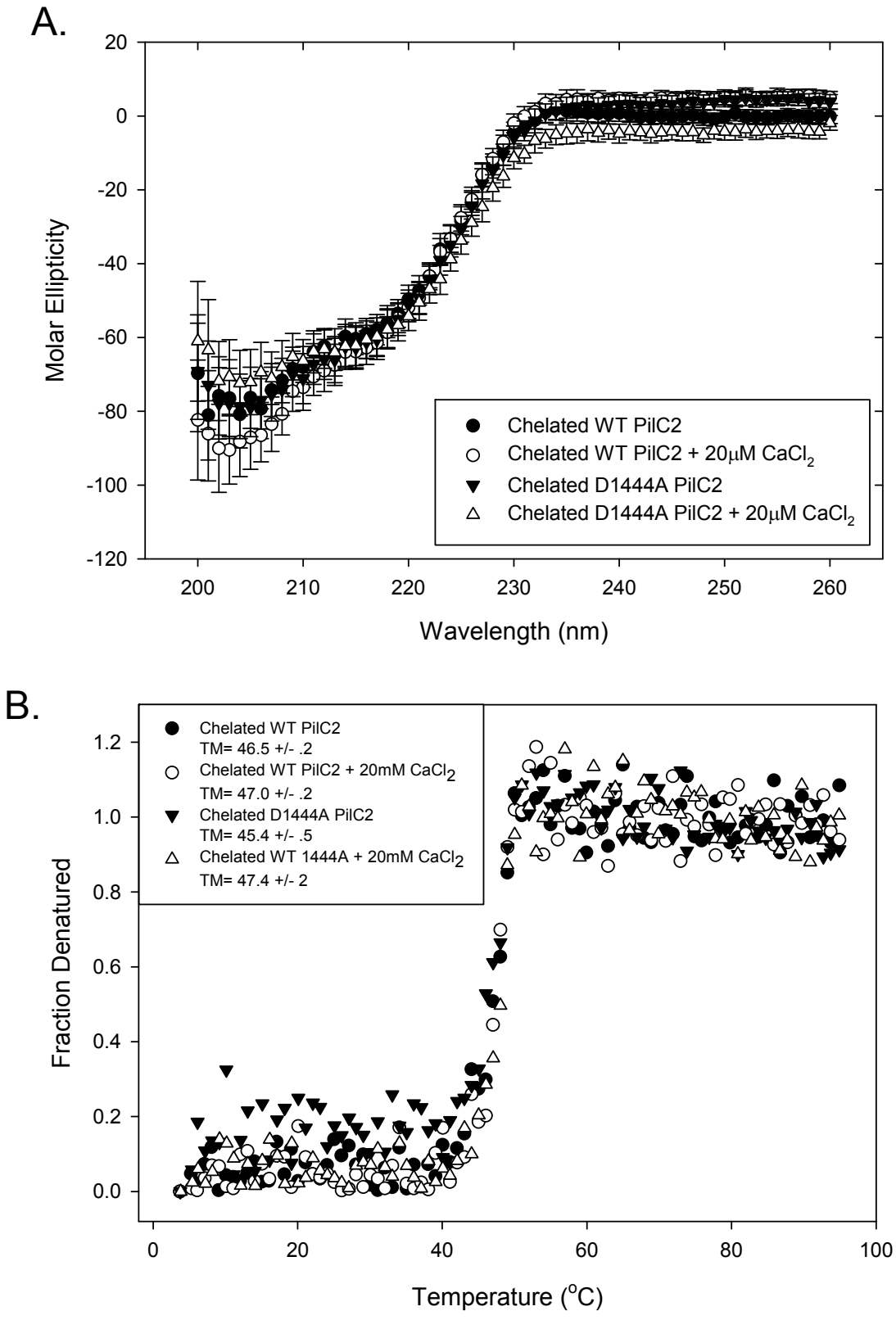
A.
Molar Ellipticity
Wavelength (nm)
Chelated WT PilC2
Chelated WT PilC2 + 20μM CaCl2
Chelated D1444A PilC2
Chelated D1444A PilC2 + 20μM CaCl2
B.
Fraction Denatured
Temperature (°C)
Chelated WT PilC2
TM= 46.5 +/- .2
Chelated WT PilC2 + 20mM CaCl2
TM= 47.0 +/- .2
Chelated D1444A PilC2
TM= 45.4 +/- .5
Chelated WT 1444A + 20mM CaCl2
TM= 47.4 +/- 2

Figure 4.7

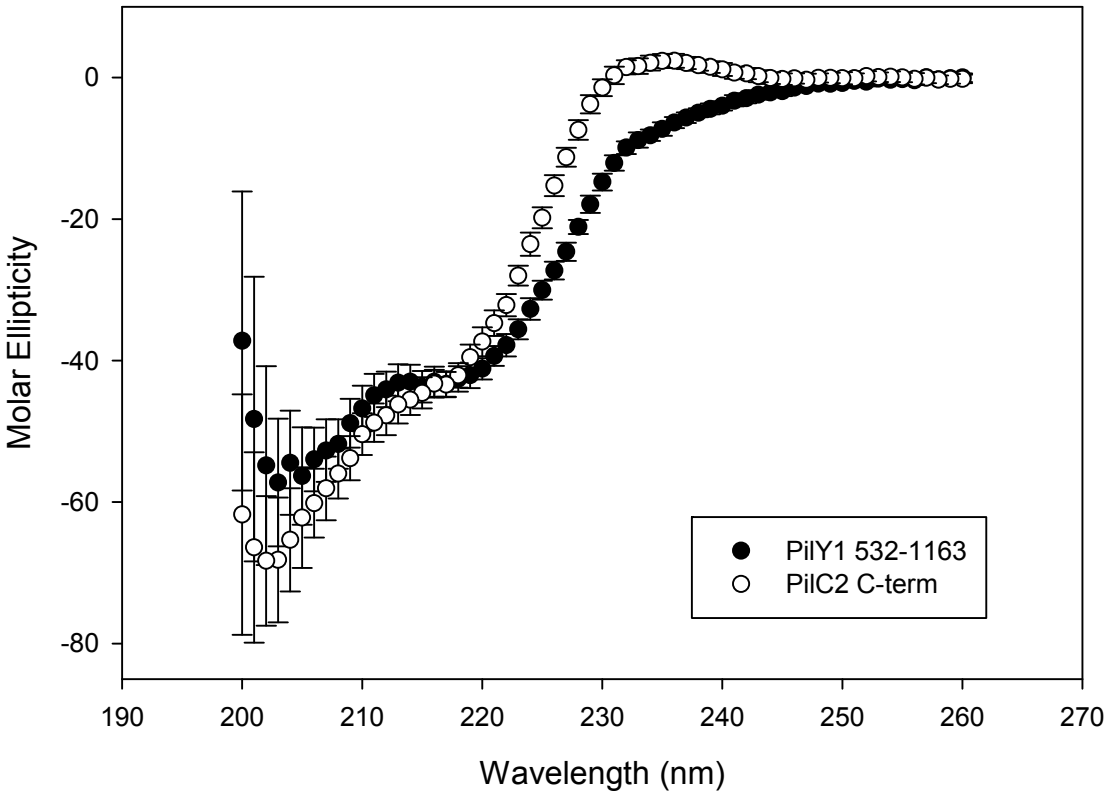
Molar Ellipticity
0
-20
-40
-60
-80
190
200
210
220
230
240
250
260
270
Wavelength (nm)
PilY1 532-1163
PilC2 C-term

Figure 4.8

A.

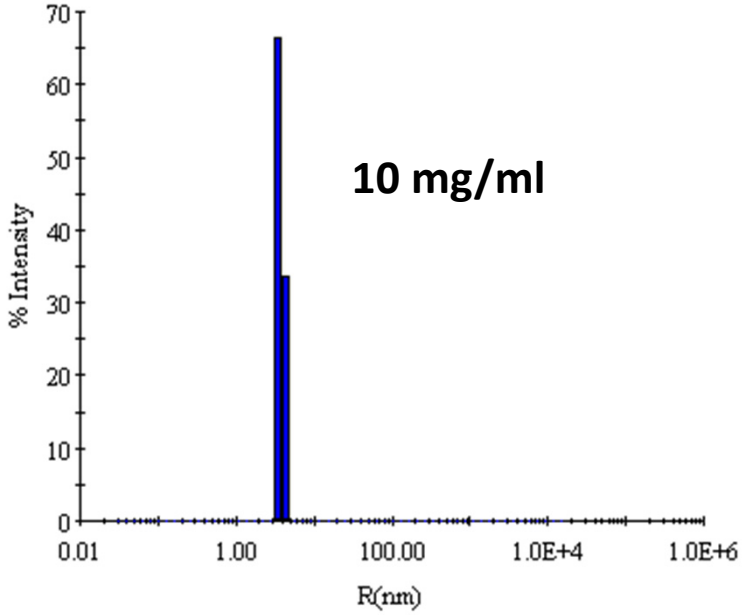

Item	R (nm)	%Pd	MW-R (kDa)
Peak 1	3.9	11.7	83

B.

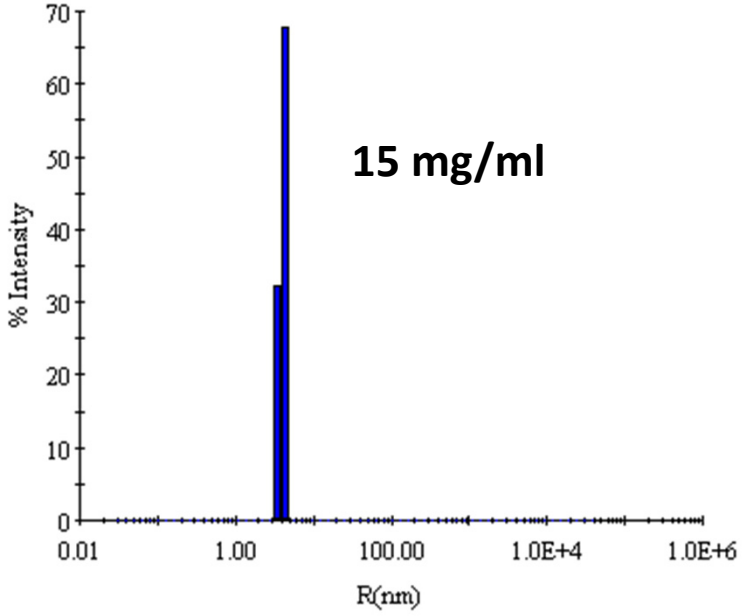

Item	R (nm)	%Pd	MW-R (kDa)
Peak 1	4.3	10.6	100

4.5 References

1. Yagupsky P, Porsch E, St Geme JW, 3rd (2011) Kingella kingae: an emerging pathogen in young children. Pediatrics 127: 557-565.

2. Orans J, Johnson MD, Coggan KA, Sperlazza JR, Heiniger RW, et al. (2010) Crystal structure analysis reveals Pseudomonas PilY1 as an essential calcium-dependent regulator of bacterial surface motility. Proc Natl Acad Sci U S A 107: 1065-1070.

3. Kehl-Fie TE, Miller SE, St Geme JW, 3rd (2008) Kingella kingae expresses type IV pili that mediate adherence to respiratory epithelial and synovial cells. Journal of bacteriology 190: 7157-7163.

4. Morand PC, Tattevin P, Eugene E, Beretti JL, Nassif X (2001) The adhesive property of the type IV pilus-associated component PilC1 of pathogenic Neisseria is supported by the conformational structure of the N-terminal part of the molecule. Mol Microbiol 40: 846-856.

5. Rudel T, Scheurerpflug I, Meyer TF (1995) Neisseria PilC protein identified as type-4 pilus tip-located adhesin. Nature 373: 357-359.

6. Higgins DG, Bleasby AJ, Fuchs R (1992) CLUSTAL V: improved software for multiple sequence alignment. Comput Appl Biosci 8: 189-191.

7. Thompson JD, Higgins DG, Gibson TJ (1994) CLUSTAL W: improving the sensitivity of progressive multiple sequence alignment through sequence weighting, position-specific gap penalties and weight matrix choice. Nucleic Acids Res 22: 4673-4680.

8. Chattopadhyaya R, Meador WE, Means AR, Quiocho FA (1992) Calmodulin structure refined at 1.7 A resolution. J Mol Biol 228: 1177-1192.

9. Roy A, Kucukural A, Zhang Y (2010) I-TASSER: a unified platform for automated protein structure and function prediction. Nat Protoc 5: 725-738.

10. Zhang Y (2008) I-TASSER server for protein 3D structure prediction. BMC Bioinformatics 9: 40.

Chapter 5

Effects of Calcium Binding on the *Neisseria gonorrhoeae* adhesin, PilC1

5.1 Summary

PilC1, a type IV pilus adhesion protein in the infectious bacterium, *Neisseria gonorrhoeae*, is a member of the PilC1-like family of adhesins found in other *Neisseria* speciesand *Pseudomonas* genera. Previous attempts to characterize the role of *N. gonorrhoeae* PilC's role in adhesion have been hampered by the inability to produce significant amounts of protein. Here, we define a method to produce recombinant full length PilC1 and demonstrate that this protein can inhibit *N. gonorrhoeae* binding to mammalian cells. In adition to adhesion, PilC1-like proteins also control pilus biogenesis. Recently, the PilC1-like protein PilY1 from *Pseudomonas aeruginosa* was shown to control pilus biogenesis through a C-terminal calcium binding site. Calcium-bound and -unbound states of PilY1 control pilus extension and retraction, respectively. We have identified a homologous calcium binding site in the C-terminal half of *N. gonorrhoeae* PilC1. Moreover, we show that the PilC1 calcium binding site mediates adhesion though regulating functional pilus biogenesis. Taken together, we establish that ion binding plays a critical role in PilC1 function.

Author wrote manuscript and contributed to Table 5.1, Table 5.2, and Figure 5.2.

5.2 Introduction

Neisseria gonorrhoeae is a Gram-negative bacterium that causes the sexually-transmitted disease gonorrhea and a variety of inflammation based human diseases. According to the CDC, there were more than 300,000 U.S. cases of gonorrhea reported in 2009. Typical *N. gonorrhoeae* infections are initiated by attachment to human epithelial cells. Adhesion is mediated by type IV pili (tfp) extended from the bacterial surface [1]. Once tfp contact is made, *N. gonorrhoeae* uses other surface machinery to solidify host attachment as it initiates invasion of epithelial cells [2]. *N. gonorrhoeae* tfp are polymeric structures predominately composed of the major pilin protein, PilE [3]. Tfp are also found in *Pseudomonas aeruginosa*, *Ralstonia solanacearum*, *Xylella fastidiosa,* and other *Neisseria* species [4]. In addition to colonizing host cells, tfp are essential for many other bacterial activities, such as twitching motility, DNA uptake, DNA conjugation, and biofilm formation [5,6].

Disruption of tfp biogenesis in *N. gonorrhoeae* is associated with abated virulence, likely due to a reduction in initial adhesion [7]. The 110 kDa *N. gonorrhoeae* PilC protein was first identified as a tfp-tip-associated adhesin and later shown to be associated with the outer-membrane of *N. gonorrhoeae* [8,9]. *N. gonorrhoeae* has two similar and functionally interchangeable *PilC* genes in its genome, *PilC1* and *PilC2* [10]. PilC1 purified from *N. gonorrhoeae* blocks bacterial adherence to human epithelial cells [11] . Furthermore, the N-terminal region of PilC was found to be responsible for the binding interaction [10]. Several experiments have suggested that the initial adherence of *N. gonorrhoeae* to human cells is facilitated by the human complement cell receptor CD46; however, there is evidence that attachment is CD46-independent [12,13,14]. Previously, the yield of purified PilC1 has been too low to meet the requirement of extensive *in vitro* studies. In this work, we have developed a new expression and purification method for PilC1 that is significantly more

efficient than previous methods. PilC is also involved in functional pilus biogenesis as with homologous proteins in other organisms such as *P. aeruginosa,* PilY1 [15,16]. Functional *P. aeruginosa* pilus biogenesis is dependent on PilY1 binding calcium; calcium bound and unbound forms corresponding to pilus extension and retraction, respectively [15]. Similarly, we have identified a PilY1-like calcium binding site in the C-terminal region of PilC1 and examined its role in *N. gonorrhoeae*.

5.3 MATERIALS AND METHODS

Protein constructs, expression and purification

Standard ligation independent cloning techniques, as described by Stols *et al.* [17], were employed in the construction of expression plasmids encoding the segments of PilC1 used in this study. Amplified DNA fragments, full-length (FL) PilC1 (residues 23-1037) and the C-terminal domain (CTD) of PilC1 (residues 519-1037), were treated and cloned into an empty pMCSG7-Lic-His expression vector. All expression plasmids used in this study were sequence verified.

Expression plasmids were transformed into *E. coli* BL21(DE3) Origami 2 cells (Stratagene). Bacteria were grown in LB medium supplemented with ampicillin, streptomycin and tetracycline at 37 ^{o}C with shaking. After the OD_{600} reached 0.6, isopropyl β-D-thiogalactoside was added to a final concentration of 0.2 mM and bacteria were grown for another 12 hours at 16 ^{o}C with shaking after which the bacteria were harvested, pelleted and stored at -80 ^{o}C. Pelleted bacteria thawed on ice were resuspended in loading buffer (50 mM $Na_xH_xPO_4$ pH 7.6, 500 mM NaCl, 25 mM imidazole) supplemented with 0.5 mM EDTA, 0.1% Triton X-100, 1 mM PMSF, one tablet of a protease inhibitor cocktail (Roche) and 1 ug/ml lysozyme. After 1 hour of gently stirring on ice, cells were sonicated on ice for 1

min and the lysate was centrifuged at 45,000 × g for 90 min at 4 °C. Using an ÄKTAxpress™ (GE HealthCare), protein from the filtered soluble fraction was nickel column purified using elution buffer consisting of 50 mM $Na_xH_xPO_4$ pH 7.6, 500 mM NaCl, 500 mM imidazole, and purified on a S200 gel filtration column (GE Healthcare) in 20 mM Tris-HCl pH 7.5, 250 mM NaCl, 2 mM DTT, 5% glycerol. Protein containing fractions were concentrated, flash frozen in liquid nitrogen and stored at -80 °C. Purified protein was >95% pure by SDS-PAGE.

Calcium binding assay

Terbium ions were used as a substitute for calcium ion due to their similar ionic radius and coordination properties. Förster resonance energy transfer (FRET) was carried out at 25 °C using a SPEX Fluorolog-3 Research T-format Spectrofluorometer (Horiba Jobin Yvon, Edison, NJ). Terbium chloride was diluted in 20 mM Tris-HCl, pH 7.5, 250 mM NaCl to a working concentration of 10 mM. Protein (400 µl at 0.2 mg/ml) was added to the cuvette, and terbium chloride was added in 0.2 µl increments. Intrinsic tryptophan fluorescence was used to excite the protein sample at 283 nm, and terbium fluorescence emission was recorded at 543 nm. The error bars represent the standard deviation of three replicates. The data was fitted to a one-site binding equation.

Circular dichroism spectroscopy

Far-UV CD spectra of wild type C-terminal PilC1 and mutants D731A, D733A, and D739A were measured with a Chirascan™ Circular Dichroism Spectrometer (Applied Photophysics) from 205-260 nm using a 1 mm path-length cell at 22 °C. Thermal denaturation of PilC1 was analyzed by monitoring ellipticity changes at 216 nm while the sample was heated at a constant rate from 10 to 80 °C. The basic protein buffer contained 25 mM HEPES, pH 7.5 and 150 mM NaF.

Cell lines and growth conditions

ME180 cells were grown in McCoy's 5A medium supplemented with 10% fetal bovine serum (FBS) at 37 ^{o}C, 5% CO_2. *N. gonorrhoeae* strains were grown on GCB-agar plates, containing Kellogg's supplement [18] at 37 ^{o}C in 5% CO_2.

Recombinant expression of PilC in *N. gonorrhoeae*

This method can be found in the Chris Thomas lab where the experiments were performed. Each western was band was quantified using NIH ImageJ software [19]. Each band was placed in the same size tight rectangle and was compared to the wild type PilC1 band that was normalized to 1.

Cell adherence assay

Cell adherence assays were performed as previously described [14] except the human epithelial ME180 cell line was employed. In necessary experiments, ME180 cells were pre-incubated with different concentrations of full-length PilC1 protein (residues 23-1037) or PilC1-CTD (residues 519-1037). ME180 cells were then incubated with the appropriate *N. gonorrhoeae* strain. After one hour, ME180 cells were washed three times with medium and lysed with 1% saponin. Colony forming units were quantified by plating serial dilutions of ME180 cell lysates. The assay was performed in triplicate and the error bars represent standard error of the normalized fraction of *N. gonorrhoeae* adherence or percent inhibition.

Cell surface exposure assay

Purified PilC1 specific monoclonal antibody, 4B5.10, was biotinylated with NHS-PEO4-Biotin. It was incubated with appropriate *Neisseria gonorrhoeae* strains for 30 min and bound antibody was detected by binding of HRP-streptavidin. HRP was then detected

by production of light in the presence of a chemiluminescent substrate. All experiments were done in triplicate.

Aggregation of *N. gonorrhoeae*

N. gonorrhoeae strains were grown at 37 ^{o}C overnight on GCB-agar plate. Bacteria were scraped off and resuspended in PBS buffer to OD_{600} ≈1. The suspension was kept at room temperature and the OD_{600} of the supernatant was measured at different time-points.

Transformation Frequency

This method can be found in the Chris Thomas lab where the experiments were performed.

5.4 RESULTS

5.4.1 Obtaining Soluble Recombinant Protein

To identify PilC1 constructs that can be expressed as soluble proteins in *E. coli*, we test-expressed a series of PilC1 constructs in numerous *E. coli* cell lines. Our results show that full-length (FL) PilC1 (residues 23-1037) and the C-terminal domain (CTD) of PilC1 (residues 519-1037) can be expressed as soluble proteins in *E. coli* BL21 (DE3) Origami 2 cells. SDS-PAGE showed that the purity of purified FL-PilC1 and PilC1-CTD was over 95% (Figure 5.1A). The expression level of PilC1-CTD is considerably higher than that of FL-PilC1. Similarly, the final obtainable concentration was more than 100 μM (>10mg/mL) for PilC1-CTD versus 0.66 μM (0.76 mg/mL) for FL-PilC1. Accordingly, these two PilC1 constructs were used in the following *in vitro* studies of PilC1.

5.4.2 Recombinant FL-PilC1 blocks *N. gonorrhoeae* Binding

Previous studies showed that purified FL-PilC1 can block the adherence of *N. gonorrhoeae* to human cells by competing with pilus-associated native PilC1 [11]. Here, we examined the impact of the recombinant proteins FL-PilC1 and PilC1-CTD on the adherence of *N. gonorrhoeae* strain FA1090 to human ME180 cells. FL-PilC1 inhibited the adherence in a dose-dependent manner with an IC_{50} in the low- to mid-nanomolar range (Figure 5.1B). As expected, our results also showed that PilC1-CTD did not affect the adherence of *N. gonorrhoeae* to human ME180 cells (Figure 5.1B). Taken together, our results suggest that the recombinant FL-PilC1 obtained in this study is likely well folded and able to mimic *in vivo* expressed PilC1.

5.4.3 Calcium Binding Domain Homology

Recent studies have identified a calcium binding site in the *Pseudomonas aeruginosa* protein, PilY1, which shares *a* high degree of homology with the PilC protein from *N. gonorrhoeae* [15]. Sequence alignment suggests that *N. gonorrhoeae* PilC1 also has the calcium binding site in the CTD (Table 5.1). We sought to determine if PilC1-CTD binds calcium and what specific residues are involved in binding. Calcium binding experiments showed that PilC1-CTD binds calcium in a manner that can be fitted with a one-site binding model (K_d = 0.9 ± 0.2 μM) (Figure 5.2A). Moreover, mutations of the putative calcium binding site aspartic acid residues to alanines (D731A, D733A and D739A) eliminate the ability of PilC1 to bind calcium (Figure 5.2A). Thus, we have both confirmed that PilC1 binds calcium and that the chelating residues include D731, D733, and D739.

It is possible that we disrupted the native protein folding state by making the aspartic acid to alanine mutations, thereby rendering the PilC1-CTD protein unable to bind to

calcium. The impact of these mutations on the secondary structure of PilC1-CTD was examined by circular dichroism (CD) spectroscopy. We saw no shift in the CD profile with any of the mutants as compared to calcium bound wild type PilC1-CTD, indicating that the mutations did not disrupt the global secondary structure of the protein (Figure 5.2B). Furthermore, we did not observe a CD profile difference between chelated and calcium-bound forms of wild type PilC1-CTD (Figure 5.2B). We also investigated the thermostability of the calcium binding domain mutations and chelated wild type PilC1-CTD as compared to calcium bound wild type PilC1-CTD. We found no significant difference in the melting temperature (T_m) between all forms of PilC1-CTD (Table 5.2). Taken together, these results show that mutations to the PilC1 calcium binding site do not change the proteins' overall secondary structure or stability.

5.4.4 Expression of Calcium Binding Mutants in *N. gonorrhoeae*

To examine the role calcium binding plays in the function of PilC1 *in vivo*, we engineered several *N. gonorrhoeae* strains in strain FA1090, which has the *pilC2* gene out of frame and therefore no PilC2 expression. We substituted the wild type *pilC1* gene with *pilC1* genes that carried different calcium binding site mutations. We first examined the expression of PilC1 mutants in engineered *N. gonorrhoeae* strains. Western-blot analysis showed that PilC1-D731A had wild-type level expression, while for unclear reasons, PilC1-D733A and PilC1-D739A had reduced expression (Figure 5.3). As a result, only the PilC1-D731A calcium binding mutant was used in the remaining studies.

5.4.5 Mutations to the Calcium Binding Site Reduce Surface PilC1 and ME180 Adherence

We next investigated the exposure of PilC1 mutants on the surface of *N. gonorrhoeae*. The monoclonal antibody 4B5.10 can recognize pilus-associated and outer-membrane associated PilC1. As expected, the non-piliated *N. gonorrhoeae* strain (PilC1^{+}/ΔPilE) was used as a negative control. Our results showed that the amount of PilC1-D731A on the bacterial surface was significantly reduced relative to wild-type PilC1 (Figure 5.4), suggesting that calcium binding promotes trafficking of PilC1 to the cell surface. In addition, the *N. gonorrhoeae* strain expressing PilC1-D731A exhibited dramatically reduced adherence to human ME180 cells compared to the *N. gonorrhoeae* strain expressing wild-type PilC1 (Figure 5.5). Together, these results indicate that the PilC1 calcium binding site impacts adhesion possibly by controlling type IV piliation.

5.4.6 PilC1 Calcium Binding Site Affects Aggregation and Transformation Frequency

To confirm that the calcium binding site affected pilus biogenesis, we examined two *N. gonorrhoeae* pilus dependent processes, aggregation and transformation frequency [20,21]. As expected, the pilus retraction deficient strain (PilC1^{+}/ΔPilT) and the piliated strain (PilC1^{+}) displayed higher levels of aggregation than the non-piliated N. gonorrhoeae strain (PilC1^{+}/ ΔPilE), which displayed the lowest levels (Figure 5.6A) [21]. The strain expressing PilC1-D731A displayed similar levels of aggregation as the non-piliated strain, suggesting that it exhibits defects in pilus biogenesis, consistent with PilY1 data from *P. aeruginosa* (Figure 5.6A) [15].

We examined the transformation frequency of the aforementioned strains of *N. gonorrhoeae*. Recall that transformation frequency is highly dependent on functional pilus

biogenesis [21]. Accordingly, the pilus retraction deficient strain (PilC1$^+$ /ΔPilT) and the non-piliated strain (PilC1$^+$/ ΔPilE) had non-detectable levels of transformation, while the piliated strain (PilC1$^+$) had functional levels of transformation efficiency (Figure 5.6B). The calcium binding deficient PilC1-D731A strain had significantly less competence than the piliated strain (Figure 5.6B). Thus, the calcium binding site in PilC1 appears to control functional pilus biogenesis.

5.5 DISCUSSION

N. gonorrhoeae is well established as a sexually transmitted pathogen and the cause of numerous inflammatory diseases, such as pharyngitis, endocarditis, and pelvic inflammatory disease [22,23]. Because adhesion though a functional tfp is a necessary step for infection, we sought to understand more about this process [3]. The focus of this study was the *N. gonorrhoeae* tfp adhesion protein, PilC1. Here, we define a new purification method for recombinant full length and C-terminal PilC1. Using these recombinant proteins, we confirmed that the adhesion domain of PilC1 was in the N-terminal region and that purified FL-PilC1 could be used as a competitive inhibitor of *N. gonorrhoeae* binding to ME180 cells. The method defined here to successfully express and purify both recombinant full-length and C-terminal PilC1 will prove beneficial in determining the specific PilC1 N-terminal domain residues responsible for adhesion and characterizing the resultant host cell binding interaction.

We also characterized a calcium binding site at residues 701-709 in *N. gonorrhoeae* PilC1. Based on the conserved PilY1 calcium binding site, we identified the residues within this site responsible for calcium chelation and showed that eliminating the ability for this site to bind calcium abolished adhesion by preventing surface piliation. As previously mentioned, PilY1's 851-859 calcium binding site controls pilus extension and retraction [15]. This

calcium binding site is not only conserved in *N. gonorrhoeae* PilC2, but in a variety of tfp containing bacteria (Table 5.1).

Tfp are used for a variety of cellular processes including motility, DNA uptake and adhesion-mediated infection [3]. Here, we continue to expound upon the importance of calcium binding sites in the PilC family of proteins. Although the mechanism by which these calcium binding sites control pilus biogenesis is unclear, we are beginning to extend the calcium bound and unbound model for the PilC family of proteins to control pilus extension and retraction, respectively.

Future work will include using purified 731A-FL-PilC1 to attempt to block *N. gonorrhoeae* from binding to ME180 cells. Given that the PilC1 binding domain is N-terminal and the calcium binding site is in the C-terminal region of the protein, we expect that purified 731A-FL-PilC1 will produce the same results as wild type protein in eliminating *N. gonorrhoeae's* ability to bind to ME180 cells. Preliminary results suggest this hypothesis is correct.

5.7 Figure Legends

Figure 5.1 Purified full-length PilC1 protein inhibits in a dose-dependent manner the adherence of *Neisseria gonorrhoeae* to human epithelial cells. (A) Full-length (FL) PilC1 (residues 23-1037) and the C-terminal domain (CTD) of PilC1 (residues 519-1037). (B) ME180 cells were preincubated with increasing concentrations of PilC1 proteins for 30 minutes before being washed and incubated with N. gonorrhoeae strain FA1090 in our cell adherence assay. The assay was performed in triplicate on three days. The error bars represent the standard error of the normalized fraction of N. gonorrhoeae adherence.

Table 5.1 Partial sequence alignment of calcium binding for various tfp containing species. Numbers correspond to residues in PilC1 *Neisseria gonorrhoeae* FA1090. **Underlined bolded** residues correspond to conserved calcium binding site. Predicted amino acid sequence in this region is identical in 9 of the 11 available gonococcal PilC sequences and 23 of the 30 *N. meningitidis* sequences. Exact matches in sequence are highlighted in blue and by a "*" at the bottom of the alignment, green and ":" indicate strongly conserved residue, and violet and "." Indicates weakly conserved residues.

Figure 5.2 Binding of Tb^{3+} to different PilC1 constructs. (A) Different PilC1-CTD constructs were titrated with increasing concentrations of $TbCl_3$ as described in our materials and methods. The solid line is computer fit of the data using one-site binding model. (B) The far-UV CD spectra of PilC1-CTD in the absence or presence of $CaCl_2$ were recorded as described in the materials and methods.

Table 5.2 Impact of calcium binding on the thermostability of PilC1. The change of ellipticity at 216 nm with the increase of temperature was recorded as described in the materials and methods. The melting temperature (Tm) indicates the temperature that the protein loses half of its ellipticity at 222 nm.

Figure 5.3 Expression of PilC1 calcium binding mutants in *N. gonorrhoeae*. Western-blot of the whole cell lysates of N. gonorrhoeae strains expressing different PilC constructs are shown here. N represents the N. gonorrhoeae strain that does not express PilC.

Figure 5.4 Impact of calcium binding on the surface exposure of PilC1 in *N. gonorrhoeae*. The surface exposure of PilC1 proteins and the adherence of different N. gonorrhoeae strains to human ME180 cells were performed as described in the materials and methods. The experiments were performed in triplicate on three days. The error bars represent the standard error of the normalized fraction of surface exposure or N. gonorrhoeae adherence.

Figure 5.5 Impact of calcium binding on the adherence of *N. gonorrhoeae* to human ME180 cells. D709A PilC1 mutation results in a significant reduction in adherence to ME180 epithelial cells in vitro. The percentage of adherent *N. gonorrhea* challenge inoculum preparation to epithelial cells was calculated and plotted from triplicate replicates in four separate experiments conducted on four successive days. Data are expressed as the mean and standard deviation. Data was compared by Repeated Measures ANOVA and Tukey analysis (P=0.0001).

Figure 5.6 Impact of calcium binding on aggregation and transformation frequency in *N. gonorrhoeae.* (A) Four ml cultures of strains 7474, 7477, 7489 and 7495 were allowed to settle over a 300 minute time course, with an OD reading taken every 50 minutes. Results starred showed significance of $p < 0.05$ by 2-way ANOVA. Differences between strains 7474 and 7477, strains 7489 and 7495, and strains 7489 and 7477 were significant ($p < 0.05$) by Tukey's Multiple Comparison Test. (B) D709A PilC1 expressing *N. gonorrhea* are less competent than WT PilC1 expressing *N. gonorrhea*. Results are expressed as percentages of recipient cells transformed described as a ratio to the wt control. Data are expressed as the means and standard deviations from 3 independent experiments. Data was analyzed by Repeated Measures ANOVA and Tukey analysis. ($P=0.0001$)

Figure 5.1

A.

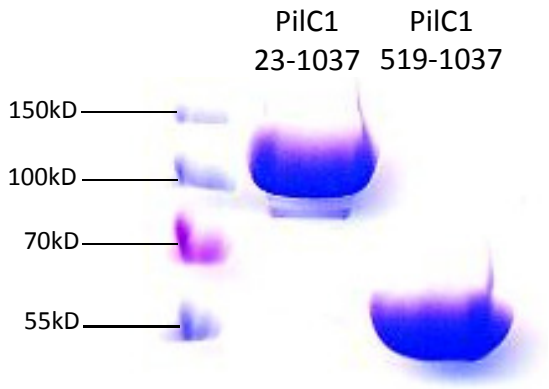
PilC1
23-1037
PilC1
519-1037
150kD
100kD
70kD
55kD

B.

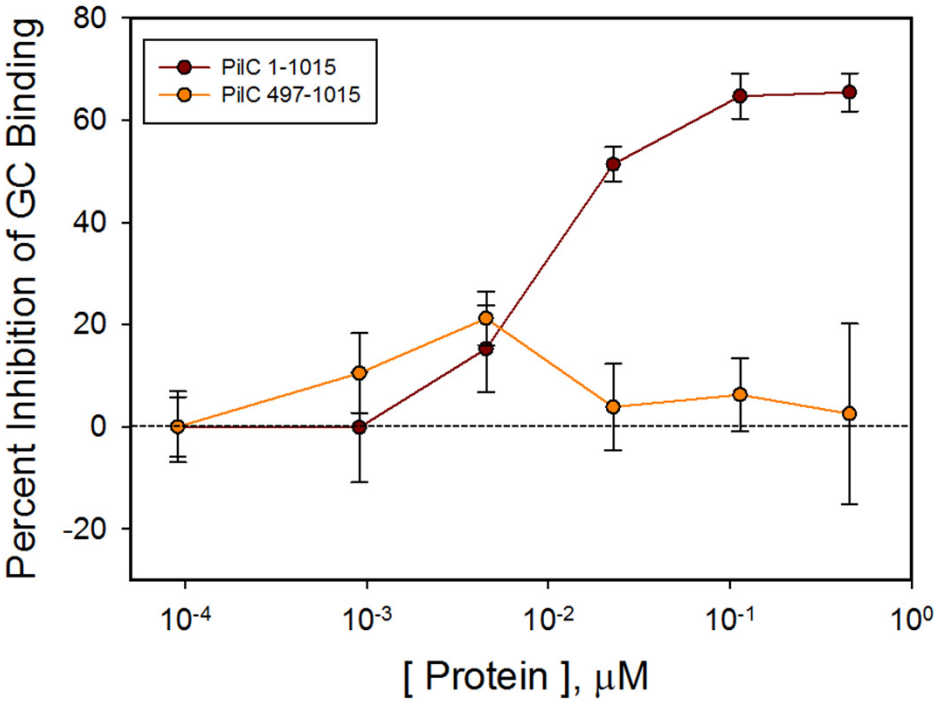
PilC 1-1015
PilC 497-1015
Percent Inhibition of GC Binding
80
60
40
20
0
-20
10-4
10-3
10-2
10-1
100
[Protein], μM

Table 5.1

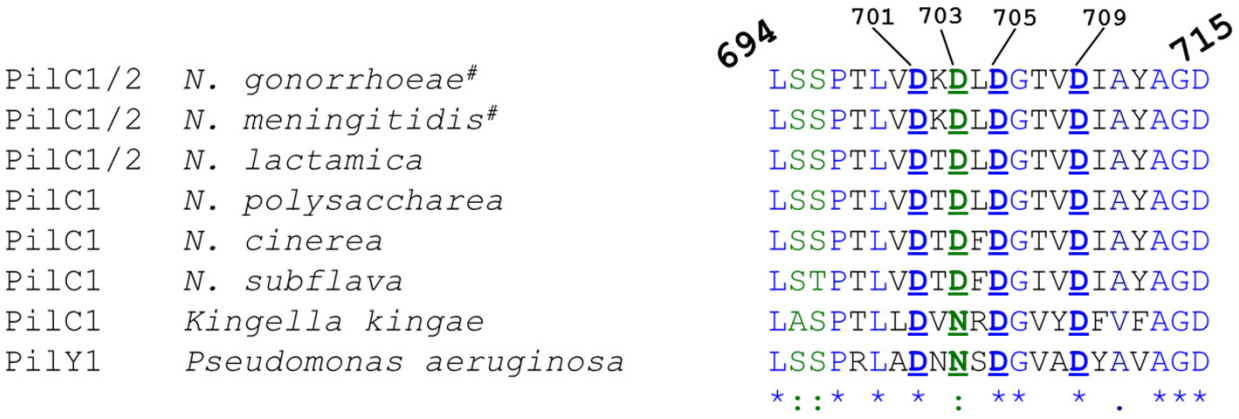
694
701
703
705
709
715
PilC1/2 N. gonorrhoeae#
PilC1/2 N. meningitidis#
PilC1/2 N. lactamica
PilC1 N. polysaccharea
PilC1 N. cinerea
PilC1 N. subflava
PilC1 Kingella kingae
PilY1 Pseudomonas aeruginosa
LSSPTLVDKDLDGTVDIAYAGD
LSSPTLVDKDLDGTVDIAYAGD
LSSPTLVDTDLDGTVDIAYAGD
LSSPTLVDTDLDGTVDIAYAGD
LSSPTLVDTDFDGTVDIAYAGD
LSTPTLVDTDFDGIVDIAYAGD
LASPTLLDVNRDGVYDFVFAGD
LSSPRLADNNSDGVADYAVAGD

Figure 5.2

A.

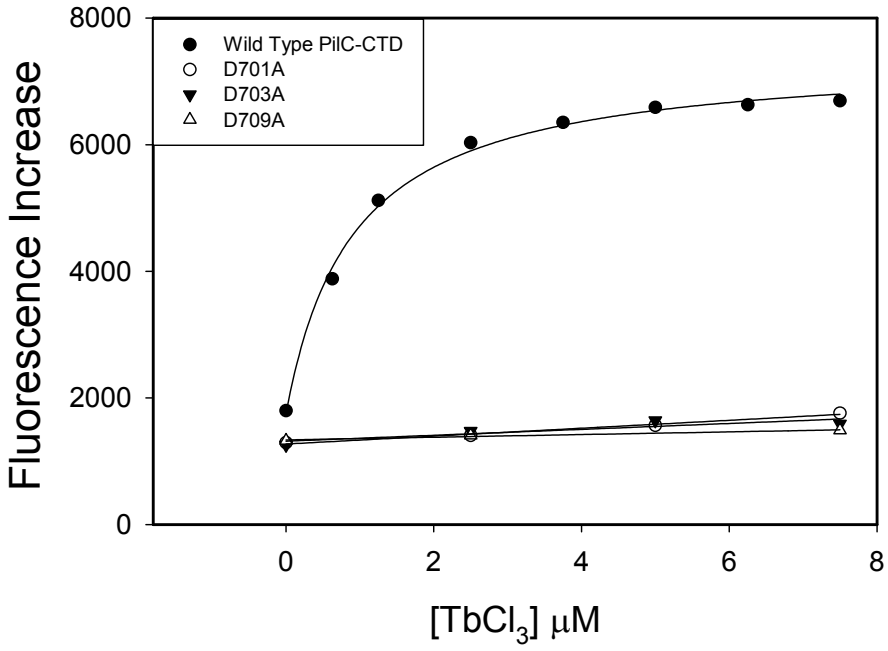
Fluorescence Increase
8000
6000
4000
2000
0
0
2
4
6
8
[TbCl3] μM
Wild Type PilC-CTD
D701A
D703A
D709A

B.

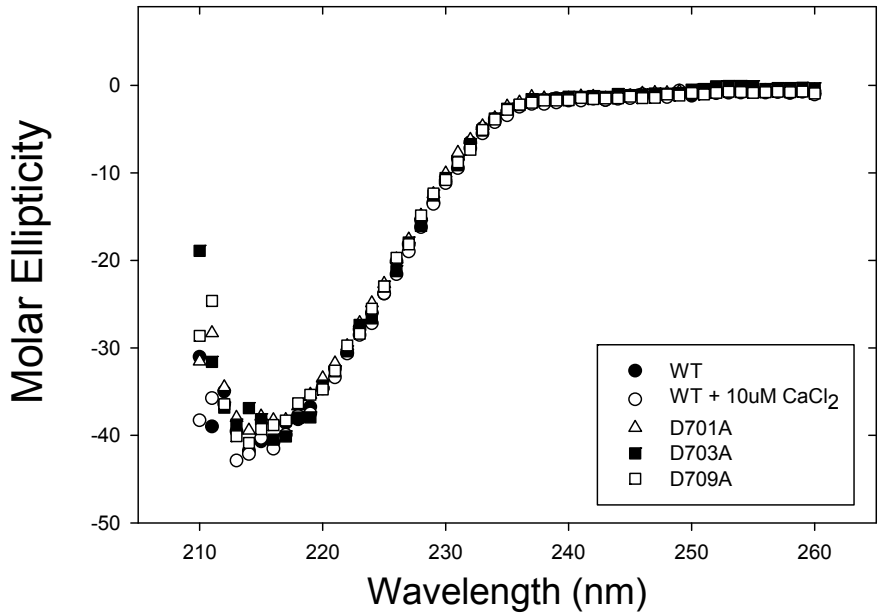
Molar Ellipticity
0
-10
-20
-30
-40
-50
210
220
230
240
250
260
Wavelength (nm)
WT
WT + 10uM CaCl2
D701A
D703A
D709A

Table 5.2

PilC1 Protein	T_m
WT + 10 µM $CaCl_2$	46.28 ± 0.10
WT no $CaCl_2$	46.17 ± 0.18
D701A	46.32 ± 0.11
D703A	47.15 ± 0.16
D709A	46.59 ± 0.19

Figure 5.3

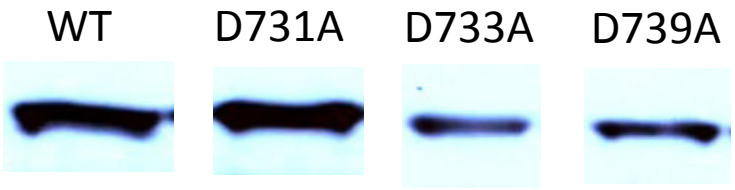

ImageJ Quantification				
	1.00	**1.07**	**0.39**	**0.54**

Figure 5.4

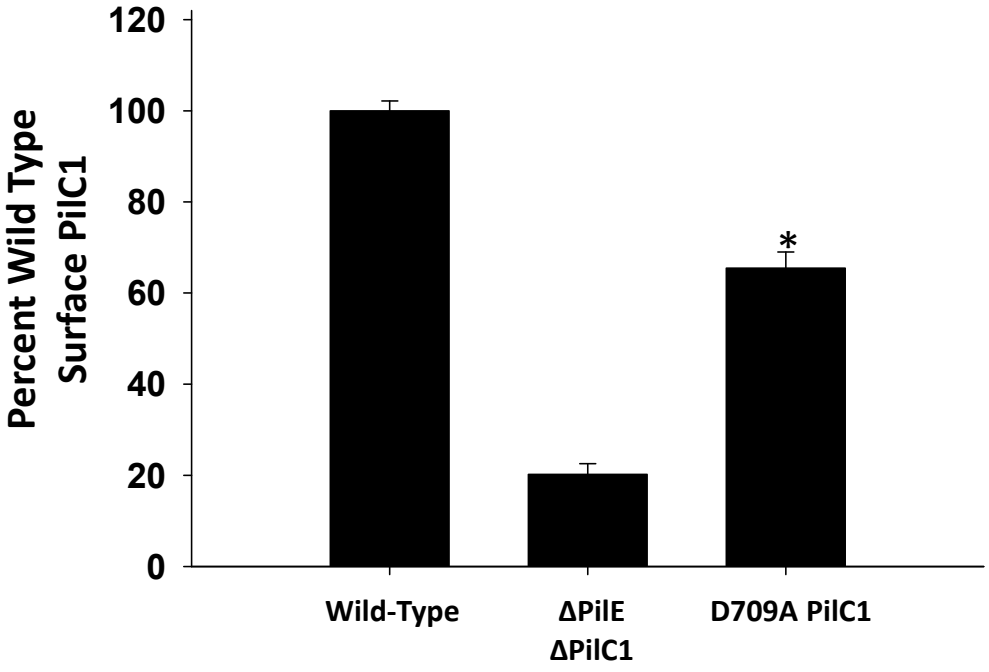
Percent Wild Type Surface PilC1
120
100
80
60
40
20
0
*
Wild-Type
ΔPilE ΔPilC1
D709A PilC1

Figure 5.5

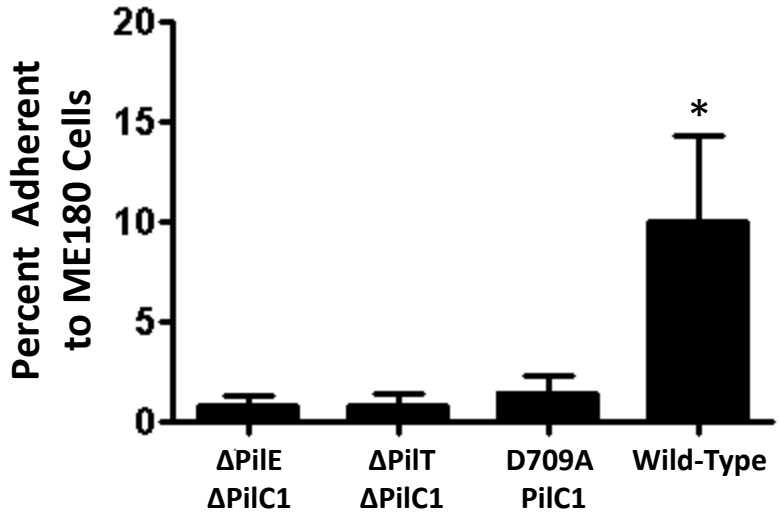
Percent Adherent to ME180 Cells
20
15
10
5
0
*
ΔPilE ΔPilC1
ΔPilT ΔPilC1
D709A PilC1
Wild-Type

Figure 5.6

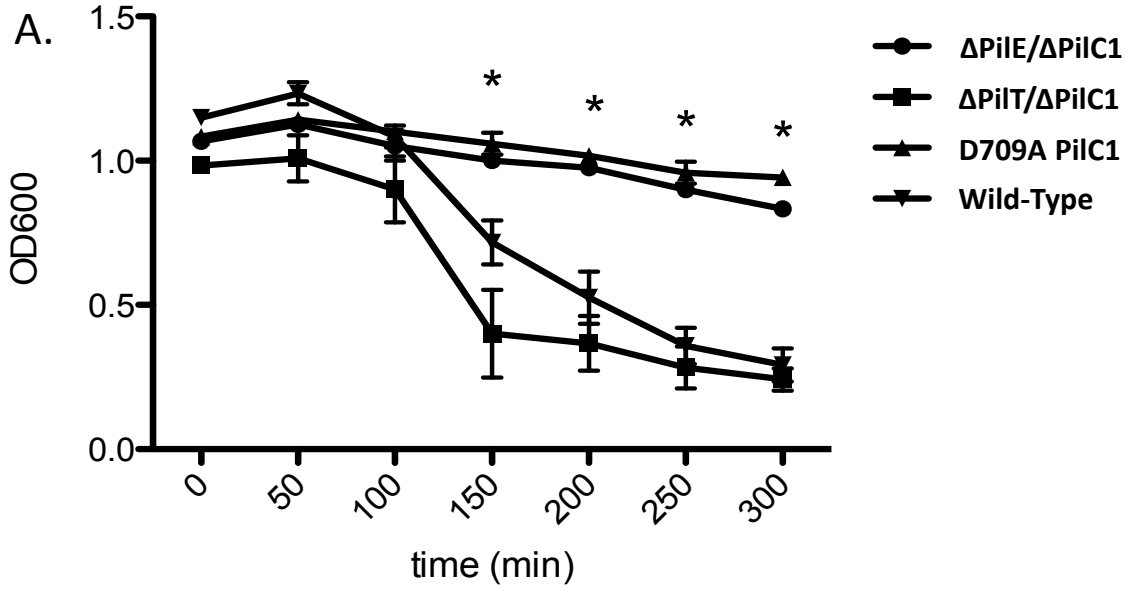
A.
1.5
1.0
0.5
0.0
OD600
0
50
100
150
200
250
300
time (min)
*
*
*
*
ΔPilE/ΔPilC1
ΔPilT/ΔPilC1
D709A PilC1
Wild-Type

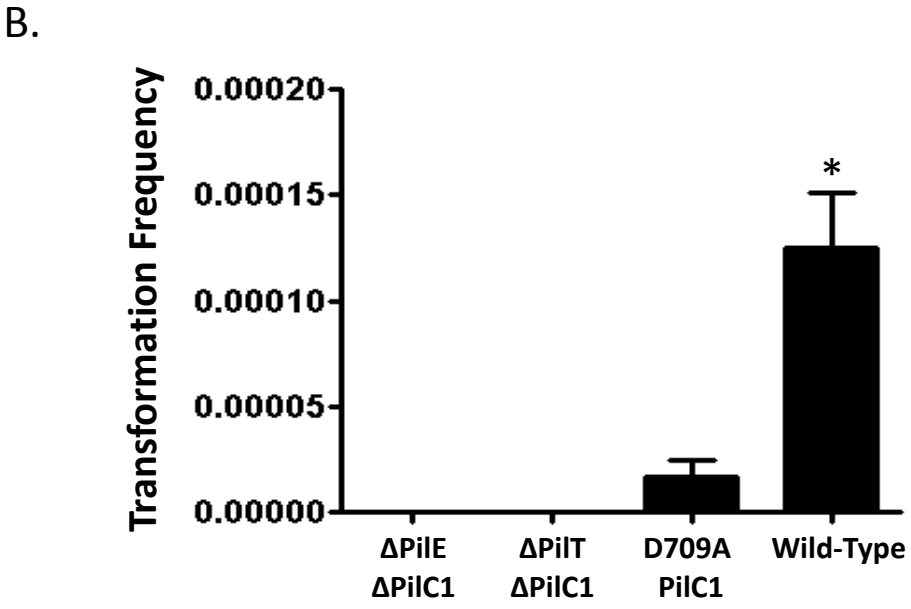
B.
Transformation Frequency
0.00020
0.00015
0.00010
0.00005
0.00000
*
ΔPilE ΔPilC1
ΔPilT ΔPilC1
D709A PilC1
Wild-Type

5.6 References

1. Swanson J (1973) Studies on gonococcus infection. IV. Pili: their role in attachment of gonococci to tissue culture cells. J Exp Med 137: 571-589.

2. McGee ZA, Stephens DS, Hoffman LH, Schlech WF, 3rd, Horn RG (1983) Mechanisms of mucosal invasion by pathogenic Neisseria. Rev Infect Dis 5 Suppl 4: S708-714.

3. Craig L, Pique ME, Tainer JA (2004) Type IV pilus structure and bacterial pathogenicity. Nat Rev Microbiol 2: 363-378.

4. Wall D, Kaiser D (1999) Type IV pili and cell motility. Mol Microbiol 32: 1-10.

5. Strom MS, Nunn DN, Lory S (1994) Posttranslational processing of type IV prepilin and homologs by PilD of Pseudomonas aeruginosa. Methods Enzymol 235: 527-540.

6. Mattick JS (2002) Type IV pili and twitching motility. Annu Rev Microbiol 56: 289-314.

7. Alm RA, Mattick JS (1997) Genes involved in the biogenesis and function of type-4 fimbriae in Pseudomonas aeruginosa. Gene 192: 89-98.

8. Rahman M, Kallstrom H, Normark S, Jonsson AB (1997) PilC of pathogenic Neisseria is associated with the bacterial cell surface. Mol Microbiol 25: 11-25.

9. Rudel T, Scheurerpflug I, Meyer TF (1995) Neisseria PilC protein identified as type-4 pilus tip-located adhesin. Nature 373: 357-359.

10. Morand PC, Tattevin P, Eugene E, Beretti JL, Nassif X (2001) The adhesive property of the type IV pilus-associated component PilC1 of pathogenic Neisseria is supported by the conformational structure of the N-terminal part of the molecule. Mol Microbiol 40: 846-856.

11. Scheuerpflug I, Rudel T, Ryll R, Pandit J, Meyer TF (1999) Roles of PilC and PilE proteins in pilus-mediated adherence of Neisseria gonorrhoeae and Neisseria meningitidis to human erythrocytes and endothelial and epithelial cells. Infect Immun 67: 834-843.

12. Kallstrom H, Liszewski MK, Atkinson JP, Jonsson AB (1997) Membrane cofactor protein (MCP or CD46) is a cellular pilus receptor for pathogenic Neisseria. Mol Microbiol 25: 639-647.

13. Kallstrom H, Blackmer Gill D, Albiger B, Liszewski MK, Atkinson JP, et al. (2001) Attachment of Neisseria gonorrhoeae to the cellular pilus receptor CD46: identification of domains important for bacterial adherence. Cell Microbiol 3: 133-143.

14. Kirchner M, Heuer D, Meyer TF (2005) CD46-independent binding of neisserial type IV pili and the major pilus adhesin, PilC, to human epithelial cells. Infect Immun 73: 3072-3082.

15. Orans J, Johnson MD, Coggan KA, Sperlazza JR, Heiniger RW, et al. (2010) Crystal structure analysis reveals Pseudomonas PilY1 as an essential calcium-dependent regulator of bacterial surface motility. Proc Natl Acad Sci U S A 107: 1065-1070.

16. Morand PC, Bille E, Morelle S, Eugene E, Beretti JL, et al. (2004) Type IV pilus retraction in pathogenic Neisseria is regulated by the PilC proteins. Embo J 23: 2009-2017.

17. Stols L, Gu M, Dieckman L, Raffen R, Collart FR, et al. (2002) A new vector for high-throughput, ligation-independent cloning encoding a tobacco etch virus protease cleavage site. Protein Expr Purif 25: 8-15.

18. Kellogg DS, Jr., Cohen IR, Norins LC, Schroeter AL, Reising G (1968) Neisseria gonorrhoeae. II. Colonial variation and pathogenicity during 35 months in vitro. J Bacteriol 96: 596-605.

19. Abramoff MD, Magalhaes, P.J., Ram, S.J. (2004) Image Processing with ImageJ. Biophotonics International 11: 36-42.

20. Strom MS, Lory S (1993) Structure-function and biogenesis of the type IV pili. Annu Rev Microbiol 47: 565-596.

21. Wolfgang M, Lauer P, Park HS, Brossay L, Hebert J, et al. (1998) PilT mutations lead to simultaneous defects in competence for natural transformation and twitching motility in piliated Neisseria gonorrhoeae. Mol Microbiol 29: 321-330.

22. Rice PA, Schachter J (1991) Pathogenesis of pelvic inflammatory disease. What are the questions? JAMA 266: 2587-2593.

23. Thompson EC, Brantley D (1996) Gonoccocal endocarditis. J Natl Med Assoc 88: 353-356.

CHAPTER 6

Past and Future Studies of *Pseudomonas aeruginosa* PilY1, PilY2, and *Neisseria gonorrhea* PilC1

6.1 Introduction

There are a number of characterization studies that were performed using *Pseudomonas aeruginosa* PilY1 and PilY2 both *in vitro* and in the organism that did not make into publications. These experiments include, but are not limited to, crystallization studies, binding experiments, and twitching assays. In addition, a number of future experiments are outlined for both *Pseudomonas aeruginosa* PilY1 and *Neisseria gonorrhea* PilC1.

6.2 Pseudomonas aeruginosa PilY1

6.2.1 PilY1 Purification

There were many constructs that were made in an attempt to get the full length or N-terminal construct of PilY1 (Table 6.1). The vectors included were in the pMCSG18 LIC-HIS vector, pET 22b(+) containing the periplasmic targeting leader sequence, pelB. There were many reasons for trying to get this protein such as for a potential crystallization target. There were also a variety of cells lines that each construct was tired in (Table 6.1). One goal would be to insert the protein in crystal trials in an attempt to elucidate the atomic structure of the

full protein. Viewing the intramolecular interactions is important for understanding other possible functions of PilY1, specifically how it might interact with the membrane or pilus. Of the additional constructs made after the two listed previously in this dissertation (615-1163 and 532-1163), six other constructs expressed, but were shorter than the 532 construct, while one longer construct weakly expressed (354-1163) with the pelB leader sequence. The 354-1163 construct degraded however, and was mostly soluble aggregate.

6.2.2 PilY1 Crystallization

A number of screens were conducted for the 532-1163 (mostly in the buffer 10mM Tris pH 7.8 50mM NaCl) at 10 mg/mL. Protein was mono-disperse up to 15 mg/mL (Figure 6.1). Screens included Morpheus, Classics, classics lite, PEG I, PEG II, PEGrx, SaltRx, PEG/ION, JCSG+, and JCSG1-4. 532-1163 PilY1 was also sent to the Hauptman-Woodward Institute. The best crystal hit appeared in 9 days at 16^{o}C was in the PEG II screen condition H6 (100mM Tris pH 8.5 8% PEG 8000) (Figure 6.2). However, the observed molecular weight of these crystals as determined by SDS page gel was degraded to ~48 kD, the same size seen in the trypsin limited proteolysis (Figure 6.3A, B). This represented the possible beginning site of the domain swap from C-terminal structure (residues 721-726); thus, constructs were designed to reflect both of these starting points [1]. Future crystallization trials with one of these constructs have yet to be conducted; even so, these constructs would most likely yield no new structural data.

6.2.3 PilY1 Metal Binding

Calcium and manganese can have the same coordination and thus, in some cases, these two elements can bind in the same location. This phenomenon is most evident in the αVβ3 structures, consensus calcium binding sites can bind to both calcium and manganese [2,3]. Therefore, we wanted to test PilY1's ability to bind manganes. To accomplish this goal, we first made sure the Oregon Green fluorescent chelater would bind to manganese, to which it did with a K_d of 3 μM, thus binding better than it does to calcium (Figure 6.4A). We then used the 615-1163 construct of PilY1 to test the manganese binding affinity of the 851-859 site. We measured a K_d of 5 μM, thus, we confirmed that these site indeed binds manganese and that said binding is roughly two-fold lower than to calcium (Figure 6.4B) [1].

6.2.4 RGD mutations in PAK PilY1 in vivo assays

R619A (AGD) and D621A (RGA) mutations were made in the PAK strain of PilY1 using the process described in chapter 2 [1]. Before testing the adherence of these bacteria to transformed cell lines, it was necessary to measure if other common bacterial attributes were affected. The first question was if the mutants would make wild type levels of PilY1 expressed in *P. aeruginosa*. Wild type levels of mutant PilY1 were expressed at 50 μM IPTG consistent with the expressed wild type protein (Figure 6.5). Recall that PilY1 was deleted from *P. aeruginosa*, and added back via the same method as the mutants were added (PilY1+).

The next things to test for were how the mutations affected twitching motility and surface piliation. Both methods were performed as in Chapter 2 [1]. Twitching motility between the aforementioned strains was also statistically similar indicating that the RGD

mutations had the same overall motility (Figure 6.6A). Also, the amount of PilA made in the R619A and D621A mutations was consistent with the PilY1+ strain (Figure 6.6B).

Finally, the mutations were tested for adherence versus HeLa cells. A monolayer of HeLa cells were grown in a 24 well dish using standard HeLa cell culturing practices. PilY1+, PilY1-, AGD, and RGA strains of *P. aeruginosa* at O.D. .08 or just media with no bacteria were incubated with the HeLa cells with the appropriate amount of IPTG for 1 hour. Wells were then washed with PBS 3 times, serial diluted, and plated. The diluted inoculum was also plated for a method of comparison. The PilY1+ bound to roughly 11% of the inoculum, which is consistent with previous reports involving wild type PilY1 and HeLa cells (Figure 6.7) [4]. The PilY1- strain was close to 0% as expected (Figure 6.7). Mutating the aspartic acid drastically reduced the adhesion by almost an order of magnitude whereas the AGD mutation seemed to have very little effect (Figure 6.7). As in Chapter 3, the aspartic acid of the RGD is absolutely necessary for integrin binding. Previously published reports suggest that the arginine might not be as necessary for adhesion, explaining why adhesion was seen in this experiment [5,6]. Perhaps the AGD mutant conveyed a small amount of binding and the cells were saturated, hence no amount of dilutions post collection would have shown less binding. If the previous hypothesis is correct, one could use a smaller amount of bacteria as the original inoculum to detect a better difference between the PilY1+ and the AGD mutation.

Adding these mutations (or the calcium binding site mutations) to the chromosome would also be advantageous. As such, they were added to PAK, but these new strains ability to produce intracellular PilA and PilY1 were not consistent with wild type PAK. Interestingly, in making each mutation, half of the crosses were not successful in that they still contained the wild type PilY1, yet, they had the same morphology of the mutations, not the wild type PAK. Therefore, these new strains could be used as attenuated forms of PAK

and inserted into various adhesion assays, contingent upon making consistent amounts of PilY1 and PilA. Ideally, these strains would be used in animal models to test for infection rates. Two interesting models of note would be in the burn wound mouse model or the CF mouse model [7]. Also interesting would be to add these mutations to a GFP *P. aeruginosa* and look for infection of transparent organism (that have the required integrins) such as zebrafish [8].

6.2.5 Potential PilY1 Small Molecule Inhibitor Assay

PilY1 calcium binding is necessary for functional pilus biogenesis [1]. Thus, eliminating the ability of PilY1 to bind calcium would yield a potential therapeutic approach. The best way to identify a small molecule inhibitor is through high-throughput screen. For this experiment, there are three essential components: the protein, calcium, and something to detect calcium binding.

Ideally, this experiment would be based on the calcium binding curve seen in Chapter 2 Figure 2.2D, where the calcium binding affinity of 615-1163 PilY1. Recall that in this experiment, Oregon Green was kept at 20 μM, the PilY1 concentration was titrated, and the calcium chloride concentration was kept 2 μM, thus leading to the competition over calcium. The PilY1 amount would be added at the EC_{50} of 3.2 μM (Figure 6.8A). Small molecules would be added to each well to detect a change in fluorescence (Figure 6.8B).

The optimal solution would be a compound that sterically blocks calcium from binding to PilY1 (Figure 6.8B). This result would be indicated with an increase in fluorescence implying the Oregon Green is binding more calcium in solution. A potential pitfall would be that the compound is a calcium or general metal chelator and the readout would show that there is no fluorescence (Figure 6.8B). Consequently, this fluorescence

could also mean that the compound caused PilY1 to bind calcium tighter. This scenario could also be an acceptable solution because the bacteria would not be able to twitch due to essentially having “dead legs” [1].

6.2.6 PilY1 H797 Mutation

A conserved histidine within *P. aeruginosa* at position 797 in PAK PilY1 makes a hydrogen bond with D859 (Figure 6.9) [1]. As can be seen in Chapter 2, this histidine is also conserved in *N. gonorrhoeae*. Without calcium bound, the residues of the 851-859 CBS could sterically force the histidine to interfere with the beta-propeller or the α-helix 6. A H797A mutation of this amino acid has been made in PilY1 but has yet to be tested. Analysis of how this mutation affects calcium binding, twitching motility and extracellular pilus production may yield new insight into how calcium mediates functional pilus biogenesis. Specifically, it may begin to provide evidence of the small structural changes that occur when PilY1 binds calcium.

6.2.7 P. aeruginosa Biofilm Formation in the Presence of Host Cells

Bacterial biofilm formation is a measure of how these organisms can sense each other in their environment. Functional biofilm development is tfp-dependent [9]. The sugar subunit of biofilms can be stained using Alcian Blue for detection; crystal violet can be used to stain the bacteria [10]. Glass slides will be inoculated and fixed after 18 hours, washed and stained with the aforementioned dyes for detection of bacteria and biofilms [10]. Because the RGD and proximal calcium mutations do not affect piliation or twitching, these strains are expected to produce wild type morphology and levels of biofilm.

6.2.8 Exotoxin Secretion

Bacterial exotoxin production can be used as a measure of how bacteria perceive their environment, specifically detection of host cells. Using wild type PAK, a baseline level of exotoxin A and exoenzyme S can be measure by examining the media of the growing bacteria without host cell stimuli. Once the baseline is established, *P. aeruginosa* with detrimental and calcium mimicking mutations in one or both sites will be measured for toxin production and secretion with and without host cell stimuli. The amount of exotoxin A and exoenzyme S will be ascertained via western blot analysis across several time points (sigma-aldrich and abcam respectively). A fold increase will be measured in the presence of host cell stimuli, which will then be normalized to the amount of bacteria added, and shown as percent increase (or decrease) in secreted virulence factors. The mutants tested would be the proximal calcium binding site mutants, D608A and D608K, and the RGD mutations. It is expected that the only mutation that gives wild type levels of toxin secretion will be the D608K mutation. Recall that in a the D859A mutation, the tfp would never make it out the cell to bind.

6.2.9 Host Cell Viability

Another measure of bacterial pathogenicity is the ability to infect and/or kill host cells. In this experiment, human corneal and lung epithelial cells will be inoculated with *P. aeruginosa* containing PilY1 with point mutations in the Ca^{2+} binding domain or of the surrounding area. After multiple time points, cell samples will be stained with annexin V, an antibody for apoptosis (BD biosciences), and examined using flow cytometry. These results should be consistent with the toxin screen results.

6.3 Pseudomonas aeruginosa PilY2

6.3.1 PilY2 Expression

PilY2 is an 114 amino acid 15 kD protein that is in the *fimU-pilVWXY1Y2E* operon that is regulated by AlgR in *P. aeruginosa* thought to play a role in fimbrial biogenesis [11]. Because *pilY2* is directly downstream *pilY1* in the operon and therefore in theory co-expressed with PilY1, it was thought that PilY2 could be a potential binding partner. Therefore we sought to purify the full length PilY2 from the PAK strain of *P. aeruginosa*. Cloning in the pMCSG18 LIC-HIS vector, we were able to solubly express full length PilY2, including the predicted signal peptide from residues 1-18 (Figure 6.10A) [12]. PilY2 appeared to be well folded mix of α-helicies and β-sheets with no significant traces of random coil on CD (Figure 6.11).

6.3.2 PilY2 Binding Experiments

We added 532-1163 PilY1 and full length PilY2 in a mixture and attempted to co-elute the proteins on a sizing column. Results show that there was no binding between the two proteins (Figure 6.10B). It is possible that these proteins do interact, but in the N-terminal domain only. Such experiments are difficult due to the insolubility problems of N-terminal PilY1. Binding experiments with 354-1163 PilY1 have not been tried, nor has any other direct binding assay.

6.3.3 PilY2 Crystallization Trials

PilY2 at 10 mg/mL in 10mM Tris pH 7.8 and 50mM NaCl was also included in crystal trials using Classics, classics lite, PEG I, PEG II, PEGrx, SaltRx, PEG/ION screens. No significant hits were observed.

6.4 Neisseria gonorrhoeae PilC1

6.4.1 Putative Neisseria gonorrhoeae PilC1 calcium binding domain

As seen in Chapter 5 of this dissertation, *N. gonorrhoeae* PilC1 has one confirmed calcium binding site. However, there could be another potential calcium binding site at residue 516 consisting of DNDKPRDLGD (Figure 6.12). This putative binding domain is located outside of the C-terminal construct tested for calcium binding. Although not identical, this putative binding site has some characteristics of the DxDxDG calcium binding motif, the consensus 9 amino acid, and 12 amino acid calmodulin-like calcium binding domains [13,14]. A BLAST search revealed that this region is conserved in roughly 75% of the other GC PilC proteins, not always distinguishing between the PilC1 and PilC2. This search also revealed that many of the sequences had the 9 amino acid putative calcium binding domain, therefore lining up with the site at 700-709 in *N. gonorrhoeae* PilC1. The region is also not present in any of the PilCs in *Neisseria meningitidis*. With the current reagent of D709A full length *N. gonorrhoeae* PilC1, this hypothesis could be tested. As seen in PilY1 (Chapter 3), putative calcium binding domain could affect the adhesion mechanism itself.

6.5 Figure Legends

Table 6.1 List of PilY1 protein constructs created.

Figure 6.1 Dynamic light scattering of 532-1163 PAK PilY1. Peak 1 and 2 show that the sample was mono-dispersed with a value 11.8% (%pd<15%).

Figure 6.2 Crystal hit of 532-1163 PilY1 in PEG II screen condition H6 (100mM Tris pH 8.5 8% PEG 8000). Bar represents 100 microns.

Figure 6.3 PilY1 protein degradation in crystal. A. SDS gel of 532-1163 Pak PilY1 crystals and protein from the entire over-nucleated drop.

Figure 6.4 PilY1 binds manganese. Assay was performed as in Chapters 2, 3 and 4 with manganese being

Figure 6.5 Infrared scan of a western blot showing IPTG induced PilY1 in whole cell PAK. Blot was scanned on an Odyssey Infrared Imaging System (LI-COR). PAK was grown in culture to O.D. =.6, lysed and diluted, and run on an SDS page gel. Gel was then transferred and stained with anti-PilY1 antibody. Secondary was infrared mouse anti-rabbit antibody.

Figure 6.6 Twitching and surface pilin expression in PAK. A. Twitching assays and B. pilus preps were performed as outlined in Chapter 2.

Figure 6.7 Adhesion assay with PAK PilY1 RGD mutations. *represents p<.05. Values represented as % inoculum. Inoculum represents bacteria from the same stock that was added to wells, but directly to the agar plate instead.

Figure 6.8 Small molecule inhibition of PilY1. A. Model of how the assay works with no inhibitor present. Fluorescence is inversely proportional to the concentration of PilY1. B. Model of how the assay works with the small molecule screen. The first panel shows what happens if the compound does nothing. The second panel shows if the molecule is a chelating compound or a compound that makes PilY1 bind more tightly to calcium. The third panel shows the theoretical result of a steric non chelating compound that blocks PilY1's ability to bind calcium.

Figure 6.9 PyMOL image of H797 interacting with the CBS of C-terminal PilY1 using the coloring found in Chapter 2

Figure 6.1. Chromatograms and SDS Page gels of PAK PilY2. A. S75 Gel filtration profile and gel of purified PilY2. B. S200 Gel Filtration profile and gel of combined 532-1163 PilY1 and PilY2 protein.

Figure 6.11 Circular dichroism wavelength scan of PilY2. Experiments were performed as in Chapters 2,3,4 and 5.

Figure 6.12 Putative *N. gonorrhoeae* PilC1 calcium binding site.

Table 6.1

	Pa PilY1 Construct	BL21	BL21 RIPL	Origami 2
1	2-614	-	-	-
2	31-614	-	-	-
3	2-491	-	-	-
4	31-491	-	-	-
5	2-326	-	-	-
6	31-326	-	-	-
7	2-292	-	-	-
8	31-292	-	-	-
9	46-287	-	-	-
10	46-330	-	-	-
11	46-489	-	-	-
12	46-618	-	-	-
13	46-1158	-	-	N/A
14	49-321	-	-	-
15	49-372	-	-	-
16	49-598	-	-	-
17	127-321	-	-	-
18	127-372	-	-	-
19	127-598	-	-	-
20	156-321	-	-	-
21	156-372	-	-	-
22	156-598	-	-	-
23	49-1158	-	-	N/A
24	127-1158	-	-	N/A
25	156-1158	-	SA	N/A
26	354-1163	-	+	N/A
27	615-1163	++++	N/A	N/A
28	532-1163	++++	N/A	N/A
29	565-1163	++++	N/A	N/A
30	565-1097	++++	N/A	N/A
31	551-1097	++++	N/A	N/A
32	551-1163	++++	N/A	N/A
33	721-1163	++++	N/A	N/A
34	726-1163	++++	N/A	N/A

Figure 6.1

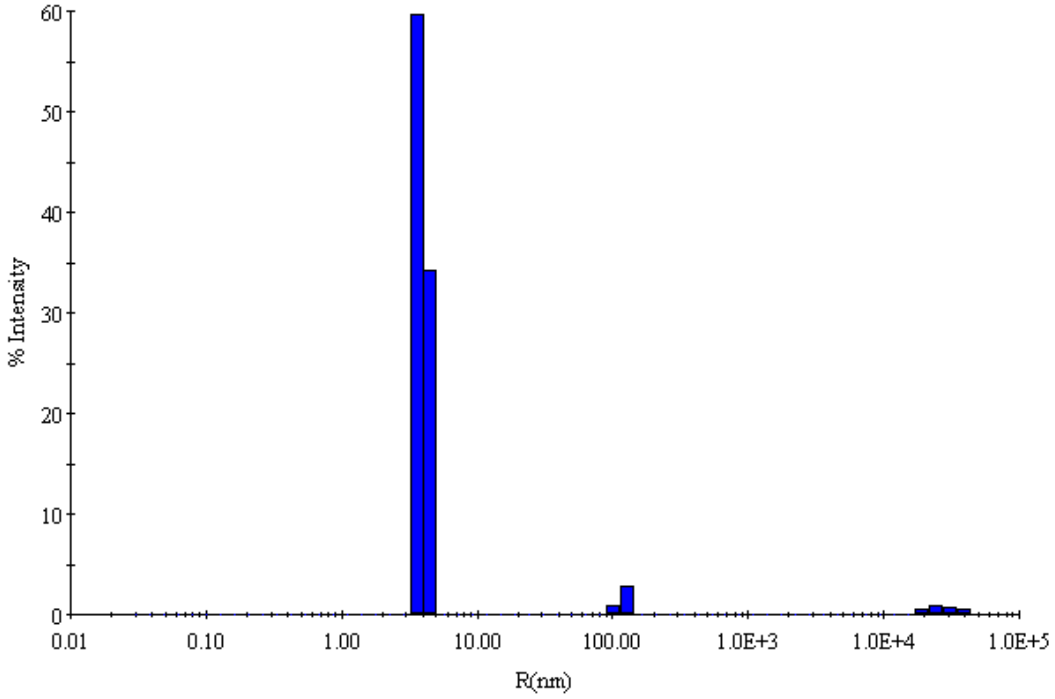

Item	R (nm)	%Pd	MW-R (kDa)	%Int	%Mass
Peak 1	0.0	11.4	0	----	----
Peak 2	4.0	11.8	84	93.8	97.8
Peak 3	121.9	9.6	255876	3.6	0.0
Peak 4	28257.2	24.1	87484200000	2.6	2.2

Figure 6.2

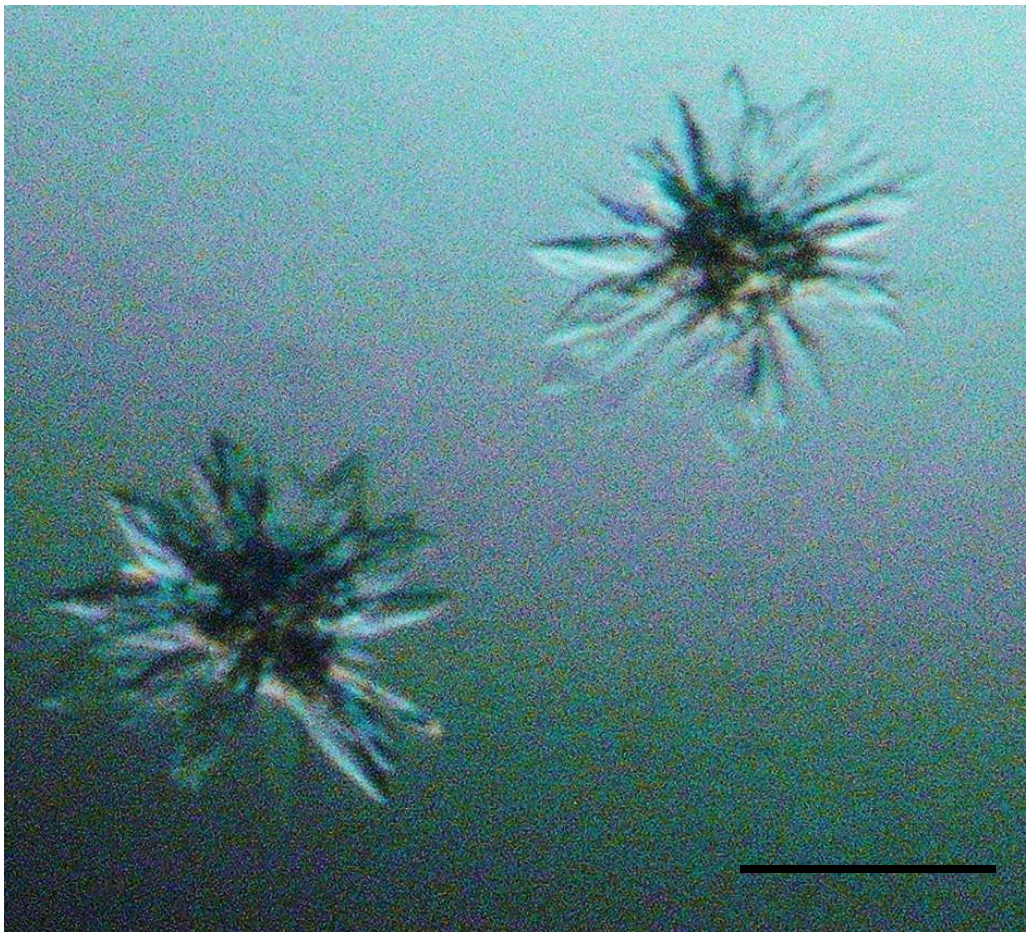

Figure 6.3

A.

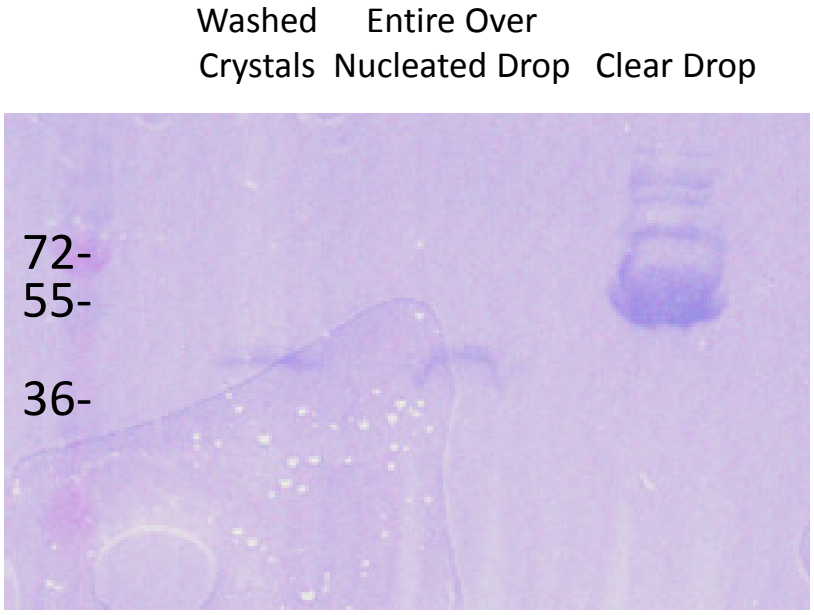
Washed Crystals
Entire Over Nucleated Drop
Clear Drop
72-
55-
36-

B.

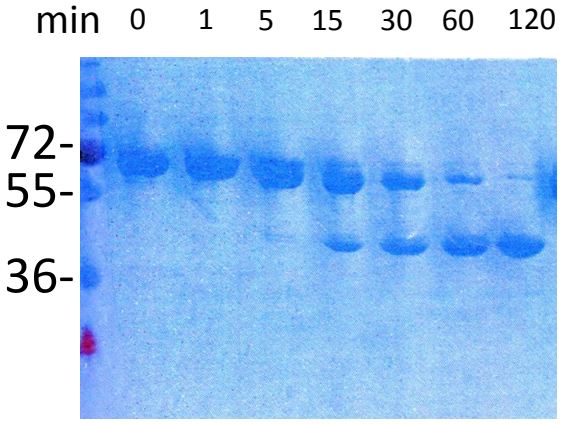
min 0 1 5 15 30 60 120
72-
55-
36-

Figure 6.4

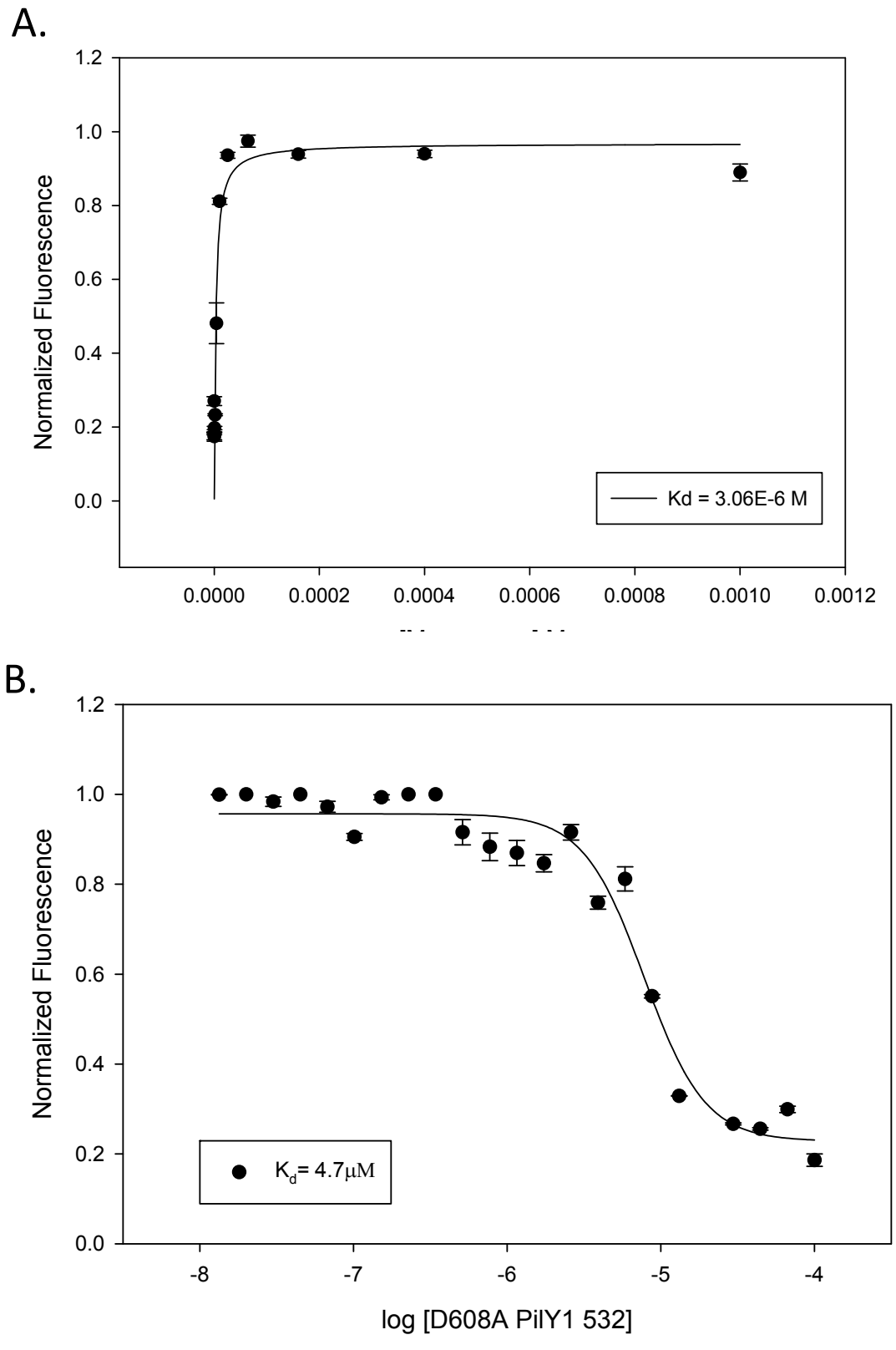
A.
Normalized Fluorescence
1.2
1.0
0.8
0.6
0.4
0.2
0.0
Kd = 3.06E-6 M
0.0000
0.0002
0.0004
0.0006
0.0008
0.0010
0.0012
B.
Normalized Fluorescence
1.2
1.0
0.8
0.6
0.4
0.2
0.0
K$_d$= 4.7μM
-8
-7
-6
-5
-4
log [D608A PilY1 532]

Figure 6.5

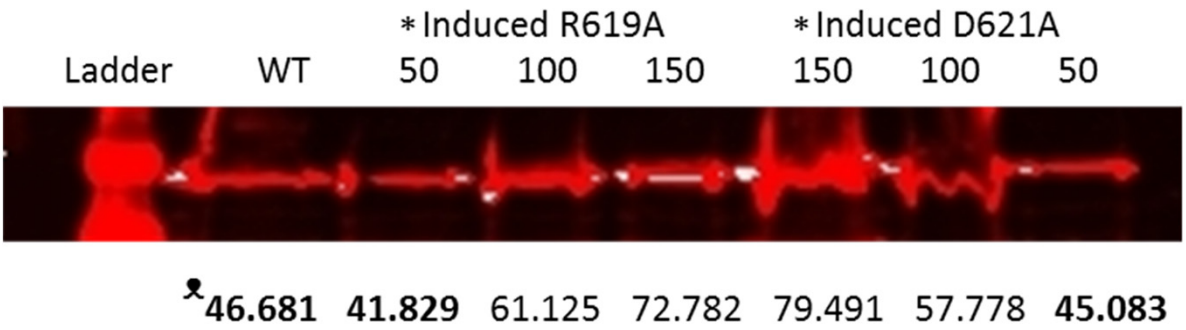

* Induced values correspond to µM IPTG concentration

Fluorescent quantification numbers measured by ImageJ

Figure 6.6

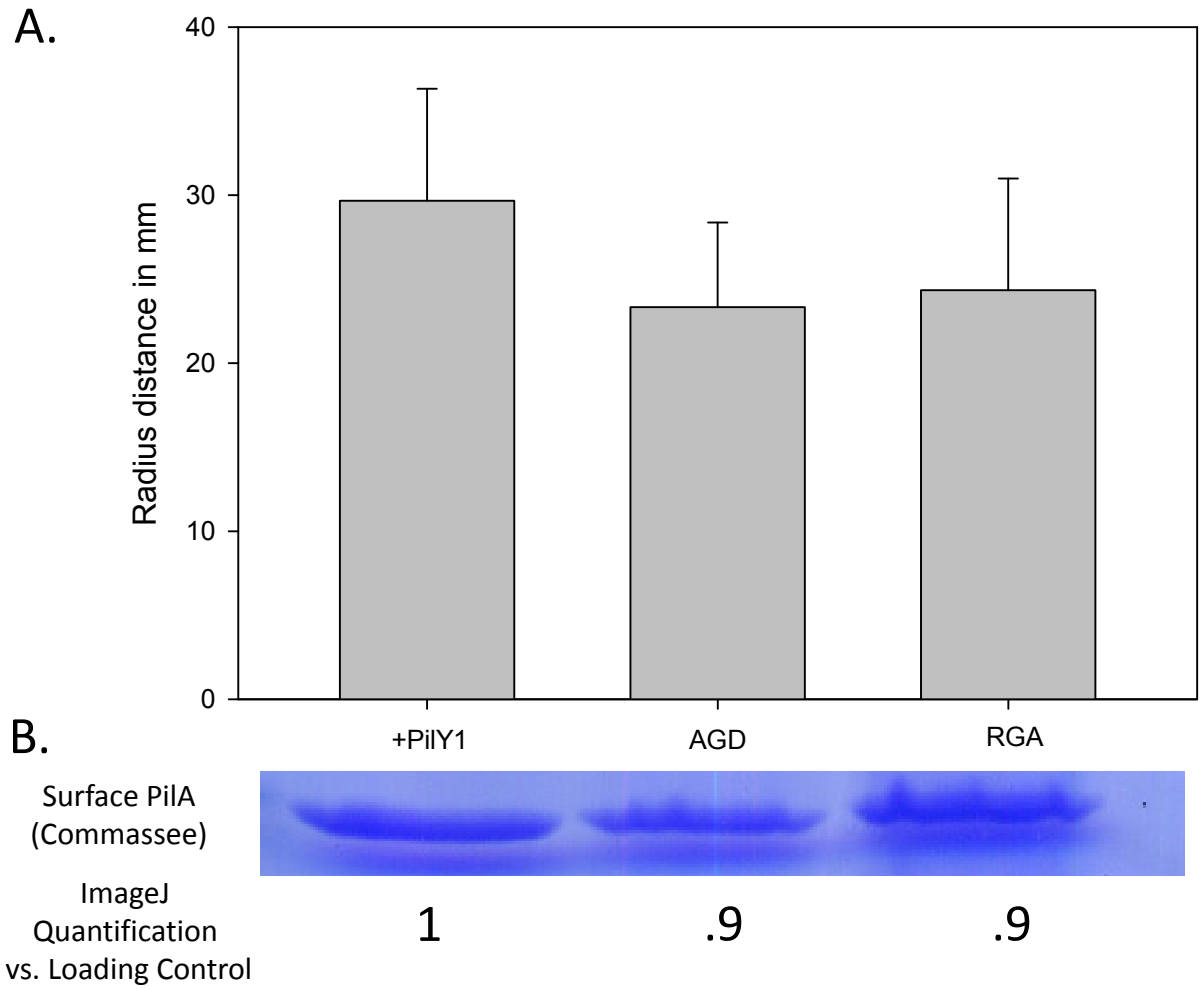
A.
Radius distance in mm
40
30
20
10
0
+PilY1
AGD
RGA
B.
Surface PilA
(Commassee)
ImageJ
Quantification
vs. Loading Control
1
.9
.9

Figure 6.7

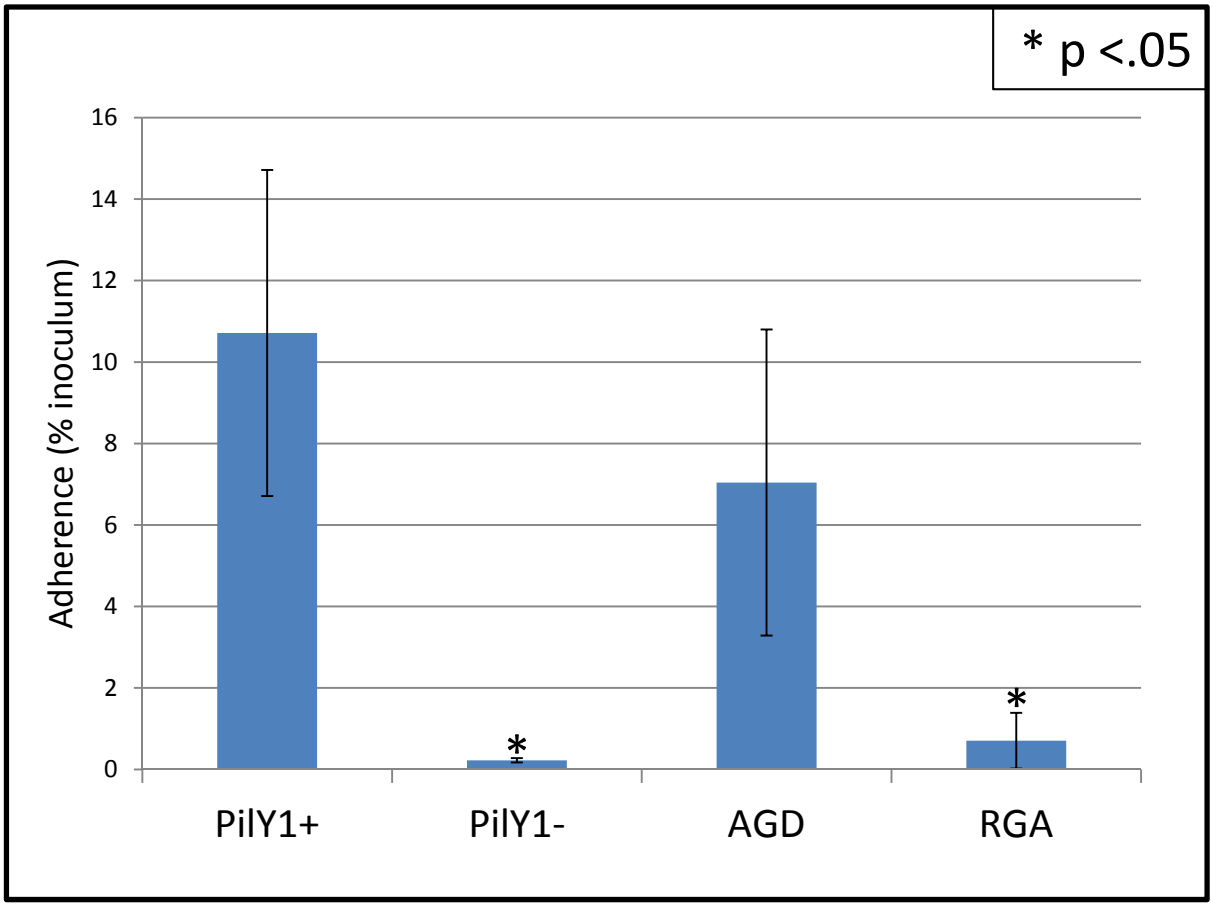

Figure 6.8

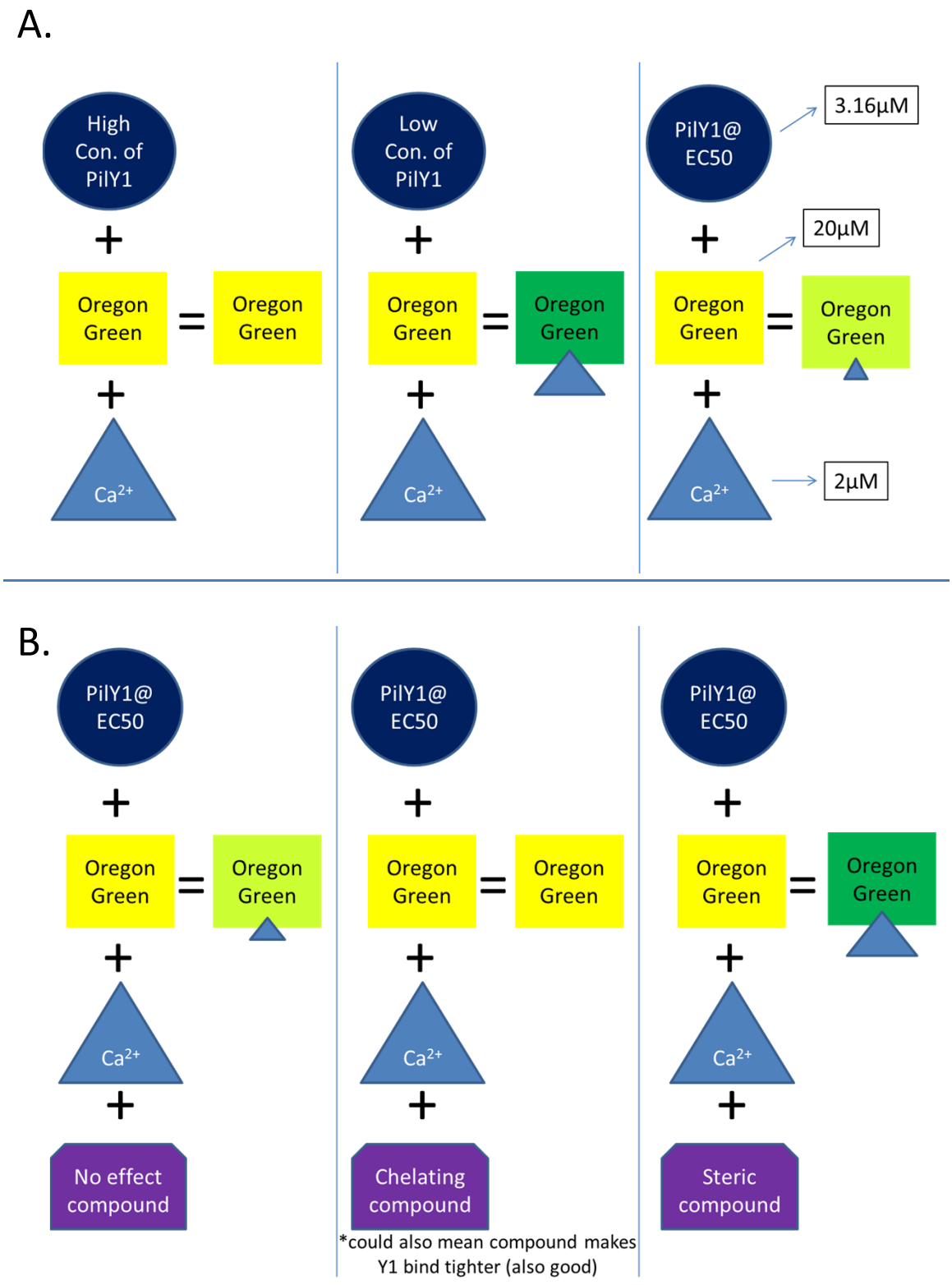
A.
High Con. of PilY1
Oregon Green
=
Oregon Green
Ca2+
Low Con. of PilY1
Oregon Green
=
Oregon Green
Ca2+
PilY1@ EC50
3.16µM
20µM
Oregon Green
=
Oregon Green
Ca2+
2µM
B.
PilY1@ EC50
Oregon Green
=
Oregon Green
Ca2+
No effect compound
PilY1@ EC50
Oregon Green
=
Oregon Green
Ca2+
Chelating compound
*could also mean compound makes Y1 bind tighter (also good)
PilY1@ EC50
Oregon Green
=
Oregon Green
Ca2+
Steric compound

Figure 6.9

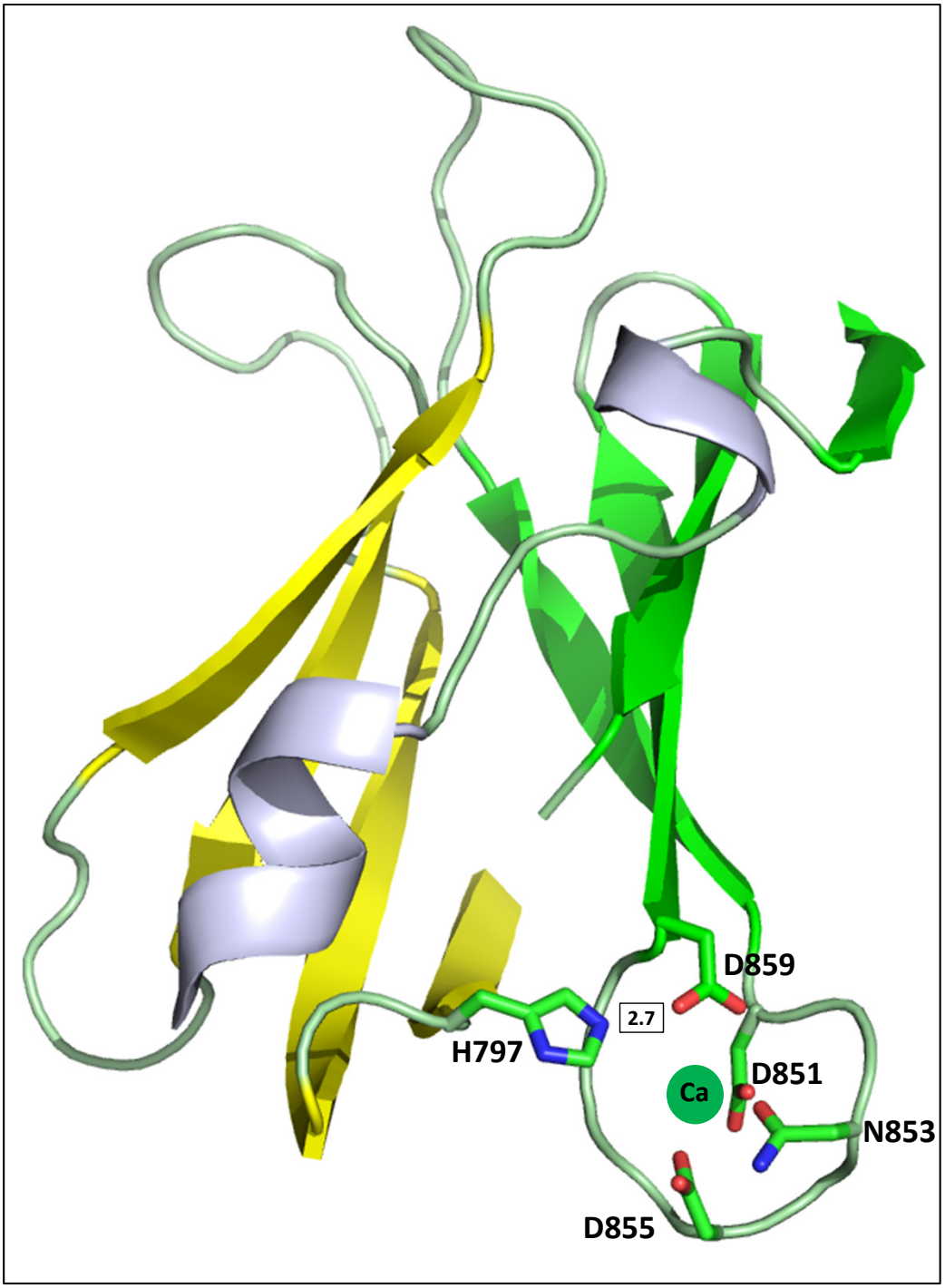

Figure 6.10

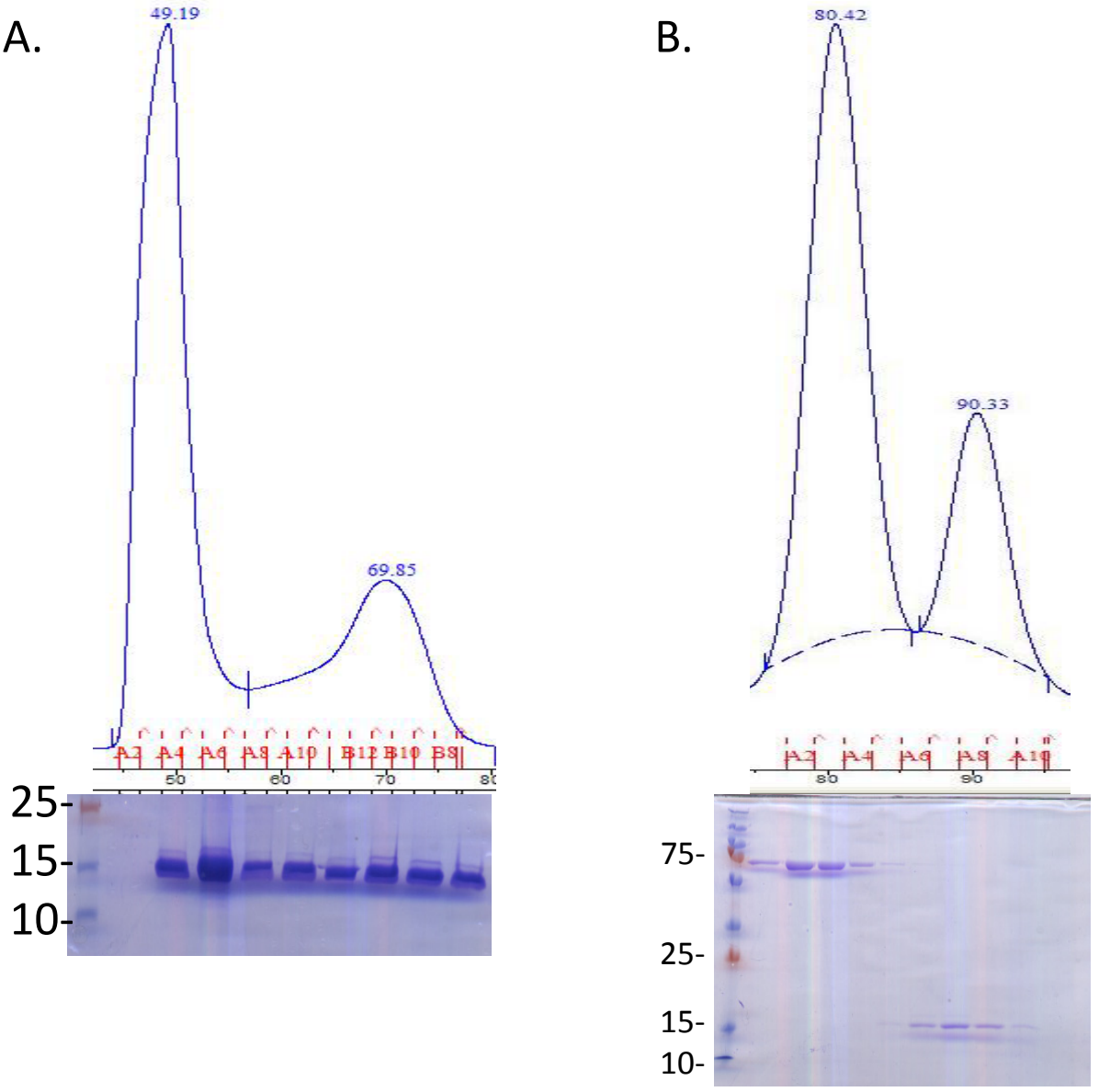

Figure 6.11

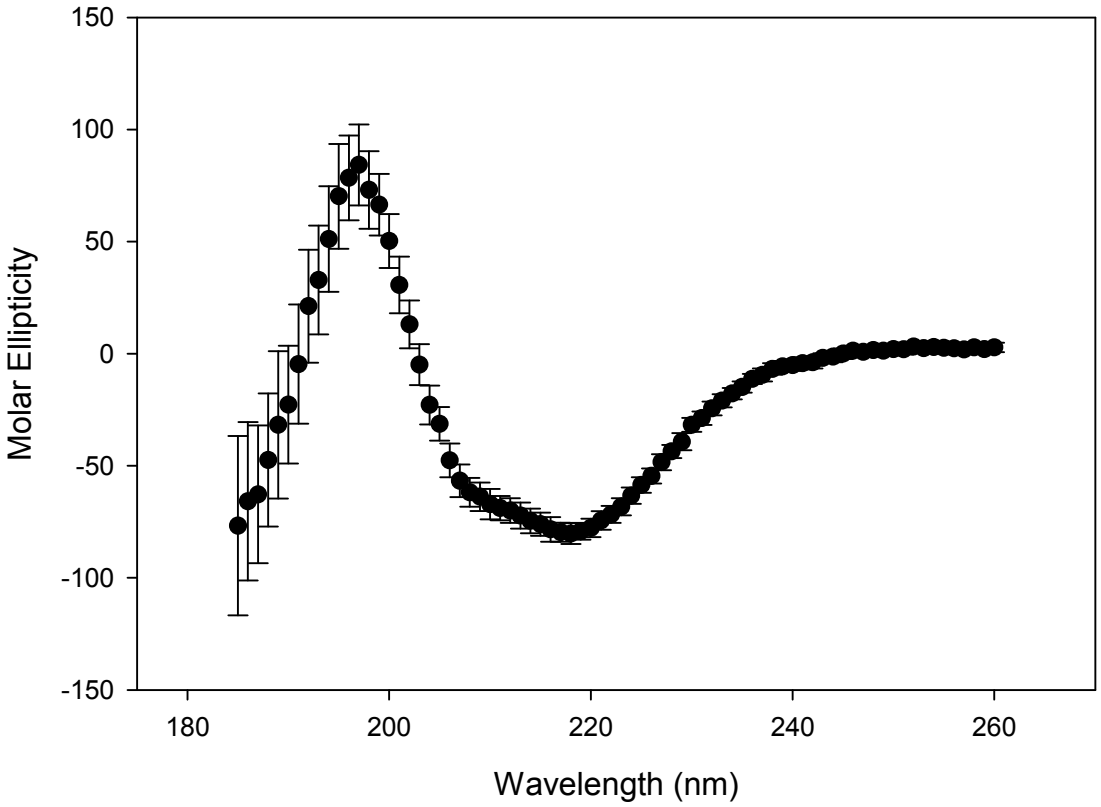
150
100
50
0
-50
-100
-150
Molar Ellipticity
180
200
220
240
260
Wavelength (nm)

Figure 6.12

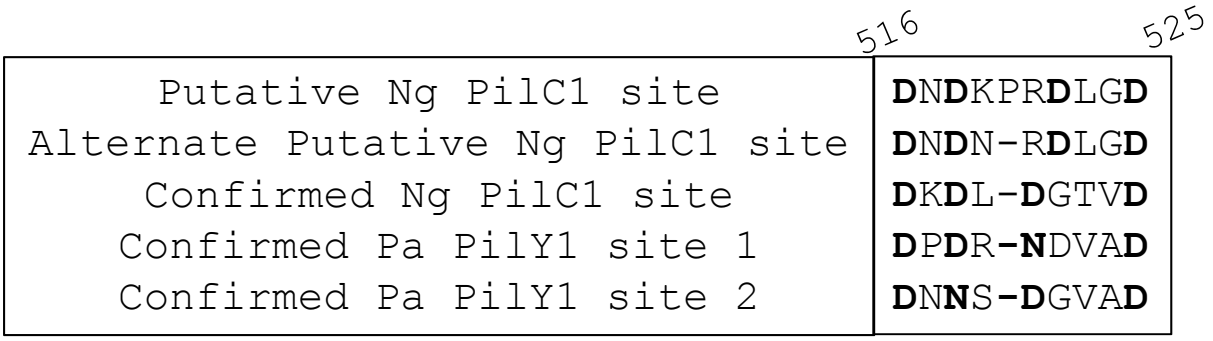
516
525
Putative Ng PilC1 site
Alternate Putative Ng PilC1 site
Confirmed Ng PilC1 site
Confirmed Pa PilY1 site 1
Confirmed Pa PilY1 site 2
DNDKPRDLGD
DNDN-RDLGD
DKDL-DGTVD
DPDR-NDVAD
DNNS-DGVAD

6.6 References

1. Orans J, Johnson MD, Coggan KA, Sperlazza JR, Heiniger RW, et al. (2010) Crystal structure analysis reveals Pseudomonas PilY1 as an essential calcium-dependent regulator of bacterial surface motility. Proc Natl Acad Sci U S A 107: 1065-1070.

2. Xiong JP, Stehle T, Diefenbach B, Zhang R, Dunker R, et al. (2001) Crystal structure of the extracellular segment of integrin alpha Vbeta3. Science 294: 339-345.

3. Xiong JP, Stehle T, Zhang R, Joachimiak A, Frech M, et al. (2002) Crystal structure of the extracellular segment of integrin alpha Vbeta3 in complex with an Arg-Gly-Asp ligand. Science 296: 151-155.

4. Comolli JC, Hauser AR, Waite L, Whitchurch CB, Mattick JS, et al. (1999) Pseudomonas aeruginosa gene products PilT and PilU are required for cytotoxicity in vitro and virulence in a mouse model of acute pneumonia. Infect Immun 67: 3625-3630.

5. Lu X, Davies J, Lu D, Xia M, Wattam B, et al. (2006) The effect of the single substitution of arginine within the RGD tripeptide motif of a modified neurotoxin dendroaspin on its activity of platelet aggregation and cell adhesion. Cell Commun Adhes 13: 171-183.

6. Sanchez-Cortes J, Mrksich M (2009) The platelet integrin alphaIIbbeta3 binds to the RGD and AGD motifs in fibrinogen. Chem Biol 16: 990-1000.

7. Cairns BA, Barnes CM, Mlot S, Meyer AA, Maile R (2008) Toll-like receptor 2 and 4 ligation results in complex altered cytokine profiles early and late after burn injury. The Journal of trauma 64: 1069-1077; discussion 1077-1068.

8. Rawls JF, Mahowald MA, Goodman AL, Trent CM, Gordon JI (2007) In vivo imaging and genetic analysis link bacterial motility and symbiosis in the zebrafish gut. Proc Natl Acad Sci U S A 104: 7622-7627.

9. Klausen M, Heydorn A, Ragas P, Lambertsen L, Aaes-Jorgensen A, et al. (2003) Biofilm formation by Pseudomonas aeruginosa wild type, flagella and type IV pili mutants. Mol Microbiol 48: 1511-1524.

10. Christensen GD, Simpson WA, Younger JJ, Baddour LM, Barrett FF, et al. (1985) Adherence of coagulase-negative staphylococci to plastic tissue culture plates: a quantitative model for the adherence of staphylococci to medical devices. J Clin Microbiol 22: 996-1006.

11. Alm RA, Hallinan JP, Watson AA, Mattick JS (1996) Fimbrial biogenesis genes of Pseudomonas aeruginosa: pilW and pilX increase the similarity of type 4 fimbriae to the GSP protein-secretion systems and pilY1 encodes a gonococcal PilC homologue. Mol Microbiol 22: 161-173.

12. Bendtsen JD, Nielsen H, von Heijne G, Brunak S (2004) Improved prediction of signal peptides: SignalP 3.0. J Mol Biol 340: 783-795.

13. Rigden DJ, Galperin MY (2004) The DxDxDG motif for calcium binding: multiple structural contexts and implications for evolution. J Mol Biol 343: 971-984.

14. Chattopadhyaya R, Meador WE, Means AR, Quiocho FA (1992) Calmodulin structure refined at 1.7 A resolution. J Mol Biol 228: 1177-1192.

CHAPTER 7

CONCLUSION

7.1 Introduction

Here, I attempt to convey the importance of looking at calcium binding sites in the PilC type IV pilus (tfp) family of proteins and formulate models in an attempt to show how PilC proteins regulate pilus biogenesis though calcium binding. I will also hypothesize how binding interactions between integrin with *Pseudomonas aeruginosa* PilY1 take place, and, explain other ways PilY1 could be mediating attachment to host integrins.

7.2 Calcium Binding Site Homology

P. aeruginosa PilY1, *Kingella kingae* PilC1/2, *Neisseria gonorrhoeae* PilC1/2, and *Neisseria meningitidis* PilC1/2 proteins all affect functional pilus biogenesis and function as adhesins (Chapter 2, 3, 4, 5, and personal communication with Dr. Joseph St. Geme III) [1,2,3,4,5,6,7,8,9]. Although it is has only been proven in *P. aeruginosa* PilY1, *K. kingae* PilC1, and *N. gonorrhoeae* PilC1 that a nine residue calcium binding site (CBS) controls functional tfp biogenesis, a BLAST search reveals well over 100 bacteria that all have the same conserved CBS in their respective PilC-like protein(s) including *N. meningitidis*, *Xylella fastidiosa*, and *Ralstonia solanacearum,* thus demonstrating that this site has a potentially wide importance (Table 7.1) (Chapter 2, 5, and personal communication with Dr. Joseph St.

Geme III) [3]. The majority of these CBSs occurred in the C-terminal domain of the protein as in *P. aeruginosa* PilY1 [3]. Studying these CBSs in PilC proteins from other organisms through processes such as structural determination, calcium binding assays, and pull-downs will continue to provide more information on host binding partners and the overall mechanism of tfp biogenesis, thus potentially leading to the identification of therapeutic targets that if inhibited by small molecules could prevent initial bacterial attachment.

7.3 Calcium Regulating Pilus Extension and Retraction

How calcium is used in PilC proteins to regulate pilus extension and retraction remains unknown. The only structure for this family of proteins solved is the C-terminal *P. aeruginosa* PilY1, which shows a seven-bladed propeller and a sheet-loop-sheet CBS [3]. Knowing the physical location of the PilC proteins is crucial to understanding how calcium plays a role in pilus biogenesis. There are differing opinions on where PilY1 is located. However, the general consensus is that PilY1 resides in the bacterial outer membrane, pilus, or both [3,10]. Using antibodies against linear PilY1 epitopes, Bohn et. al. showed that PilY1 is present in bacterial cell membrane blebs, but not in the pilus; however in Orans et. al. upon sheared pilus preps, using an antibody for purified PilY1 C-terminal domain, PilY1 appears in the pilus fraction [3,10]. Perhaps the antibody made to these epitopes was for inaccessible portions of the structured protein, and thereforw did not bind, thus, through electron microscopy, not visualized in the pilus [10]. This antibody production technique does not at all devalue the PilY1 that was seen in the membrane, it simply cast doubt on a conclusion based protein that was unseen.

Assuming that PilY1 is found in both the pilus and the membrane, one can begin to envision a mechanism on how calcium binding might mediate pilus extension and retraction.

In referencing only the PAK PilY1 851-859 CBS, one hypothesis is that the membrane bound PilY1 is the calcium unbound form and the pilus bound PilY1 is the calcium bound form, thus fitting with the model that when calcium is bound to this site, there is pilus extension, and when calcium is not bound, there is pilus retraction (Figure 7.1A) [3]. Note that there are many pili on the surface extending and retraction, hence in theory; there would always be PilY1 present on the membrane in the wild type organism (Figure 7.1A, B. For pilus extension to occur, the PilA subunit polymerization needs to overcome the retractionary force of PilT [11,12]. The calcium bound state of PilY1, via a subtle local structural change, could initiate attachment to the pilin-like protein cuff to oppose PilT mediated pilus retraction by acting as a notch in the pilus, preventing PilA retraction/depolymerization back through the PilQ pore protein (Figure 7.1A). When the calcium is pried away from this site by either a separate protein or more likely, a small steric change that makes binding calcium unfavorable in comparison to binding the pilin-like protein cuff, the notch in PilY1 is alleviated, thus allowing PilT mediated retraction to commence (Figure 7.1B). As the pilus is being retracted through PilQ, PilY1 is trafficked back into the membrane, ready to reinsert itself into the next pilus extension process (Figure 7.1C, D).

7.4 Calcium Affecting Integrin Binding

Integrins are non-covalently linked heterodimeric cell adhesion and signaling receptors found in a variety of organisms from invertebrate to mammals [13]. The heterodimer of these surface proteins consists of an α-domain and a β-domain. Integrins are commonly found in the extracellular matrix and in tight junction regions between cells. Integrins, such as αVβ3 are known to have six metal (manganese or calcium) binding sites

in the apo structure and eight sites in the ligand bound structure with five metals bound in the α-domain of each respective structure [14,15]. None of these binding sites fit either the consensus calmodulin binding site or the nine residue site seen in PilY1. However, some sites do fit the consensus DxDxDG calcium binding motif [16]. Integrin metal binding is thought to be structural, however not much is known about the binding affinities of each site. One would have to make the low yield protein with calcium mimic mutations to each site except for one in question to determine the affinity of each respective site. Assuming each of the calcium mimics worked, even in the non-conventional metal binding sites, metal would need to be chelated out of the remaining site hoping the structural integrity stayed intact. This situation would also make it difficult to study how metal binding affinity would change in attached proteins.

In Chapter 3, PilY1 was shown to binds integrin in an RGD- and calcium-dependent manner. It was also proposed that the 600-608 CBS in PilY1 could be interacting with an integrin consensus CBS to help chelate calcium in order to mediate better integrin binding. We know both CBSs play a role in integrin binding (Chapter 3). Surprisingly, the D859A mutation could overcome the detrimental D608A mutation. The forms of PilY1 that had calcium present or mimicked calcium at the 600-608 site could be responsible for an initial lower affinity integrin interaction that was not discernible by the assay used. However, the D859A mutation, specifically with calcium present or mimicked at the 600-608 site, leads to higher than wild type binding for PilY1. Accordingly, the moment of pilus attachment to a target (via PilY1 or some other protein) could act as a catch bond, therefore having a long range motions in the pilus; one effect being the elimination of calcium from the 851-859 site leading to pilus retraction thus leading to PilA depolymerization (Figure 7.2A, B). In reintegrating PilY1 back into the bacterial membrane, the target, in theory, would also stay

attached and thus, be in closer proximity to the bacterial cell, leading to higher avidity and ultimately a greater ability for the bacteria to infect (Figure 7.2C, D).

Another way in which calcium binding may be affecting integrin binding is controlling the interaction PilY1 might be having with itself. Ligands using RGD bind in the integrin α- and β-subunit interface, mostly interacting with the residues phenylalanine-tyrosine-tryptophan (FYW) [15]. PilY1 has a conserved phenylalanine-threonine-tryptophan (FTW) similar to FYW and is 13 residues upstream of the promixal 600-608 CBS in the PAK strain of *P. aeruginosa* (Figure 7.3). Although the match is not exact, the differing middle amino acids share a side chain –OH group. In the 600-608 calcium bound state of PilY1, the RGD could be sterically out of reach from the FTW located in PilY1 and therefore be available for binding to the integrin FYW. In the 600-608 non-calcium bound form of PilY1 the distance between RGD and FTW could be close enough to initiate binding, and therefore compete for integrin binding. Also, from what we have shown in Chapter 3, the 851-859 non-calcium bound form of PilY1 must be able to overcome this putative blocking on integrin binding. It should be noted that the FTW is also conserved in the PA14 strain, which has the RGD and putative CBS occur much earlier in the protein sequence.

7.5 Other Putative Integrin Binding Mechanisms

There are other potential mechanisms that explain why PilY1 binds to integrins. A BLAST search shows that PilY1 is homologous to proteins that have FG-GAP motifs, which are commonly found in seven bladed β-propellers [17]. These repeats have been found in both the α-integrin subunits and in ligands such as fibronectin and epidermal growth factor [17]. Many of these proteins have known CBSs which are homologous to the two found in PilY1 [17]. PilY1 has also been found to share the nine residue CBS homology and both N-

terminal and C-terminal homology with the integrin binding protein von Willebrand factor type a [18]. Mimicking the fold and calcium binding site of an integrin binding ligand, or integrin itself, could provide PilY1 with yet another mechanism, besides the RGD, in which to bind integrin.

7.6 Figure Legends

Table 7.1 Bacteria that have homologous calcium binding sites found in Orans et. al. Bolded bacteria were examined in this study.

Figure 7.1 Model of calcium mediated pilus biogenesis. psPil represent pseudopilins. Proteins are not represented to scale, but for simplicity of the overall model. In reality, the ratio of pseudopilins to PilA is much lower [19]. (a) Model representing tfp extension where a small change in the represented PilY1 occurs in the non-calcium bound form as compared to the calcium bound form. (b) A small conformational change occurred in PilY1 (loss of the "notch") leading to pilus depolymerization/retraction. (c) Tfp is retracting and PilY1 is being trafficked back into the membrane. (d) Tfp is fully retracted with calcium unbound PilY1 located in the membrane.

Figure 7.2 Model of calcium mediated pilus biogenesis based on target binding. Labeling and scale is consistent from figure 7.1. (a) Model representing tfp extension where a small change in the represented PilY1 occurs in the non-calcium bound form as compared to the calcium bound form. PilY1 is attached to RGD binding integrin. (b) A small conformational change occurs in PilY1 post binding leading to loss of the "notch" and thus pilus depolymerization/retraction. (c) Tfp is retracting and PilY1 is being trafficked back into the membrane with integrin still attached. (d) Tfp is fully retracted with calcium unbound PilY1 located in the membrane with integrin attached

Figure 7.3 Alignment of PilY1 in various *P. aeruginosa* strains. FTW, 600-608 CBS and RGD are highlighted. Three varying strains of *P. aeruginosa* PilY1 were aligned using the biology workbench server [20,21]. Blue residues and an "*" corresponds to identical residues throughout the three strains, green residues and a ":" correspond to highly conserved residues, and navy residues and a "." corresponds to mildly conserved residues (e.g. alanine and leucine). Reference numbers are for PAK_287 PilY1 (the strain used in this study).

Table 7.1

Bacteria that have homologous CBS found in Orans et. al.
Acidovorax delafieldii
Acinetobacter baumannii
Acinetobacter calcoaceticus
Acinetobacter haemolyticus
Acinetobacter lwoffii
Acinetobacter radioresistens
Aeromonas caviae
Aeromonas hydrophila
Aeromonas salmonicida
Aeromonas veronii
Alcanivorax borkumensis
Alicycliphilus denitrificans
Alteromonadales bacterium
Alteromonas macleodii
Azoarcus sp.
Cardiobacterium hominis
Chromobacterium violaceum
Cupriavidus metallidurans
Cupriavidus necator
Cupriavidus taiwanensis
Deferribacter desulfuricans
Delftia sp.
Desulfatibacillum alkenivorans
Desulfobacterium autotrophicum
Desulfohalobium retbaense
Desulfotalea psychrophila
Desulfuromonas acetoxidans
Dichelobacter nodosus
Eikenella corrodens
Endoriftia persephone
Enhydrobacter aerosaccus
Ferrimonas balearica
Geobacter metallireducens
Geobacter sulfurreducens
Glaciecola agarilytica
Hahella chejuensis
Hippea maritima
Hydrogenivirga sp.
Hydrogenobacter thermophilus
Kingella denitrificans
Kingella kingae
Kingella oralis
Lutiella nitroferrum
Marichromatium purpuratum
Marinobacter adhaerens
Marinobacter aquaeolei
Methylobacter tundripaludum
Methylococcus capsulatus
Methylomonas methanica
Methylophaga aminisulfidivorans
Methyloversatilis universalis
Moritella sp.
Myxococcus xanthus
Neisseria bacilliformis
Neisseria cinerea
Neisseria elongata
Neisseria flavescens
Neisseria gonorrhoeae
Neisseria lactamica
Neisseria macacae
Neisseria meningitidis
Neisseria polysaccharea
Neisseria sicca
Neisseria subflav
Neisseria weaveri
Nitrococcus mobilis
Nitrosococcus halophilus
Nitrosococcus oceani
Nitrosococcus watsonii
Nitrosomonas europaea
Oceanobacter sp.
Oceanospirillum sp.
Oxalobacteraceae bacterium
Pelobacter carbinolicus
Persephonella marina
Polaromonas naphthalenivorans
Populus trichocarpa
Pseudoalteromonas atlantica
Pseudoalteromonas haloplanktis
Pseudoalteromonas tunicata
Pseudogulbenkiania sp.
Pseudomonas aeruginosa
Pseudomonas fulva
Pseudomonas mendocina
Pseudomonas stutzeri
Psychrobacter arcticus
Psychromonas sp.
Ralstonia eutropha
Ralstonia solanacearum
Ralstonia syzygii
Ramlibacter tataouinensis
Reinekea sp.
Shewanella amazonensis
Shewanella baltica
Shewanella benthica
Shewanella denitrificans
Shewanella frigidimarina
Shewanella halifaxensis
Shewanella loihica
Shewanella oneidensis
Shewanella pealeana
Shewanella piezotolerans
Shewanella putrefaciens
Shewanella sediminis
Shewanella violacea
Shewanella violacea
Shewanella woodyi
Simonsiella muelleri
Teredinibacter turnerae
Thermodesulfovibrio yellowstonii
Thermovibrio ammonificans
Thioalkalivibrio sp.
Tolumonas auensis
Variovorax paradoxus
Verminephrobacter eiseniae
Xanthomonas axonopodis
Xanthomonas gardneri
Xylella fastidiosa

Figure 7.1

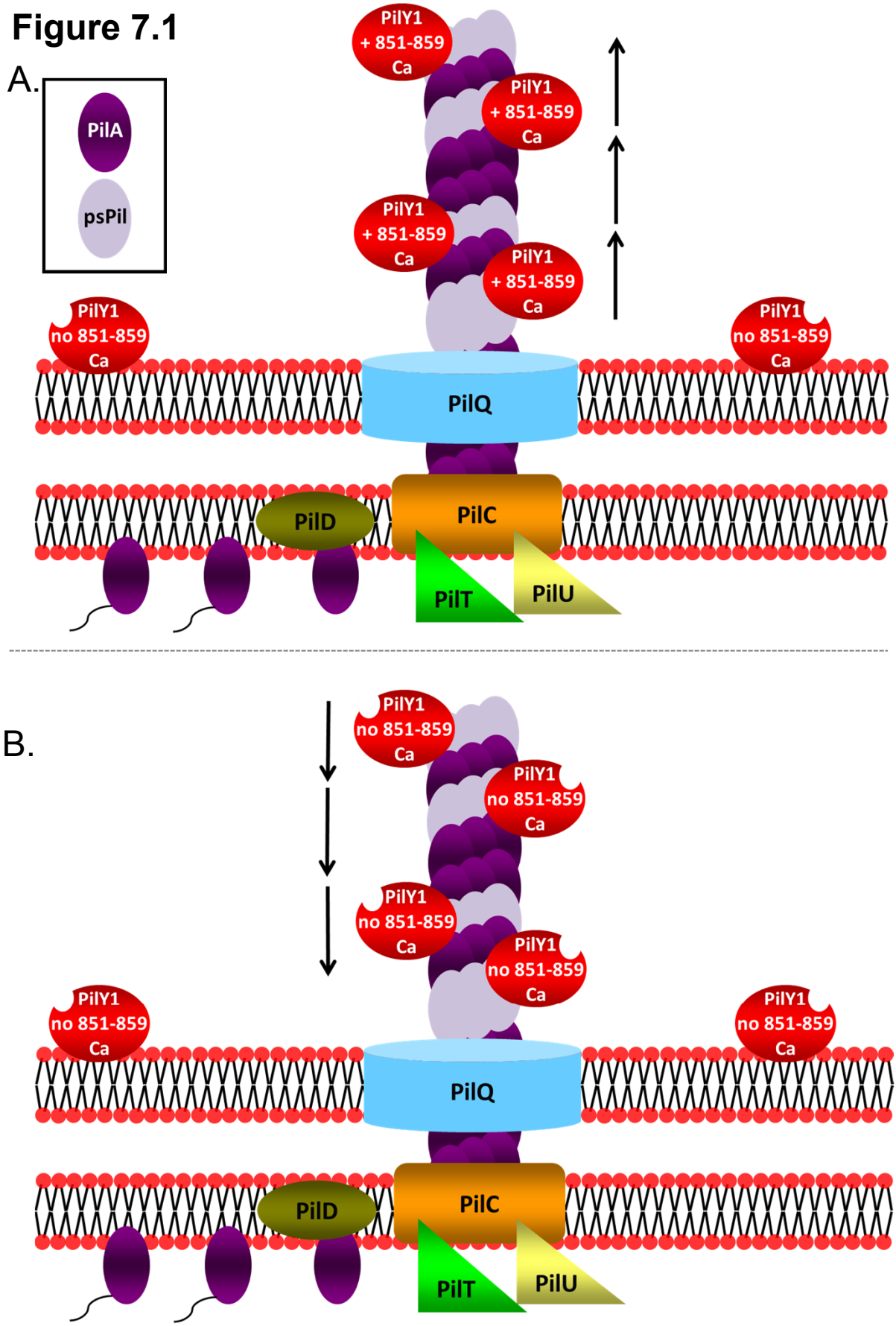
A.
PilA
psPil
PilY1
+ 851-859
Ca
PilY1
no 851-859
Ca
PilQ
PilC
PilD
PilT
PilU
B.

C.

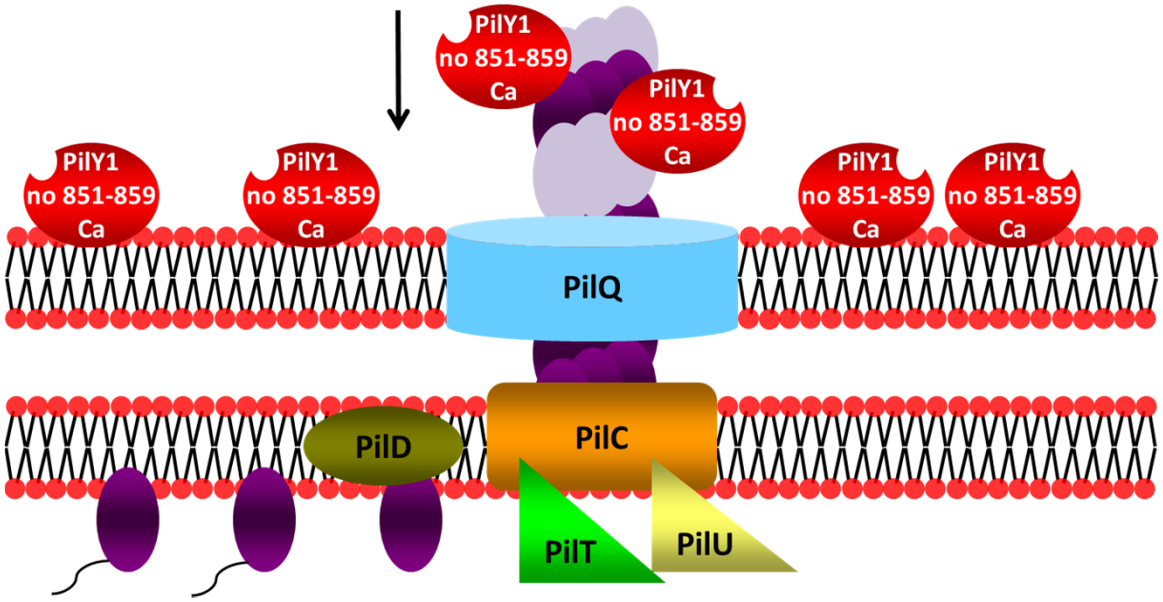
PilY1
no 851-859
Ca
PilY1
no 851-859
Ca
PilY1
no 851-859
Ca
PilY1
no 851-859
Ca
PilY1
no 851-859
Ca
PilY1
no 851-859
Ca
PilQ
PilD
PilC
PilT
PilU

D.

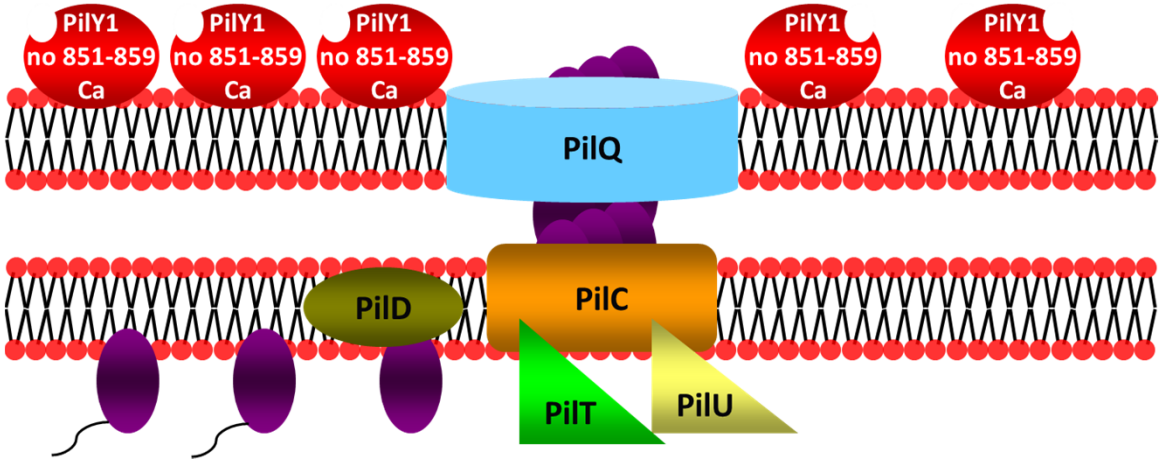
PilY1
no 851-859
Ca
PilY1
no 851-859
Ca
PilY1
no 851-859
Ca
PilY1
no 851-859
Ca
PilY1
no 851-859
Ca
PilQ
PilD
PilC
PilT
PilU

Figure 7.2

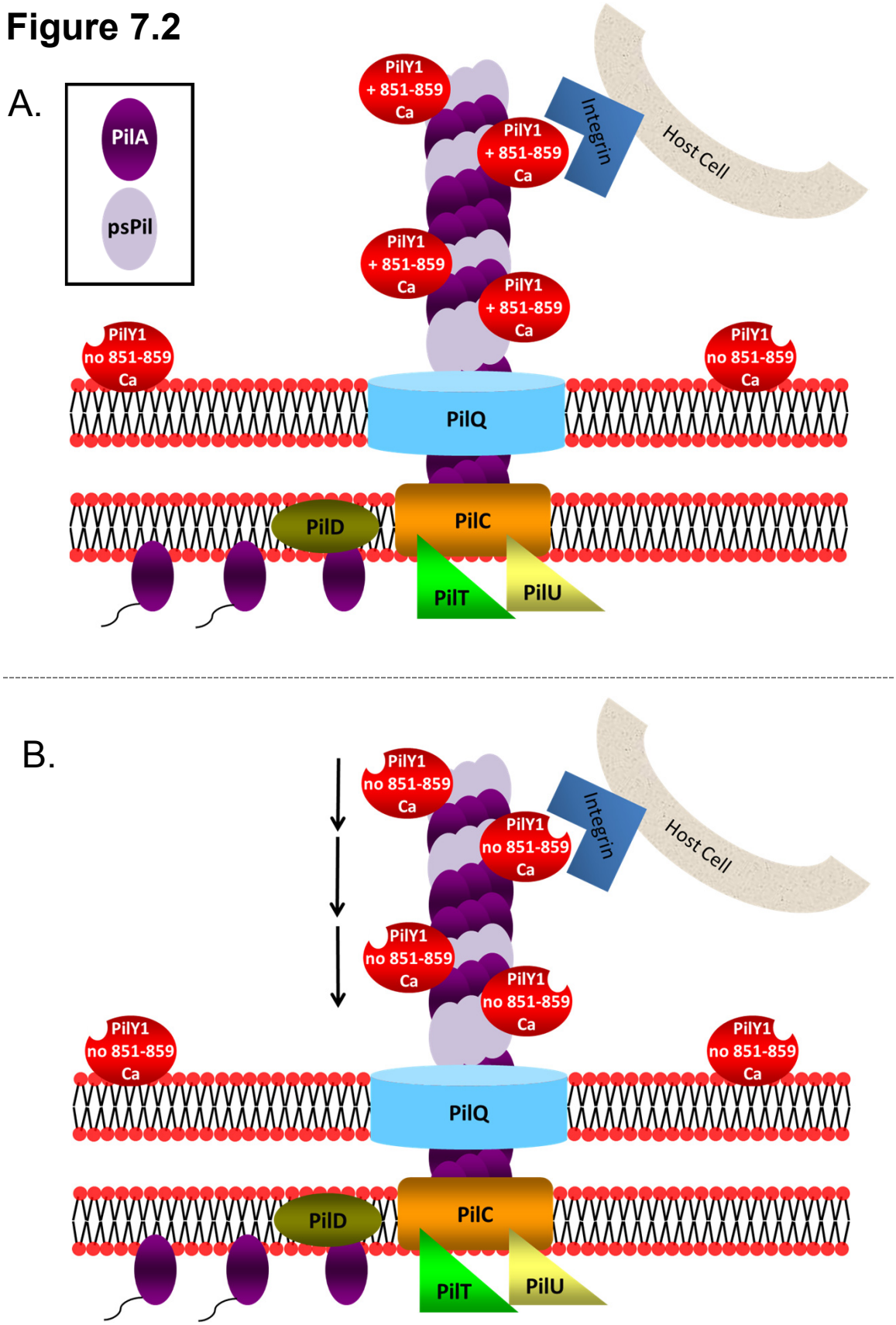
A.
PilA
psPil
PilY1
+ 851-859
Ca
PilY1
no 851-859
Ca
Integrin
Host Cell
PilQ
PilC
PilD
PilT
PilU
B.

C.

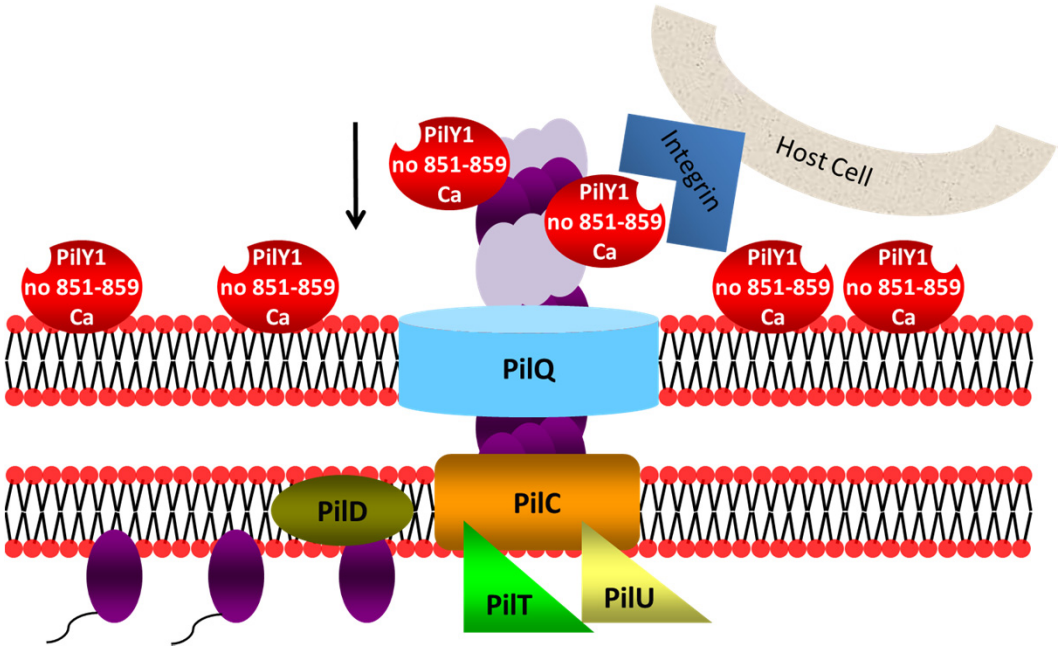
PilY1
no 851-859
Ca
PilY1
no 851-859
Ca
PilY1
no 851-859
Ca
PilY1
no 851-859
Ca
PilY1
no 851-859
Ca
PilY1
no 851-859
Ca
Integrin
Host Cell
PilQ
PilC
PilD
PilT
PilU

D.

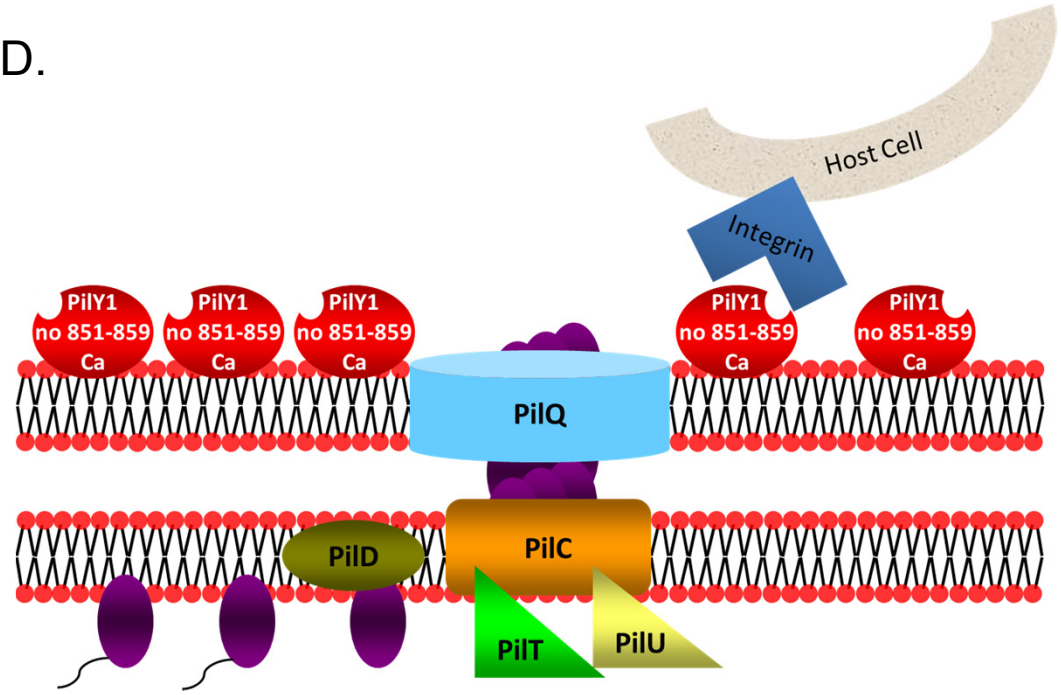
PilY1
no 851-859
Ca
PilY1
no 851-859
Ca
PilY1
no 851-859
Ca
PilY1
no 851-859
Ca
PilY1
no 851-859
Ca
Integrin
Host Cell
PilQ
PilC
PilD
PilT
PilU

Figure 7.3

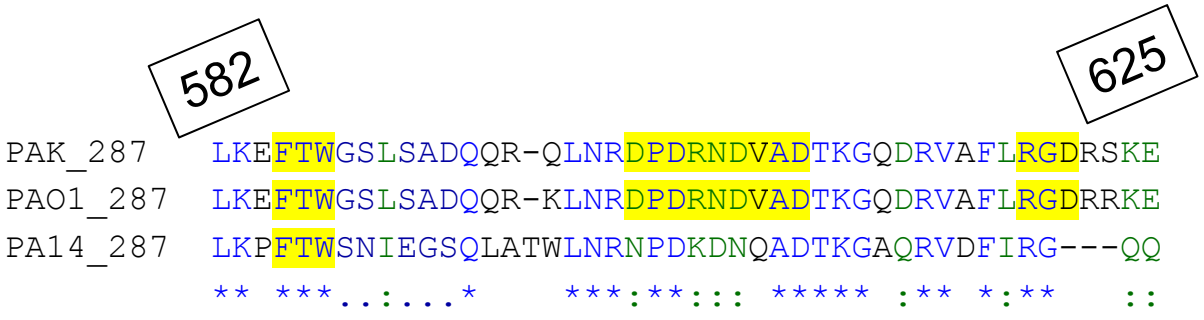
582
625
PAK_287 LKEFTWGSLSADQQR-QLNRDPDRNDVADTKGQDRVAFLRGDRSKE
PAO1_287 LKEFTWGSLSADQQR-KLNRDPDRNDVADTKGQDRVAFLRGDRRKE
PA14_287 LKPFTWSNIEGSQLATWLNRNPDKDNQADTKGAQRVDFIRG---QQ

7.7 References

1. Morand PC, Tattevin P, Eugene E, Beretti JL, Nassif X (2001) The adhesive property of the type IV pilus-associated component PilC1 of pathogenic Neisseria is supported by the conformational structure of the N-terminal part of the molecule. Mol Microbiol 40: 846-856.

2. Morand PC, Bille E, Morelle S, Eugene E, Beretti JL, et al. (2004) Type IV pilus retraction in pathogenic Neisseria is regulated by the PilC proteins. Embo J 23: 2009-2017.

3. Orans J, Johnson MD, Coggan KA, Sperlazza JR, Heiniger RW, et al. (2010) Crystal structure analysis reveals Pseudomonas PilY1 as an essential calcium-dependent regulator of bacterial surface motility. Proc Natl Acad Sci U S A 107: 1065-1070.

4. Jonsson AB, Nyberg G, Normark S (1991) Phase variation of gonococcal pili by frameshift mutation in pilC, a novel gene for pilus assembly. Embo J 10: 477-488.

5. Kehl-Fie TE, Miller SE, St Geme JW, 3rd (2008) Kingella kingae expresses type IV pili that mediate adherence to respiratory epithelial and synovial cells. Journal of bacteriology 190: 7157-7163.

6. Kirchner M, Heuer D, Meyer TF (2005) CD46-independent binding of neisserial type IV pili and the major pilus adhesin, PilC, to human epithelial cells. Infect Immun 73: 3072-3082.

7. Kirchner M, Meyer TF (2005) The PilC adhesin of the Neisseria type IV pilus-binding specificities and new insights into the nature of the host cell receptor. Mol Microbiol 56: 945-957.

8. Nassif X, Beretti JL, Lowy J, Stenberg P, O'Gaora P, et al. (1994) Roles of pilin and PilC in adhesion of Neisseria meningitidis to human epithelial and endothelial cells. Proc Natl Acad Sci U S A 91: 3769-3773.

9. Rudel T, Scheurerpflug I, Meyer TF (1995) Neisseria PilC protein identified as type-4 pilus tip-located adhesin. Nature 373: 357-359.

10. Bohn YS, Brandes G, Rakhimova E, Horatzek S, Salunkhe P, et al. (2009) Multiple roles of Pseudomonas aeruginosa TBCF10839 PilY1 in motility, transport and infection. Mol Microbiol 71: 730-747.

11. Wolfgang M, Lauer P, Park HS, Brossay L, Hebert J, et al. (1998) PilT mutations lead to simultaneous defects in competence for natural transformation and twitching motility in piliated Neisseria gonorrhoeae. Mol Microbiol 29: 321-330.

12. Misic AM, Satyshur KA, Forest KT (2010) P. aeruginosa PilT structures with and without nucleotide reveal a dynamic type IV pilus retraction motor. J Mol Biol 400: 1011-1021.

13. Humphries JD, Byron A, Humphries MJ (2006) Integrin ligands at a glance. Journal of cell science 119: 3901-3903.

14. Xiong JP, Stehle T, Diefenbach B, Zhang R, Dunker R, et al. (2001) Crystal structure of the extracellular segment of integrin alpha Vbeta3. Science 294: 339-345.

15. Xiong JP, Stehle T, Zhang R, Joachimiak A, Frech M, et al. (2002) Crystal structure of the extracellular segment of integrin alpha Vbeta3 in complex with an Arg-Gly-Asp ligand. Science 296: 151-155.

16. Rigden DJ, Galperin MY (2004) The DxDxDG motif for calcium binding: multiple structural contexts and implications for evolution. J Mol Biol 343: 971-984.

17. Springer TA (1997) Folding of the N-terminal, ligand-binding region of integrin alpha-subunits into a beta-propeller domain. Proc Natl Acad Sci U S A 94: 65-72.

18. Kuchma SL, Ballok AE, Merritt JH, Hammond JH, Lu W, et al. (2010) Cyclic-di-GMP-mediated repression of swarming motility by Pseudomonas aeruginosa: the pilY1 gene and its impact on surface-associated behaviors. Journal of bacteriology 192: 2950-2964.

19. Giltner CL, Habash M, Burrows LL (2010) Pseudomonas aeruginosa minor pilins are incorporated into type IV pili. J Mol Biol 398: 444-461.

20. Higgins DG, Bleasby AJ, Fuchs R (1992) CLUSTAL V: improved software for multiple sequence alignment. Comput Appl Biosci 8: 189-191.

21. Thompson JD, Higgins DG, Gibson TJ (1994) CLUSTAL W: improving the sensitivity of progressive multiple sequence alignment through sequence weighting, position-specific gap penalties and weight matrix choice. Nucleic Acids Res 22: 4673-4680.